

Aus der Medizinische Klinik und Poliklinik V der
Ludwig-Maximilians-Universität München

Direktor: Prof. Dr. med. Jürgen Behr

Thema der Dissertation:

**Analysis of altered intracellular pathways leading to a
reduced Toll-like receptor-4 (TLR-4) expression in cystic
fibrosis**

zum Erwerb des Doktorgrades der Humanbiologie an der
Medizinischen Fakultät der Ludwig-Maximilians-Universität zu
München

vorgelegt von

Gaurav Vilas Sarode

aus Nashirabad, (MH) India

2017

**Mit Genehmigung der Medizinischen Fakultät der Ludwig-
Maximilians- Universität München**

Berichterstatter:	Prof. Dr. med. Jürgen Behr
Mitberichterstatter:	Prof. Dr. Fritz Krombach Prof. Dr. med. Matthias Griese
Mitbetreuung durch den promovierten Mitarbeiter:	PD. Dr. med. Markus Henke
Dekan:	Prof. Dr. med. dent. Reinhard HICKEL
Tag der mündlichen Prüfung:	29 th August 2017

Table of contents

Summary	7
Zusammenfassung	9
1 Introduction	11
1.1 Cystic fibrosis	11
1.2 Innate immunity	13
1.3 Toll-like receptors (TLRs)	15
1.3.1 Toll-like receptor-4	16
1.4 ENaC channel	19
1.5 Transforming growth factor-β	22
1.6 microRNAs	24
1.6.1 microRNAs in cystic fibrosis	25
1.7 Iron homeostasis	27
1.7.1 Hypoxia-inducible factor-1 α	29
1.7.2 Ferroportin	30
1.8 Hypothesis and aims:	31
2 Materials and methods	32
2.1 Materials	32
2.1.1 Chemicals and biochemicals.....	32
2.1.2 Instruments and software's	34
2.1.3 Primary and secondary antibodies:.....	35
2.1.4 Medium and serums	36
2.1.5 Kits	36
2.1.6 Miscellaneous	37
2.1.7 Buffers and Solutions	38
2.1.7.1 1-Buffers for SDS-PAGE and Electrophoresis	38
2.1.7.2 2 Buffers for immunofluorescence	40
2.1.7.3 3 Buffers for immunohistochemistry	40
2.1.7.4 4 Buffers for ELISA	41

2.1.8	Primers of mRNA.....	41
2.1.9	Primers for miRNA.....	42
2.1.10	Cell lines.....	42
2.2	Methods.....	42
2.2.1	Cell culture.....	42
2.2.2	RNA analysis.....	43
2.2.2.1	RNA isolation.....	43
2.2.2.2	cDNA synthesis.....	44
2.2.2.3	Amplification of cDNA.....	45
2.2.2.4	cDNA synthesis for miRNA expression.....	46
2.2.2.5	Quantitative Real-Time PCR analyzes for miRNA profiling:.....	47
2.2.3	Protein expression analysis.....	48
2.2.3.1	Protein isolation from CFBE41o- and 16HBE14o-.....	48
2.2.3.2	Protein quantification.....	49
2.2.3.3	Sodium dodecyl sulfate-polyacrylamide gel electrophoresis (SDS-PAGE) and immunoblotting.....	49
2.2.3.4	Enzyme-linked immunosorbent assay (ELISA).....	52
2.2.3.5	Immunofluorescence:.....	54
2.2.4	Transfections.....	55
2.2.4.1	Transfection of miRNA mimics and inhibitor:.....	55
2.2.4.2	Transfection of TLR-4-yfp plasmid:.....	56
2.2.5	Statistical analysis.....	57
3	Results.....	58
3.1	TGF-β expression in CFBE41o- and 16HBE14o- cells.....	58
3.1.1	mRNA expression of TGF- β by q-PCR.....	58
3.1.2	Protein expression of TGF- β by immunoblotting.....	59
3.1.3	Level of TGF- β by ELISA.....	60
3.1.4	Expression of TGF- β by immunofluorescence.....	61
3.1.5	TGF- β expression in corrCFBE41o- cells.....	62
3.2	miRNA-16 dependent TGF-β expression.....	63
3.2.1	miR-16 expression.....	63

3.2.2	TGF- β expression upon miR-16 mimic and anti-miR-16 transfection in 16HBE14o- cells and CFBE41o- cells	64
3.3	Hypoxia stabilization associated TGF-β expression	66
3.4	Decreased expression of ferroportin in CF	67
3.4.1	mRNA expression of ferroportin by q-PCR.....	68
3.4.2	Protein expression of ferroportin by western blot	68
3.4.3	Expression of ferroportin by immunofluorescence	69
3.4.4	Ferroportin expression in corrCFBE41o- cells	70
3.5	Hypoxia stabilization associated ferroportin expression.....	71
3.6	Effect of TGF-β treatment on expression of ferroportin expression	73
3.7	Effect of TGF-β treatment on expression of TLR-4 expression	75
3.8	ENaC- channel inhibition by amiloride upregulates the expression of Ferroportin.....	77
3.9	ENaC channel inhibition by amiloride restores TLR-4 expression in CFBE cell lines	79
3.9.1	Transfection of TLR-4-yfp to CFBE41o- and 16HBE14o- cells	81
3.10	TLR-4 expression upon DFO, TGF- β and EIPA treatments	83
4	Discussion.....	85
4.1	TGF- β expression is reduced in CF	86
4.2	miR-16 downregulate TGF- β expression in CF cells	88
4.3	Hypoxia regulates the TGF- β expression	88
4.4	Ferroportin expression is reduced in CF and regulated by hypoxia	90
4.5	Exogenous TGF- β upregulates the ferroportin and TLR-4 expression.....	91
4.6	Direct inhibition of ENaC up-regulate the ferroportin and TLR-4 expression.....	94
5	Conclusion	96
6	References.....	98

7	Abbreviation	109
8	Curriculum vitae	113
9	Eidesstattliche Versicherung.....	116
10	Acknowledgements	117

Summary

Cystic fibrosis (CF) is caused due to the dysregulation of cystic fibrosis transmembrane conductance regulator (CFTR) and epithelial sodium channel (ENaC). CFTR is a negative regulator of the amiloride-sensitive ENaC that constitutes the limiting pathway for sodium (Na^+) and fluid absorption. Mutation in CFTR gene leads to ENaC channel overexpression and results in Na^+ hyper-absorption in airways. Defective CFTR leads to enhanced mucus viscosity, decreased muco-ciliary clearance and bacterial colonization. It is assumed that impaired toll-like receptor-4 (TLR-4) mediated innate and adaptive immune responses affect chronic bacterial infection of CF airways. The reduced TLR-4 surface expression might be associated with increased iron concentration and hypoxia via downregulation of hemoxygenase-1 in CF airways.

Iron transport in the epithelium is associated with transcellular movement of Na^+/K^+ -ATPase and ENaC. We speculate that increased intracellular iron might be a result of ENaC mediated high Na^+ and subsequent iron bypass in CF airways. Alterations in iron homeostasis have been previously studied in CF. However, expression of ferroportin, which is the only known iron exporter, has not been well studied in CF epithelial cells.

Recent studies suggest that microRNA-16 (miR-16) and transforming growth factor- β (TGF- β) regulate the ENaC channel in acute lung injury (ALI) and are involved in CFTR regulation in CF. We hypothesized that miR-16 and TGF- β might have a role in modulating ENaC channels and regulate the ferroportin and TLR-4 expression in CF epithelial cells. Therefore, we investigated *in vitro* roles of miR-16 on TGF- β expression in CF. Further, we studied *in vitro* effects of

exogenous TGF- β mediated direct inhibition of ENaC, ferroportin and subsequent TLR-4 expression in CF.

Cystic fibrosis bronchial epithelial cell line (CFBE41o-) and normal human bronchial epithelial cell lines (16HBE14o-) were used for *in vitro* analysis for protein and mRNA expression via immunoblotting, qPCR, immunofluorescence, enzyme-linked immunosorbent assay and transfection. Immunohistochemistry analysis of TGF- β was performed on lung sections from CF patients and donor.

We observed reduced TGF- β and ferroportin expression in CFBE41o- cells as compared to 16HBE14o- cell lines. Additionally, hypoxic condition showed up-regulation of the TGF- β and ferroportin expression, suggesting a role of hypoxia in downregulation of TGF- β and ferroportin expression in CF cells. Exogenous application of TGF- β revealed the increase of ferroportin and TLR-4 surface expression. Direct inhibition of ENaC by EIPA also resulted in increased ferroportin and TLR-4 expression in CFBE41o- cells. Immunofluorescence studies confirmed the increase of ferroportin and TLR-4 surface expression upon TGF- β and EIPA treatments.

To conclude, our *in vitro* results demonstrate that miR-16 and hypoxia might be responsible for reduced TGF- β and ferroportin expression in CFBE41o- cells. Further exogenous supplement of TGF- β and direct inhibition of ENaC by EIPA was correlated with increased ferroportin expression and improve TLR-4 surface expression in CFBE41o- cells.

Zusammenfassung

Zystische Fibrose (CF) wird durch eine Dysregulation des Cystic Fibrosis Transmembrane Conductance Regulator Kanals (CFTR) und des epithelialen Na^+ Kanals (Epithelial Sodium Channel, ENaC) verursacht. CFTR wirkt als ein negativer Regulator für den amiloride-sensitiven epithelialen Na^+ Kanal (ENaC), dies ist was die limitierende Signalkaskade für Na^+ und der Flüssigkeitsabsorption bildet. Mutationen in CFTR-Genen führen zu einer Überexpression von ENaC-Kanälen und resultiert in eine Na^+ Hyperabsorption in den Atemwegen. Dies führt zu einer erhöhten Schleimviskosität, veringertes Mukoziliärer-Clearance und Bakterienkolonisation. Es wird angenommen, dass eine chronische Bakterienbesiedelung der CF Atemwege durch Toll Like Rezeptor-4 (TLR-4) vermittelte Immunantwort beeinflusst wird. Wir konnten feststellen, dass TLR-4 bei CF verringert an der Oberfläche exprimiert wird. Dies könnte mit einer erhöhten Eisenkonzentration und beeinträchtigter Hypoxie durch Runterregulation von Hämoxxygenase-1 in CF Atemwegen assoziiert sein.

Der epitheliale Eisentransport ist mit einer transzellulären Bewegung der Na^+/K^+ -ATPase und dem epithelialen Na^+ Kanal assoziiert. Wir vermuten, dass erhöhtes intrazelluläres Eisen, durch den ENaC-Kanal vermittelten hohen Na^+ Gehalt mit anschließender Eisenumleitung in CF Atemwege, assoziiert ist. Veränderungen in der Eisenhomöostase wurden bereits früher bei CF vermutet. Jedoch, die Expression von Ferroportin, der einzig bekannte Eisenexporter, wurde in CF epithelialen Zellen noch nicht untersucht.

Aktuelle Untersuchungen deuten darauf hin, dass microRNA-16 (miR-16) und transforming growth factor- β (TGF- β) bei akutem Lungenversagen (ALI) die ENaC Kanäle regulieren und auch in der CFTR-Regulierung bei CF beteiligt sind. Wir vermuten, dass miR-16 und TGF- β eventuell eine Rolle in der Modulation der ENaC Kanäle und der Regulation von Ferroportin und TLR-4 Expression in der

CF Epithelzelle hat. Daher haben wir *in vitro* die Rolle von miR-16 on TGF- β bei CF Epithelzellen untersucht. Des Weiteren untersuchten wir den *in vitro* Effekt von exogener TGF- β vermittelter direkter Inhibition von ENaC, Ferroportin und der folgender TLR-4 Expression bei CF.

Zystische Fibrose bronchiale Epithelzelllinien (CFBE41o-) und normale humane bronchiale Epithelzelllinien (16HBE14o-) wurden für *in vitro* Analysen von Proteinen und mRNA Expression via Immunoblotting, qPCR, Immunofluorescence, enzyme-linked immunosorbent assay und Transfektion verwendet. Immunohistochemie Analysen von TGF- β wurden an Lungenschnitten von CF-Patienten und Kontrolllungenschnitten ausgeführt.

Wir sahen eine verringerte TGF- β und Ferroportin Expression in CFBE41o- Zellen im Vergleich zu 16HBE14o- Zellen. Zusätzlich bestand unter hypoxischen Bedingungen eine Hochregulation der TGF- β und Ferroportin Expression, was andeutet, dass veränderter Hypoxie, in runterregulierter TGF- β und Ferroportin Expression in CF Zellen, eine Rolle spielt. Exogene Zufuhr von TGF- β zeigte einen Anstieg von Ferroportin und TLR-4 Oberflächenexpression. Direkte Inhibition von ENaC durch EIPA resultierte in eine erhöhte Ferroportin und TLR-4 Expression in CFBE41o- Zellen. Immunofluoreszens Experimente bestätigten den Anstieg von Ferroportin und TLR-4 Oberflächenexpression durch TGF- β und EIPA Behandlung.

Zusammenfassend, zeigen unsere *in vitro* Ergebnisse, dass miR-16 und Hypoxie eventuell für eine verringerte TGF- β und Ferroportin Expression in CFBE41o- Zellen verantwortlich sind. Des Weiteren, dass Zusatz von TGF- β und direkte Inhibition von ENaC durch EIPA mit erhöhter Ferroportin Expression und verbesserter TLR-4 Oberflächenexpression in CFBE41o- Zellen korrelieren.

1 Introduction

1.1 Cystic fibrosis

Cystic fibrosis (CF) is a life-limiting inherited disorder that affects ~70,000 individuals worldwide. CF mostly affects the Caucasians; however, it has been reported in all races and ethnicities. It is an autosomal recessive disease caused by one or more mutations in the gene encoding cystic fibrosis transmembrane conductance regulator (CFTR) [1-3]. Mutation in CFTR gene leads to CFTR protein dysfunctions. This condition is autosomal recessive which means both copies of the gene are mutated in each cell [4]. Individuals whose parent carries one functional copy of mutated CFTR gene do not exhibit any signs and symptoms of cystic fibrosis. One copy of the gene can also exhibit the complete function of CFTR protein [5]. CFTR not only functions in regulation of apical epithelial chloride channel but also regulates other channels such as epithelial Na⁺ channel (ENaC) [6], Ca²⁺-activated chloride conductance (CaCC), renal outer medullary K⁺ (ROMK) channel, sodium/proton exchanger 3 (NHE3), and aquaporin channel [7].

Currently, there are nearly 2,000 mutations noted in CFTR gene [8]. Depending upon the abnormalities in this gene, these mutations are divided into 5 types ranging from complete loss of protein synthesis to normal apical membrane expression of the protein with poor chloride conductance [7]. The most common mutation is the deletion of phenylalanine at 508th position ($\Delta F508$ del mutation) of the gene. In this mutation, CFTR gene is synthesized in an immature form that leads to improper folding of CFTR protein in the endoplasmic reticulum (ER) and further degraded by ER-chaperons. It causes reduction of its function and affects the chloride transport at the apical plasma membrane [9].

In healthy airways, CFTR acts as cyclic adenosine 3',5'-monophosphate (cAMP)-regulated chloride channels [10]. Thus, defective CFTR impairs chloride-ion

transport across epithelial surfaces and mucosal membranes [9]. Organs containing epithelia such as lungs, pancreas, gastrointestinal system, hepatobiliary system, reproductive system, and sweat glands are all severely affected in CF disease. Among these, the pulmonary airways display distinct changes with a basic genetic defect, which results in the significantly reduced life expectancy of CF patients [11, 12].

Defective CFTR causes alteration of epithelial salt and water transport within the cells and excessive sodium reabsorption lead to dehydrated airway surface fluid and impaired muco-ciliary clearance (Figure-1). Further, it results into abnormal viscous mucus secretions in the lung airways thereby causing difficulty in breathing and declination of lung functions.

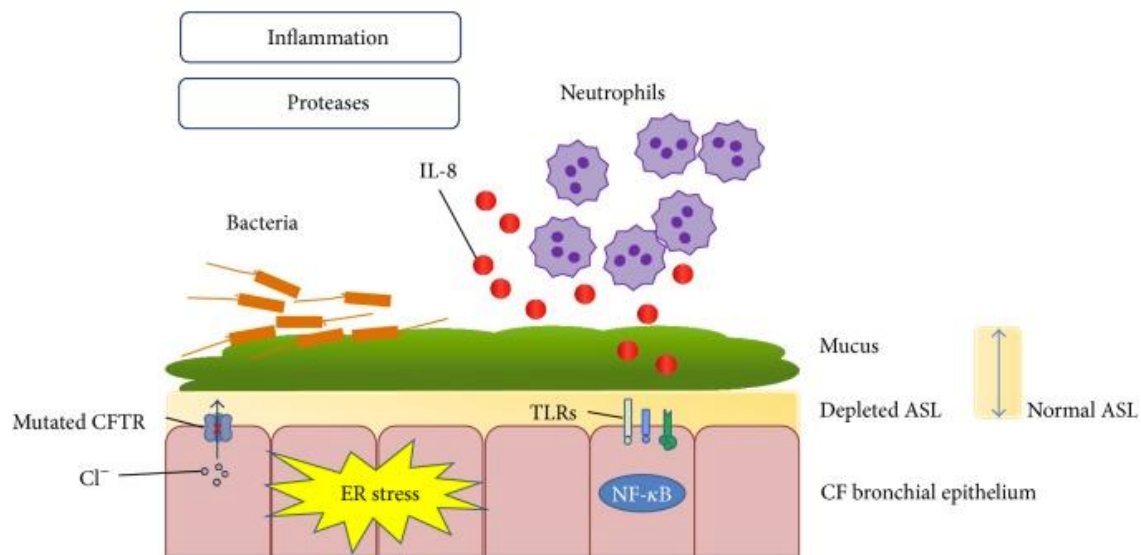


Figure 1: Cystic fibrosis epithelium [13]

Thickened mucus secretion provides a suitable environment for bacterial growth. Over the time of CF progression, CF patients are infected with various pathogens such as *Pseudomonas aeruginosa* (*P. aeruginosa*), *Staphylococcus aureus* (*S. aureus*) and *Burkholderia cenocepacia* (*B. cenocepacia*).

Chronic infection with *P. aeruginosa* is known as a major perpetrator in CF, that leads to epithelial surface damage and airway blocking, which further impairs the airway conductance [14]. These result in decline of pulmonary functions and contribute to over 85-90% of deaths in CF patients [15]. An exaggerated inflammatory response due to chronic bacterial infection is one of the contributing factors in worsening of CF [16]. Several studies have suggested that defective CFTR may directly affect airway immunity with exaggerated production of pro-inflammatory mediators and impaired immune responses to pathogens [17].

1.2 Innate immunity

Clinical data suggest that CF initiates due to altered host defense system of the airways and failure to clear the bacterial infection. This leads to chronic inflammation and contributes to obstructive lung diseases eventually associated with the respiratory failure [18]. The innate immune system is the first line of defense against pathogens, which additionally signals to acquire immune system for activation of T and B cells to specific antigens. The innate immune system not only provides barriers to colonization and infection but also determines antigen specificity and the nature of the response to be carried out by acquired immunity [19]. Innate immunity prevents bacterial infections by rapid recruitment of phagocytic cells, effective signal transduction systems, muco-ciliary escalator, proteases, anti-proteases, antimicrobials, immediate production of reactive oxygen species (ROS), and pattern recognition receptors (PPRs) [20].

The response of innate immunity in the detection of pathogens relies on the recognition of various pathogen-associated molecular patterns (PAMPs), which include complex lipids, lipopolysaccharides, carbohydrates, unmethylated cytosine-guanosine, DNA sequences, and double-stranded RNAs [21]. PAMPs are recognized by the host's pattern recognition receptors (PRRs). Upon recognition, it signals to the host about the presence of infections and initiates immune responses by activation of the intracellular cascade to trigger pro-

inflammatory and antimicrobial agents to clear the infections [22].

PPR mediated signaling ultimately leads to the activation of gene expression and synthesis of various cytokines, chemokines, cell adhesion molecules, and immune receptors [21], which together play roles in early host response to infections and initiate the link for adaptive immune responses. This, in turn, promotes the repair of damaged tissues, and assist in the restoration of tissue functions. The basic underlying mechanisms for innate immune recognition are highly conserved among all species.

The key components of the innate immunity include epithelial cells, neutrophils, and alveolar macrophages. These cells not only function in clearing pathogens but also co-ordinate the immune responses against the infections. Airway secretions, which contain anti-microbial peptides and proteins directly acts on pathogens and modulate the inflammatory responses [18]. Defective CFTR leads to impairment of epithelial cell functions such as bacterial killing, transport of glutathione (GSH) and cytokine production. Also, there is deterioration of neutrophil functions such as phagocytosis, degranulation, apoptosis, anti-microbial activity, cytokine production and TLR-2, 4, 5 expressions. Furthermore, macrophage functions such as clearance of apoptotic cells, cytokine production, phagocytosis acidification of lysosomes and antigen presentation are affected.

In CF patients, mutation in CFTR causes critical impairment of innate host immune responses. Mechanisms of how faulty CFTR result in impaired immune responses is not fully understood. This compromised immune response results in an early and severe form of chronic airways disorders, featuring thick mucus obstruction with chronic bacterial infections, neutrophil-dominated airway inflammation, finally leading to progressive pulmonary damage with bronchiectasis and emphysema [23].

1.3 Toll-like receptors (TLRs)

TLRs are the first line of defense key sensors in innate immune response and constitute a highly conserved family of pattern recognition receptors. These are expressed by epithelial and immune cells, which allow the host to detect the presence of microbial infections. TLRs mediate response by sensing pathogen-associated molecular patterns (PAMPs), and danger-associated molecular patterns (DAMPs).

Upon detection of these conserved molecular patterns in microbial factors and endogenous danger signals, TLRs provide rapid stimulation of intracellular signaling cascades of innate immunity for the expression of various inflammatory mediators including tumor necrosis factor alpha (TNF- α), nuclear factor kappa-light-chain-enhancer of activated B cells (NF- κ B) and interleukin-8 to coordinate the early host response to infection. Thirteen TLRs have been identified up to date and their respective ligands are as follows:

Table 1- Toll like receptors and their ligands [22, 24, 25]

Receptors	Ligands
TLR-1	Bacterial lipopeptides, soluble factors
TLR-2	Lipopeptides, lipoteichoic acid, peptidoglycan
TLR-3	Double-stranded RNA, polyinosine: cytosine
TLR-4	LPS, heat-shock protein 60, fusion protein
TLR-5	Flagellin
TLR-6	Zymosan, lipopeptides
TLR-7	Single-stranded viral RNA, imiquimod (R837)
TLR 8	Single-stranded RNA
TLR-9	Unmethylated CpG DNA
TLR-10, TLR-11, TLR-12, TLR-13	Uncertain

TLR ligands activate the most important cell types such as antigen-presenting cells (APCs), dendritic cells (DCs), macrophages, B cells, and T cells [26]. TLRs signaling act via MyD88-dependent (myeloid differentiation primary response protein 88) or MyD88-independent pathways [27]. Signaling occurs through the adaptor protein MyD88 and its TLR binding partner toll-IL-1 receptor domain-containing adaptor protein (TIRAP) and induces activation of NF- κ B via the Pelle-like kinase interleukin-1 receptor-associated kinase (IRAK) to activate expression of pro-inflammatory genes such as TNF, IL-1 β , IL-6, and IL-8 [28, 29].

Previous studies have shown that TLR signaling is involved in mucin gene regulation. Stimulation of TLR-2 and TLR-3 persuade mucin expression, activating mitogen-activated protein kinases (MAPK) and inducing epidermal growth factor receptor (EGFR) signaling [30]. Ueno and colleagues showed that MUC1 acts as anti-inflammatory agent by negatively regulating TLR-2, -3, -4, -5, -7, and -9 mediated inflammatory signaling [31].

In CF, apical expression of TLR-2 and TLR-5 in cystic fibrosis epithelial cells is increased and associated with hyper-inflammatory responses to bacterial products whereas, surface expression of TLR-4 is reduced and restricted to the endosome [32].

1.3.1 Toll-like receptor-4

TLR-4 is a member of toll-like receptor family of proteins and has been very well known for identifying lipopolysaccharide (LPS). TLR-4 ligands also recognize several viral proteins, polysaccharides, and a variety of endogenous proteins such as low-density lipoprotein, β -defensin, and heat shock proteins [33]. Lipopolysaccharide (LPS) is a component of the outer cell membrane of gram-negative bacteria such as *P. aeruginosa* and activates a wide variety of mammalian cell types [34]. LPS recognition leads to oligomerization of TLR-4, which leads to recruitment of its downstream adaptors through interactions with

TIR (Toll-interleukin-1 receptor) domains. The TIR domains play important role in TLR-4 mediated signal transductions because any mutation in the TIR domains can lead to the elimination of LPS response [35]. Upon recognition of LPS, TLR-4 has been shown to initiate multiple intracellular signaling events. TLR-4 exhibit MyD88-dependent and MyD88-independent (TRIF-dependent) pathway, which induces the release of critical pro-inflammatory cytokines such as interleukin-1 (IL-1), interleukin-6 (IL-6), interleukin-8 (IL-8), and tumor necrosis factor-alpha via activation of NF-kB pathways [34].

In CF, along with bacterial infections, Cohen and Prince stated that the CFTR dysfunction affects several components of innate immunity and that the initial predisposition to infection in infants with CF may represent a primary defect in local mucosal immunity [32]. Studies by Henke et al. have shown that defective CFTR cells have reduced TLR-4-mediated innate immune responses and decreased interferon- γ inducible protein-10 (IP-10) mediated adaptive immune responses in CF. They also postulated that reduced TLR-4 surface expression might be due to defective translocation of TLR-4 onto the cell surface caused by defective CFTR [36, 37].

Altered processing and localization of TLR-4 on the epithelial cell surface might lead to the altered or limited immune responses in CF. Furthermore, the CF bronchial airway epithelium may fail early detection of bacterial infection and delay of neutrophil chemotaxis and migration across the epithelium. These late activations of neutrophils may support the growth and biofilm formation in the CF lungs. Neutrophil absence or degradations increase sputum tenacity and are associated with reduced muco-ciliary clearance due to the release of large amounts of DNA [38-40]. In healthy people, CFTR may also act as pattern recognition receptor (PRR) to clear *P. aeruginosa* infections by activating pro-inflammatory cytokines. In CF, defective CFTR function leads to impaired muco-ciliary clearance and results into increased *P. aeruginosa*, *S. aureus*, and *Haemophilus influenzae* infections in airway epithelial cells, thereby

compromising the clearance ability of the airways of CF patients. It not only affects components of innate immunity like a dysregulated TLR-4 trafficking and signaling, but also a diminished ability to counteract the oxidative stress induced by constitutive and exogenous activated inflammation. This further causes an exaggerated and ineffective airway inflammation that fails to eradicate pulmonary pathogens and contributes to the persistent airway bacterial infections as seen in CF patients (Figure-2). Exact molecular mechanisms or pathways for reduced TLR-4 surface expression in CF are still unknown. We believe that reduced TLR-4 surface expression might be one of major contributor for chronic infections in CF.

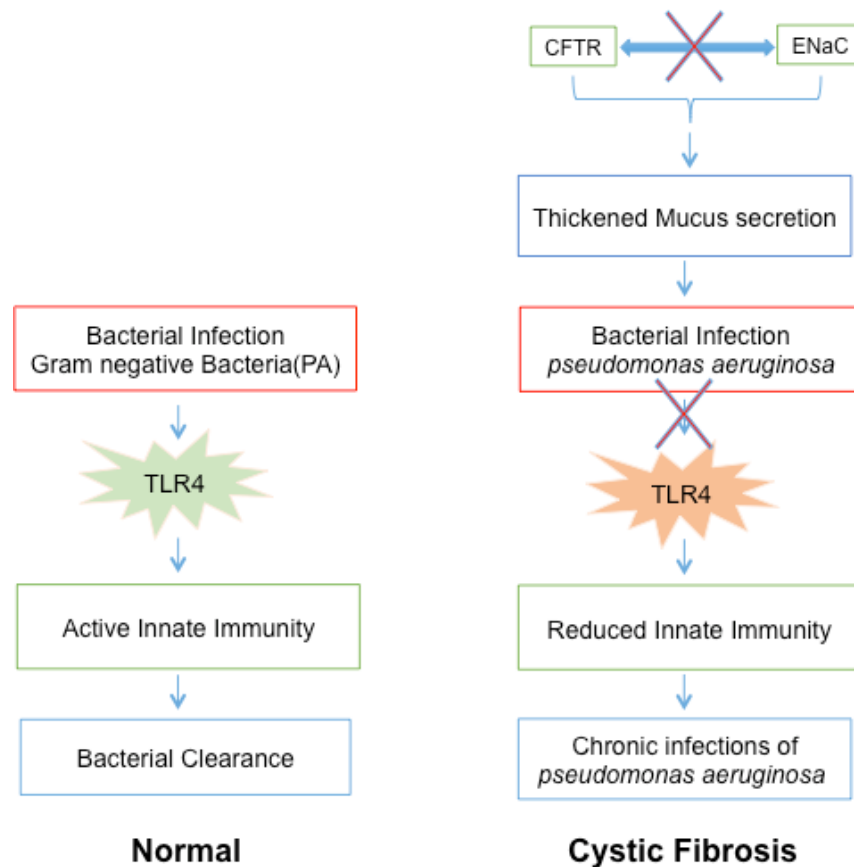


Figure 2: Defective CFTR and TLR-4 dysregulation in CF.

1.4 ENaC channel

The epithelial sodium channel (ENaC) or amiloride-sensitive sodium channel is a membrane-associated ion channel and plays role in transportation of Na⁺ ions in and out of the cells. It is expressed at the apical plasma membrane of epithelial cells in the urinary bladder, lung airway, colon, and ducts of salivary and sweat glands [41]. Trans-epithelial Na⁺ transport is carried out by Na⁺/K⁺-ATPase at the basolateral membrane of the epithelial cell by creating an electro-chemical gradient. This gradient provides the driving force for Na⁺ influx into the cell via ENaC, which mediates the transport of sodium ions (Na⁺) across the epithelium [42]. The movement of Na⁺ ions across the epithelium establishes the osmotic gradient and further accelerates the movement of water in the cells [43]. So, active trans-epithelial sodium transport plays an important role in maintaining the volume and the composition of epithelial lining fluid across the epithelial cell layer. ENaC has been shown to play a crucial role in the electrolyte balance and blood pressure regulation [44]. In 1986, Palmer and Frindt first identified the single ENaC channel. They studied single channel activity in the apical membrane of cortical collecting duct cells from rat kidneys using the patch-clamp technique. In 1993, Canessa et al. showed that ENaC consists of α , β and γ subunits in rat colon. Each subunit has two membrane-spanning domains with a large extracellular loop, intracellular N-terminal, and C-terminal. The activity of ENaC is regulated by many extrinsic and intrinsic factors. Extrinsic factors are hormone activation, mechanical stretch, and/or proteolytic cleavage. While, intrinsic factors include intracellular trafficking, ubiquitination, various kinases, sodium, and metabolic substrates. These factors affect the regulation of ENaC channel expression/synthesis, intracellular channel trafficking, and single-channel properties such as open probability (P_o) [45]. Amiloride is a potassium-sparing diuretic and is very well known to block the activity of ENaC [42].

Epithelial sodium channel plays a crucial role in maintaining lung fluid balance by transportation of Na⁺ ions across the lung epithelium. ENaC channel in the lungs,

alveolar type II cells and airways epithelial cells appear to be involved in the regulation of sodium transport [46]. In addition, the functional evidence from Hummler and colleagues demonstrated that genetically knocking out α ENaC in mice is associated with defective lung fluid clearance and results in the premature deaths of newborn mice [47]. In contrast, airway epithelial cells absorb Na^+ ions and actively secrete chloride/bicarbonate ions to maintain the volume of airways surface liquid (ASL) levels and composition. The airway surface liquid is composed of the peri-ciliary layer (PCL) and mucus layer which play important role in bacterial clearance. ENaC and CFTR channels regulate critical components of muco-ciliary clearance (MCC) such as PCL height, viscosity, and pH. Impaired MCC leads to chronic bacterial infections and exaggerated inflammatory responses in many diseases including CF and chronic obstructive pulmonary disease (COPD) (Fig.3).

It has been shown that amiloride-sensitive epithelial Na^+ ions are increased in CF airways epithelia, which might be due to defective CFTR in CF [48]. Loss of CFTR functions lead to dysregulated ENaC channel [49] and mutation in the β -subunit of ENaC is correlated to severe CF-like symptoms [50].

CFTR is a negative regulator of ENaC, although the exact mechanism of how CFTR regulates ENaC is still unknown. The idea that CF is a result of dysregulation of ion channels including CFTR and ENaC channels, which is associated with Na^+ ions hyperabsorption and Cl^- ions reduction. This further lead to the formation of contracted viscous surface liquid layer causing muco-ciliary transport defects, bacterial infections, inflammatory responses, and eventually lung failure. Several factors such as lipopolysaccharide, protein kinase C, reactive oxygen species (ROS) and hypoxic stress, are involved in regulation of ENaC activity [51]. ENaC-blocking is thought to facilitate restoration of the airway surface liquid volume and subsequently allow normal muco-ciliary clearance, which might be interesting therapy in the management of lung disease in CF patients [52].

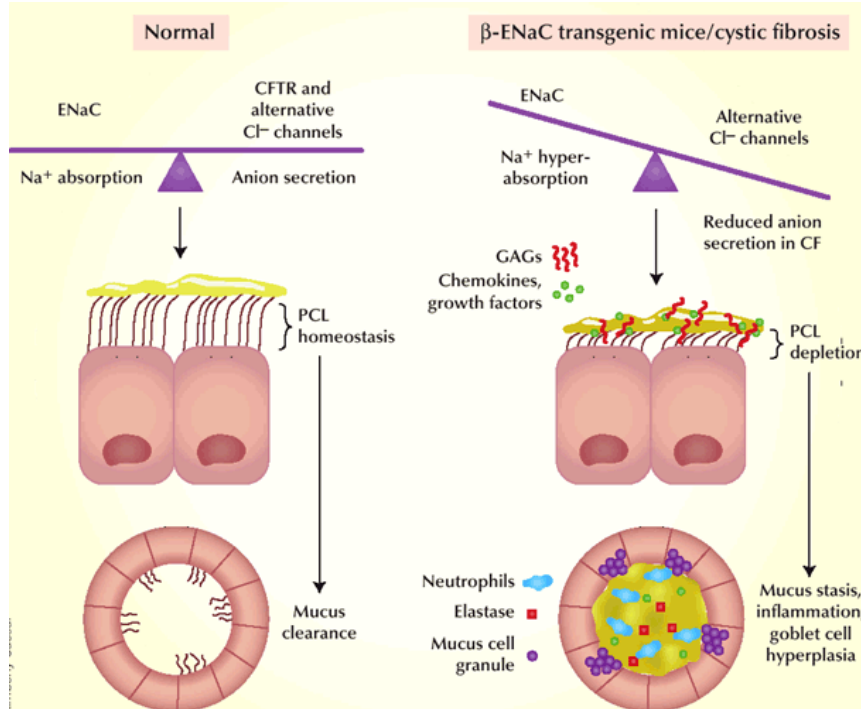


Figure 3: CFTR and ENaC regulation in CF [53]

Recent literature showed that transforming growth factor- β (TGF- β), a multifunctional cytokine, regulates the immune, inflammatory systems and downregulates ENaC channels in acute lung injury (ALI) [54]. It is also shown that microRNAs (miRNAs), a major class of gene expression regulator, is involved in ENaC regulation. miR-16 has been reported to downregulate ENaC channel through inhibition of serotonin transporter (SERT), which is involved in the 5-HT transmitter system and downregulate TGF- β in alveolar type II cells of ALI [55].

1.5 Transforming growth factor- β

TGF- β was first identified by Richard K. Assoian and his colleagues in 1983 [56]. It is derived from human platelets, hence known as platelet-derived TGF- β . It consists of two subunits of 12.5 kDa each, which are bound with disulfide bonds [56]. Up to date, several isoforms of TGF- β have been determined. It is considered as a multifunctional cytokine. Currently, TGF- β family consists of more than 60 structurally related members including five activins, eight bone morphogenic proteins (BMPs) and three TGF- β s [57]. These members play an important role in the regulation of multiple cellular functions, including cell proliferation, cellular differentiation, cell migration, organization, and apoptosis [58]. The three isoforms of TGF- β are TGF- β 1, 2 and 3, which contains around 40 different related proteins [59]. TGF- β is synthesized as a latent precursor molecule (LTGF- β), which consists of an amino-terminal hydrophobic signal peptide region, the latency associated peptide (LAP) region and the C-terminal potentially bioactive region. TGF- β related proteins are categorized into 2 subfamilies: TGF- β /activin/nodal subfamily and the bone morphogenetic protein (BMP)/growth/differentiation factor (GDF)/Muellerian inhibiting substance (MIS) subfamily [59]. These subfamilies play a diverse role in the regulation of cellular functions in embryonic development, tissue homeostasis, tissue repair remodeling as well as disease pathogenesis [60, 61].

In human lungs, TGF- β is expressed in multiple cells types such as airway epithelium, alveolar macrophages, endothelial and mesenchymal cells [62, 63]. TGF- β is secreted in a latent form, which complexes with two polypeptides, latent TGF-beta binding protein (LTBP) and latency-associated peptide (LAP). TGF- β signal transduction is initiated by binding of TGF- β to its serine/threonine kinase receptors namely, the type II (T β RII) and type I (T β RI) receptors on the cell membrane. Upon ligand binding, T β RII activates T β RI by phosphorylation of threonine and serine residues on T β RI. Further, the activated T β RI activates SMAD family messenger. SMAD family is the family of intracellular proteins,

which play important role in extracellular signaling for activation of TGF- β pathways. These are categorized in 3 different classes such as receptor-regulated SMADs (R-SMADs) which include SMAD1, SMAD2, SMAD3, SMAD5 and SMAD8/9 [64], common partner SMADs (Co-SMADs) which includes only SMAD4 [65] and inhibitory SMAD (I-SMAD) which includes SMAD6 and SMAD7 [66]. Activated T β RI phosphorylates the R-SMAD, SMAD2/3 which are coupled to co-SMAD SMAD4 to form a heterocomplex. These complexes enter the nucleus and regulate the target gene transcription. TGF- β receptors can also lead to ubiquitination-mediated degradation with the help of inhibitory SMADs. SMAD-7 acts as an inhibitor to block the phosphorylation of R-SMADs [67]. A schematic overview of TGF- β signaling is presented in Fig.4 adapted from [68].

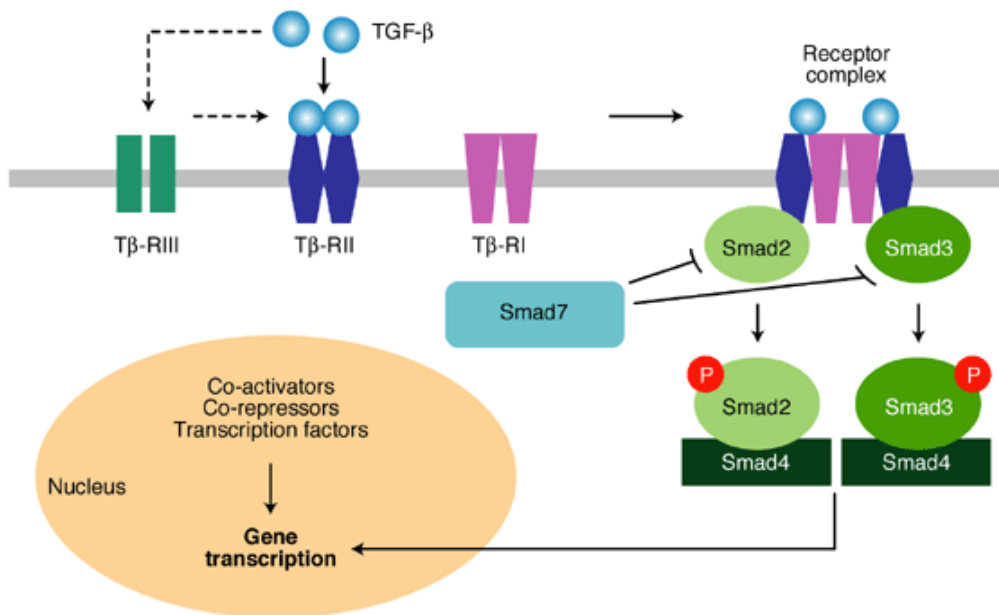


Figure 4: TGF- β signaling pathways [68]

TGF- β levels in plasma from CF patients were found to be elevated compared to controls [69]. Also, TGF- β levels were increased in bronchoalveolar lavage fluid (BAL) from children with CF and it was shown to be associated with neutrophilic inflammation with reduced lung function [70]. Further, TGF- β signaling is

significantly increased in lung tissue sections from CF patients [71]. Previous data also suggested the role of TGF- β in downregulation of CFTR channels in CF [72]. Contradictory to this, TGF- β is known as crucial ENaC channel blocker and shown to inhibit the ENaC channel in ALI [54, 55, 73].

1.6 microRNAs

miRNA is an epigenetic modification and novel approach towards understanding various gene expression in infections and diseases. The first miRNA (lin-4) was discovered in 1993 in *Caenorhabditis elegans*. Further, let-7 was discovered in human in 2000 [74]. Currently, there are 24,521 precursor miRNA expressing 30,424 mature miRNAs [75]. miRNA is small, non-coding single-stranded RNA, consisting of 19-25 nucleotides and has been shown to play role in gene regulation by transcription repression, which involves various biological processes such as, cellular differentiation, cell cycle regulation and metabolism [76-78]. MicroRNA is transcribed in the nucleus as distinct transcription unit by RNA polymerase II or III. It is then subjected to the formation of a long fragment of double-stranded hairpin structured RNA, which is called as primary miRNA (pri-miRNA). Then Drosha, a RNase type III enzyme and RNA-binding protein DGCR8 process the pri-miRNA to form ~60-100 nucleotide long hairpin-structured precursor miRNA (pre-miRNA). After pre-miRNA formation, exportin 5 and RAN-GTP export the pre-miRNA from the nucleus to cytoplasm. Dicer, which is RNase III endonuclease, processes pre-miRNA and leads to the formation of a 22 nucleotides double stranded RNA molecule called miRNA/miRNA duplex. Further, these duplex form a mature single stranded RNA which is incorporated into RNA-induced silencing complex (RISC) consisting of dicer, TRBP, and argonaute protein (Figure-5) [79]. Finally, This RISC complex identifies the target mRNA sequence, binds it and leads to gene silencing by transcription repression or degradation of target mRNA sequences.

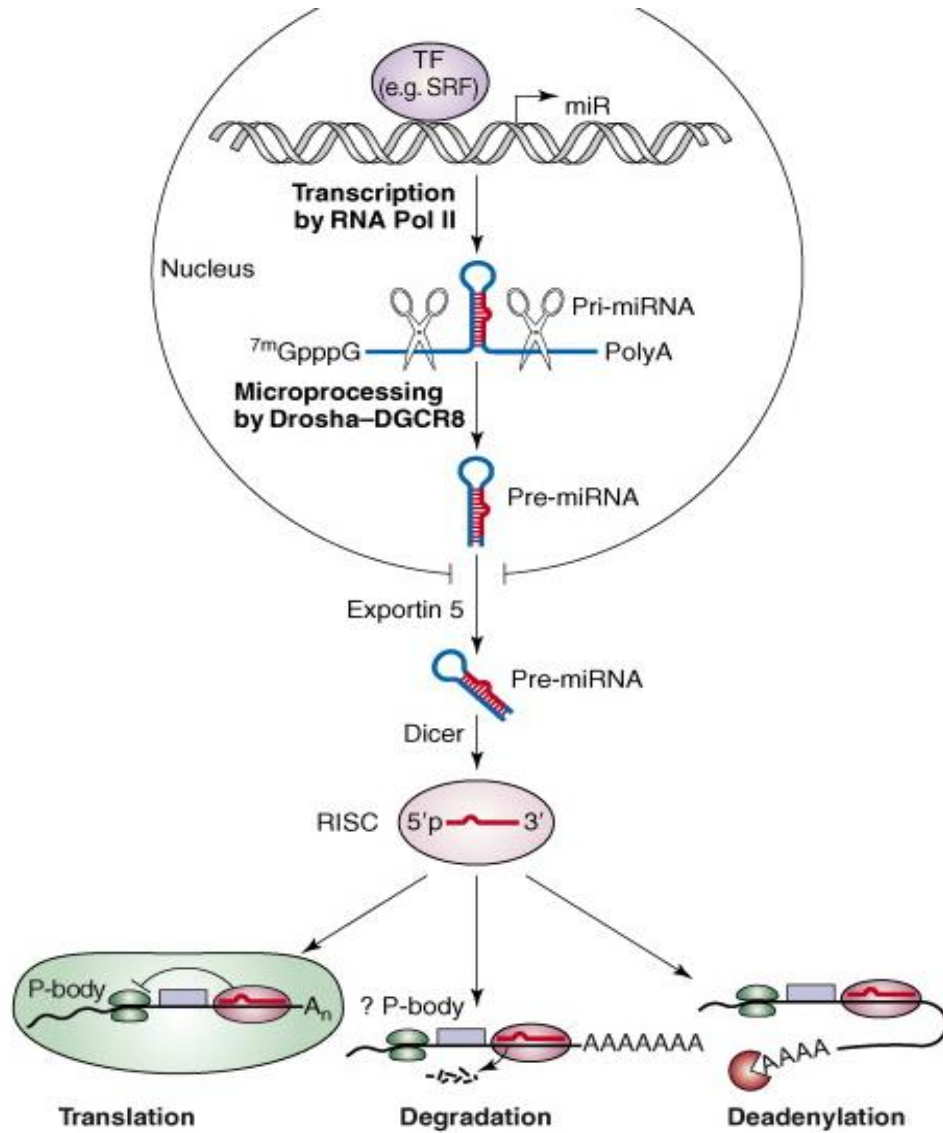


Figure 5: The formation and fate of a microRNA [80]

1.6.1 microRNAs in cystic fibrosis

Previously reported studies revealed the impacts of miRNAs on the development of lung diseases including chronic obstructive pulmonary disease (COPD), asthma, lung inflammation and cystic fibrosis [81]. Since defective CFTR and chronic inflammation are the major features of CF, miRNAs might play an important role in the regulation of CFTR, inflammation, innate immune response,

endoplasmic reticulum stress, lung cell development and differentiation. miRNAs could downregulate CFTR expression by binding to the 3'-UTR segment of the transcript, which was firstly shown by Gillen et al. in 2011 [82]. They identified 13 miRNAs, which could regulate CFTR expression in various cells lines. Further, miRNAs such as miR-145, miR-223, and miR-494 have been shown to be up-regulated in CF bronchial epithelial cells suggesting a role in repression of CFTR gene in cystic fibrosis bronchial epithelial cells (CFBE cells) [83]. Furthermore, the role of miR-101, miR-144, and miR-145 in downregulation of CFTR gene expression was confirmed in 16HBE14o- cell line and in primary human airway cells [84].

In response to innate immunity and inflammation, Oglesby and colleague performed first miRNAs profiling on bronchial brushing of CF patients. They identified 92 differential expressed miRNAs of which 56 were down-regulated and 36 were up-regulated. In this study, it was found that miR-126 was significantly reduced in lungs of patients with CF as compared to that of healthy controls, which is correlated with a significant up-regulation of TOM-1 mRNA.

Target of Myb protein-1 (TOM-1) acts as an anti-inflammatory agent by negatively regulating NF-kB, TLR-2, TLR-4, and IL-1 β induced signaling pathways in CFBE cells [85]. The second miRNA is miR-155, which was found to be up-regulated in lung epithelial cells and neutrophils from patients with CF and associated with activation of IL-8 dependent inflammation via PI3K/Akt signaling pathway. Further studies also confirmed that exposure of the anti-inflammatory cytokine IL-10 or following inhibition of IL-1 β signaling result into reduced levels of miR-155 with a reduction of IL-8 production [86].

As discussed earlier, defective CFTR leads to ENaC over-expression. Recently published data suggest the role of miRNAs in ENaC regulation. Studies by Tamarapu et al. demonstrated that miR-16 suppresses the expression of TGF- β , thereby indirectly leading to the up-regulation of ENaC expression in ALI [55]. As

TGF- β is known to inhibit the expression of ENaC [73], miR-16 seems to rescue F508del-CFTR function in native cystic fibrosis epithelial cells [87].

miRNAs can be used as therapeutics by 2 methods which include inhibition of miRNA by its artificially made complementary sequence also called as anti-oligonucleotide (anti-miR). When delivered to the cells, anti-miR binds to target miRNA and relieves inhibition of endogenous target genes. Sometimes it can also degrade the target miRNA. The second method is supplementation of miRNA in which artificially made miRNA also called as miRNA-mimic is used to suppress the expression of endogenous genes [88].

miRNA that targets IL-8 have the potential to decrease IL-8 expression and correct the over exuberant neutrophils influx in CF. In contrast, inhibition of miRNA such as miR-145, miR-223 and miR494 using anti-miR approach, aberrant CFTR expression might be corrected and chloride ion conductance can be restored. So, finding and targeting miRNAs can provide a newly emerging field in the regulation of innate immunity, inflammation, and correction of CFTR in CF. However, there are some challenges such as numerous molecular targets for miRNA, tissue-specific delivery, degradation by nucleases optimal chemistry and delivery systems have to be developed.

1.7 Iron homeostasis

Iron is a redox active metal which is essential for the normal function of a wide range of cellular proteins [89]. Iron shuttles between two oxidation states, Fe (II) (Fe^{2+} ; ferrous iron) and Fe (III) (Fe^{3+} ; ferric iron). Fe^{2+} is very aqua soluble and is transported across the membranes. However, Fe^{2+} is easily oxidized to the Fe^{3+} , which is highly insoluble at physiological pH. Many proteins bind iron in its Fe^{3+} form. Fe^{3+} is relatively non-toxic. However, Fe^{2+} is a potent pro-oxidant and free iron generates ROS via the Fenton or the Haber-Weiss reaction

rendering it into quite toxic form [90-92]. Cells of the lungs obtain their iron supplies from the plasma, where it is bound to the protein transferrin (Tf). Most of the iron delivered to cells is imported via transferrin receptor-1 (TfR-1), but may also be utilized by nonreceptor-mediated mechanisms [93, 94]. Intracellular iron is also supplied by hemoxygenase-1 (HO-1) via conversion of heme into the equal concentration of Fe^{2+} , carbon monoxide, and biliverdin. Intracellular iron is stored in a non-toxic form within ferritin [95]. Stored iron can be exported via the only known iron exporter ferroportin (FPN). Airway epithelial cells up-regulate FPN expression in the presence of iron, and FPN is thought to play a role in lung iron detoxification [96, 97]. Many proteins are involved in iron transport and regulation, such as divalent metal transporter-1 (DMT-1), hephestin, transferrin receptor-2 (TFR-2), ferroportin (FPN), hepcidin, duodenal cytochrome b (DCYTB), hemojuvelin (HJV) and heme carrier protein 1 (HCP1) [98]. Most proteins associated with iron metabolism are expressed in the lung and are likely to play important role in lung health and lung defense [99-102].

These iron-associated proteins are synthesized in the lung mainly by two types of cells, the airway epithelial cells and the alveolar macrophages (AM). Airway epithelial cells serve as the first line of defense in the upper airways against harmful environmental insults, including toxic heavy-metal-containing particles and very efficient in removing non-transferrin-bound iron, which converts it to less toxic protein-bound iron.

CF airways contain large amounts of iron and ferritin during acute exacerbations or non-acute form [103]. Moreau-Marquis and colleagues demonstrated that airway epithelial cells expressing ΔF508 -CFTR releases more iron into the extracellular medium than the cells expressing wild-type protein [104]. As discussed earlier, CF is involved in dysregulation of ion channels including ENaC channel, which is responsible for the transportation of Na^+ ions into the cell. Turi et al. suggested that epithelial transport of Na^+ ions into the cell is associated with transcellular movement of metals, particularly

iron [105]. Vice versa, iron itself can induce ENaC expression and amiloride-sensitive Na⁺ transport in fetal lung epithelial cells [106]. Supporting to this data Henke et. al. confirmed the increase of intracellular iron which further lead to impaired hypoxia-inducible factor-1 causing the downregulation of hemeoxygenase-1 expression in CF epithelial cells [107]. Downregulation of HO-1 is associated with iron accumulation in multiple cell types. Increased iron-mediated ROS might alter the microenvironment of airways epithelial cells in chronic CF, thereby leading to low partial pressure of oxygen inside the lungs and thus causing hypoxia [108, 109].

1.7.1 Hypoxia-inducible factor-1 α

HIF-1 α is a transcription factor, which is activated in response to hypoxia and is controlled at the protein level, through enzymes called prolyl hydroxylases (PHDs). This enzyme continuously targets HIF-1 α for proteasomal degradation [110]. Importantly, iron is required for activation of PHD, which play a crucial role in the degradation of HIF-1 α in normoxic condition [110]. It was shown that HIF-1 α expression is up-regulated via NF- κ B [111, 112] and TLR-4 [113]. Further, it was shown that HIF-1 α enhanced the expression of TLR-4 mRNA and protein. HIF-1 α mediated up-regulation of TLR-4 expression enhances the cellular response to LPS resulting in increased expression of IL-6 and interferon- γ -inducible protein-10 (IP-10) [114].

HIFs are major regulators of several genes involved in iron homeostasis and inflammation, which includes TfR-1, hemeoxygenase-1, natural resistance-associated macrophage protein-1 (Nramp-1), DMT-1, erythropoietin, and ferroportin [115].

1.7.2 Ferroportin

Ferroportin (FPN) is a transmembrane protein encoded by FERROPORTIN (SLC40A1), which transports iron from inside to outside of the cell. It is the only known iron exporter and plays a crucial role in maintaining iron homeostasis. Mutation or lack of ferroportin leads to iron accumulation, which further causes iron overload in the cells. The regulations of FPN can be carried out by transcriptional, post-transcriptional, and post-translational manner [116].

At transcription level factors like transition metals, heme, inflammatory cytokines and hypoxia have been shown to be involved in regulation of ferroportin. Iron-responsive element (IRE) at FPN mRNA is involved in post-transcription regulation [117]. Post-translational regulation of FPN is associated with the iron regulatory hormone hepcidin, which plays a crucial role in ferroportin internalization and degradation [116].

The ferroportin expression has been shown to be up-regulated in lung tissue from CF patients [118]. Up to date, the area of studies, which emphasize on the relation between FPN and CF has not been explored. It will be interesting to understand molecular pathways and its involvement in the altering iron homeostasis in CF.

1.8 Hypothesis and aims:

The reduced TLR-4 surface expression might be responsible for a reduced detection of gram-negative bacteria (for example *Pseudomonas aeruginosa*) and causing worsening of CF. Therefore, identifying the molecular mechanism and the factors involved in TLR-4 trafficking might assist to resolve the immune response in CF (Figure. 6).

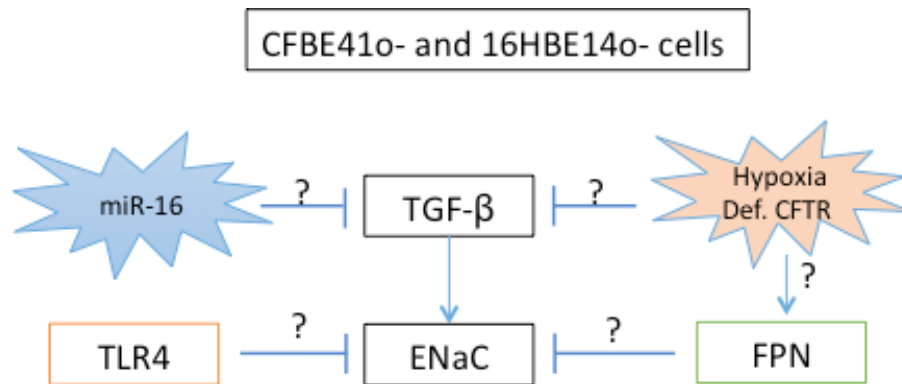


Figure 6: Schematic representation of factors which might involve in TLR-4 and ferroportin expression in CF.

Study goals based on the hypothesis:

1. To analyze expression of TGF- β and its regulating factors in CFBE41o- and 16HBE14o-cells.
2. The role of miR-16 in TGF- β regulation in CF.
3. To evaluate ferroportin expression and its regulating factors in CFBE41o- and 16HBE14o- cells.
4. To identify TGF- β mediated iron-related proteins (FPN) and TLR-4 expression in CFBE41o- and 16HBE14o- cells.
5. To investigate the effect of ENaC inhibition on FPN and TLR-4 expression in CFBE41o- and 16HBE14o-cells.

2 Materials and methods

2.1 Materials

2.1.1 Chemicals and biochemicals

Table 2: Chemicals and biochemicals

Reagents	Company
2,2'-dipyridyl	Sigma-Aldrich
Acetic acid	Carl Roth
Ammonium persulfate	Carl Roth
Bovine serum albumin 30% solution	PAA
β mercaptoethanol	Sigma, USA
Bromophenol blue	Carl Roth
BSA solution (2mg/mL) Bio-Rad, USA	Bio-Rad, USA
Chloroform	Carl Roth, Germany
Calcium chloride	Sigma-Aldrich
Clarity western ECL substrate	Bio-Rad
DAPI	Invitrogen, USA
DFO	Sigma, USA
Dimethyl sulfoxide	Sigma, USA
DNA ladder (100bp,1Kb)	Fermentas, Germany
D(+)-saccharose	Carl Roth
Developer	AGFA
EDTA	Carl Roth
EIPA	Sigma-Aldrich
Ethanol absolute	Sigma-Aldrich
Fluorescence mounting medium	Dako, Germany
Glycerol	Merck
Glycine	Carl Roth

MATERIALS AND METHODS

Hydrochloric acid 37%	Sigma-Aldrich
Iron (II) sulphate heptahydrate	Carl Roth
Isol-RNA lysis reagent	VWR
Isopropanol	Sigma-Aldrich
LPS from PA	Sigma-Aldrich
Lipofectamine 2000	Invitrogen, USA
Milk powder	Merck
Manual fixing bath	AGFA
Mercaptoethanol	Sigma-Aldrich
Methanol	Sigma-Aldrich
N,N,N',N'-tetramethyl-1,2-diaminomethane (TEMED)	Sigma, USA
Ponceau S solutionA	Sigma, US
Potassium dihydrogen phosphate	Carl Roth, Germany
Potassium phosphate monobasic	Carl Roth, Germany
PageRuler prestained protein ladder 10-170kDa	Thermo Scientific
PBS 1x	Gibco
Penicillin-streptomycin	Gibco
Pierce BCA protein assay reagent A	Thermo Scientific
Pierce BCA protein assay reagent B	Thermo Scientific
PMSF	Carl Roth
Primers	Eurofins
Rotiphorese® Gel 30	Carl Roth
SDS	Carl Roth
Sodium chloride	Sigma-Aldrich
Sodium hydroxide standard solution (4M)	Sigma-Aldrich
Supersignal west Femto maximum sensitivity chemiluminescent substrate	Pierce
SYBR® green PCR master mix	Life Technologies

TaqMan® fast advanced master mix	Life Technologies
TaqMan® microRNA RT kit	Life Technologies
TEMED	Sigma-Aldrich
Tris	Carl Roth
Triton-X-100	Sigma-Aldrich
Trypsin/EDTA(1x)	Gibco
Tryptone	Sigma-Aldrich
Tween® 20	Carl Roth
Western blotting luminol reagent	Bio-Rad
Xylol	Carl Roth, Germany

2.1.2 Instruments and software's

Table 3: *Instruments and Manufacturer*

Instrument	Manufacturer
AccuBlock™ digital dry baths	Labnet Internationals
Amersham hybon-p (PVDF transfer membrane)	GE Health Care
Analytical balance	John Morris Scientific
Autoclave	Systec
Centrifuge (table top)	Heraeus Instruments
Filtropur S 0.2 (sterile filters)	Sarstedt
Incubator	Heraeus Instruments
Infinite® 200 PRO	Tecan
Inkjet syringe (20 mL)	Braun
MicroAmp® fast optical 96-well reaction plate	Applied Biosystems
MicroAmp® optical adhesive film	Applied Biosystems
Mini-PROTEAN® tetra cell	Bio-Rad

Mini spin table centrifuge	Kobe
Nanodrop spectrophotometer	peQLab Biotechnology
PCR system	PE Applied Biosystems
PowerPac™ HC power supply system	Bio-Rad
Roller	Kobe
SevenCompact™ pH/ion	Mettler Toledo
Shaker	Kobe
Sonifier	Branson
Trans-blot SD system	Bio-Rad
ViiA™ 7 real-time PCR system	Applied Biosystems
Vortex-Genie 2	Scientific Industries
ImageJ	National Institutes of Health USA
Graph Pad Prism	GraphPad Software, La Jolla, USA
Leica application suite advanced fluorescence (LAS AF) software	Leica Mikrosysteme Vertrieb GmbH

2.1.3 Primary and secondary antibodies:

Table 4: *Antibodies and companies*

Antibody	Company
Immunoblotting	
Anti-goat immunoglobulins	Dako
Anti-HIF 1 α antibody	Life Span Biosciences
Anti-FPN antibody	Nivus Bio
Anti-FPN antibody	Santa Cruz Biotechnology
Anti-mouse immunoglobulins	Dako
Anti-rabbit immunoglobulins	Dako

Anti- TGF- β antibody	Santa Cruz Biotechnology
Anti-TLR-4 antibody	Abcam
Anti-TLR-4 antibody	Santa Cruz Biotechnology
Anti- β -actin antibody	Sigma-Aldrich
Immunofluorescence	
Donkey anti-rabbit 488 green alexafluor® 488	Invitrogen
Donkey anti-rabbit 594 green alexafluor® 594	Invitrogen
Donkey anti-rabbit 594 mouse alexafluor® 594	Invitrogen

2.1.4 Medium and serums

Table 5: Media and companies

Medium	Company
DMEM/HAM's F12 growth medium	Promocell
MEM with L-glutamine	Gibco
Opti-MEM	Gibco
Fetal calf serum	Gibco
Bovine serum albumin	Thermo Scientific, Rockford, IL, USA

2.1.5 Kits

Table 6: Kits and suppliers

Kits	Suppliers
cDNA reverse transcription kits	Applied Biosystems Carlsbad, CA

GeneAmp RNA PCR kit applied biosystems, carlsbad, CA	Applied Biosystems, Carlsbad, CA
Pierce BCA protein assay kit	Thermo Scientific, Rockford, IL, USA
Clarity™ western ECL blotting substrate	Bio-rad Germany
ZytoChem plus broad spectrum	Zytomed systems
DuoSet® ELISA development systems	R&D Systems, USA

2.1.6 Miscellaneous

Table 7: products and companies

Name	Company
6-well culture plate, sterile	Greiner Bio-One
12-well culture plate, sterile	Greiner Bio-One
Amersham hybon-p (PVDF transfer membrane)	GE Health Care
Cell scrapers 16cm 2-position blade	Sarstedt
Conical tubes	BD Falcon™
Culture slide 8-well	BD Falcon™
Deoxynucleotide set, 100mM	Sigma-Aldrich
Disposable cuvettes plastibrand®	Carl Roth
Dual-luciferase reporter assay system	Promega
Eppendorf pipettes	Eppendorf
Eppendorf safe-lock tubes	Eppendorf
Eppendorf phase-lock tubes	Eppendorf

Filtropur syringe filter 0.20µM sterile	Sarstedt
Nunc immunoplate F96 Maxi sorp nunc	Sigma-Aldrich
Parafilm	Pechiney
Pasteur pipette	Hirschman
Pipette tips	Tip-One
Röhren tubes	Sarstedt
Serological pipettes	Greiner Bio-One
Thermo Scientific CL-XPosure film	Pierce
Thin-walled PCR tubes 600µL	Stratagene
Tissue culture dish 100X20mm	Sarstedt
Whatman blotting paper	Whatman

2.1.7 Buffers and Solutions

2.1.7.1 1-Buffers for SDS-PAGE and Electrophoresis

Table 8: Buffers and Compositions

Buffers	Composition
Protein extraction (lysis buffer) Lysis buffer	50mM tris 150mM NaCl 5mM EDTA 1% triton-X-100 0.5% Na-deoxycholate 1mM PMSF (100mM PMSF stock)
Resolving gel buffer	1.125M tris HCl pH 8.8 30% saccharose volume make up to 100 mL

MATERIALS AND METHODS

Stacking gel buffer	0.625M tris HCl pH 6.8 volume make up to 250 mL
4X loading buffer	5g of SDS 25 mL stacking gel buffer 40 mL glycerol 0.005g Bromophenol blue Adjust the volume up to 100 mL with distilled water
Running buffer	30g tris 144g glycine 10g SDS
Transfer buffer	20mM tris 159mM glycine 20% MeOH
Blocking buffer	5% milk powder in 1xTBST
TBST washing buffer	0.5M NaCl 0.5M tris HCl pH 7.5 20g tween20 (after adjusting pH)

2.1.7.2 2 Buffers for immunofluorescence

Reagents	Composition
4% paraformaldehyde	4 g PFA dissolve in 100 mL PBS (add few drops of NaOH). Heat at 55°C until PFA is dissolved. Cool and adjust the pH to 6-7
0.1% saponin	
1% BSA	1g of BSA in 100mL PBS

2.1.7.3 3 Buffers for immunohistochemistry

Reagents	Composition
PBS	8 g NaCl 0.2 g KCl 1.44 g Na ₂ HPO ₄ 0.24 g KH ₂ PO ₄ Dissolve in 800 mL of dH ₂ O, adjust pH to 7.4 and add H ₂ O q.s. to 1 l
Antigen retrieval buffer	2.49 g of sodium citrate 800mL of H ₂ O and adjust the pH to 6 500 µL Triton-x-100 Add H ₂ O q.s to 1l

2.1.7.4 4 Buffers for ELISA

Reagents	Composition
Phosphate buffered saline (PBS)	137mM NaCl, 1.5mM KH ₂ PO ₄ , 8.1mM Na ₂ HPO ₄ ·2H ₂ O, 2.7mM KCl, diluted with distilled water to a final volume of 1 liter pH=7.4, 0.2µM filtered
Wash buffer	0.05% Tween 20 in PBS, pH=7.2-7.4
Block buffer	5% Tween 20 in PBS
Reagent diluent	1.4% delipidized BSA, 0.05 % Tween 20 in PBS pH=7.2-7.4, 0.2 µM filtered
Stop solution	2 N sulfuric acid

2.1.8 Primers of mRNA

Table 9: Primers and sequences

Genes	Tm	Sequence
FERROPORTIN	58.68	F-CTACTTGGGGAGATCGGATGT
SLC40A1	58.37	R-CTGGGCCACTTTAAGTCTAGC
α-ENaC	66.9 69.7	F-GGTGGACTGGAAGGACTGGAAGATCG R-ATGAAGTTGCCAGCGTGTCTCCTC
TGF-β	59.8 61.9	F-CCCAGCATCTGCAAAGCTC R-GTCAATGTACAGCTGCCGCA

2.1.9 Primers for miRNA

Table 10: miRNA primers and company

miRNA	Company
hsa-miR-16	Applied Biosystems

2.1.10 Cell lines

Table 11: cell lines

Cell line	Description
16HBE14o-	Human Bronchial epithelial cell line
CFBE41o-	Cystic Fibrosis Bronchial Epithelial cell line
corrCFBE41o-	Corrected Cystic Fibrosis Bronchial Epithelial cell line

2.2 Methods

2.2.1 Cell culture

Cystic fibrosis bronchial epithelial cell line (CFBE41o-), with homozygous DF508-CFTR, its isogenic wild-type CFTR-complemented counterpart (corrCFBE41o-) and normal human bronchial epithelial cell lines (16HBE14o-) were received from Dr. Dieter Gruenert.

Cells were sub-cultured on tissue culture plastic plate coated with a solution containing fibronectin (BD Biosciences, San Diego, CA) and grown in Minimum Essential Medium (MEM) with Earl's salts (Gibco, Karlsruhe, Germany), supplemented with 10% fetal calf serum (FCS; Gibco) and 1% Penicillin/Streptomycin (PAA, Pasching, Austria) at 37°C in 5% CO₂. Complemented CF airway epithelial cells (corrCFBE41o-) were cultivated in medium containing 200 mg/mL Hygromycin B (Invitrogen, Carlsbad, CA). The

cells were maintained in 10 cm² flasks at 37°C incubator. Upon confluence, cells were sub-cultured in a ratio of 1:3 or counted by using hemocytometer for spilled according to numbers of cells.

Cells were either treated with Transforming Growth Factor-β1 (TGF-β1) Human Recombinant Protein (EMD Millipore), Deferoxamine mesylate salt (DFO, Sigma-Aldrich) and 5-(N-Ethyl-N-isopropyl) amiloride (EIPA, Sigma-Aldrich). Controls were treated with PBS or respective vehicles. Cells were reversed transfected with miR-16 Mimics and anti-MiR 16 using, siPORT (Ambion).

2.2.2 RNA analysis

2.2.2.1 RNA isolation

RNA isolation was carried out to analyze mRNA expression and miRNA expression. Trizol method (VWR Germany) was used for the RNA isolation. Cells media was removed from the plate followed by PBS washing. 1mL of trizol was added to the plate and collected into 1.5 mL tube. Cell lysate with trizol was immediately frozen and stored in -80°C freezer until the further procedure.

Samples were thawed and 200uL ice-cold chloroform was added to each sample. Sample tubes were inverted 15-20 times and kept for 3 min at RT and centrifuged (pre-cooled) at 13000 rpm for 15 min at 4°. The upper aqueous phase (300-400μL) was transferred to a new tube and repeated the step one more time. Further, the upper aqueous phase was transferred to a new tube and 1μL of glycobblue and 500μL of pre-cooled isopropanol was added to each tube followed by gentle inverting for 3-5 times. Samples were stored in -80°C for overnight. Following day, the samples were centrifuged for RNA pelleting at 13,000 rpm for 30 min at 4°C. Supernatants were discarded and the blue colored pellet was washed twice with 1mL of 75% ice-cold ethanol and centrifuged at 10,000 rpm for 15 min at 4°C. All ethanol was removed and the pellets were left to air dry at 52°C. RNA was dissolved in 30μL of RNase free water. RNA

concentrations of samples were measured by using the Nano-Drop 2000c photometer (PeqLab).

2.2.2.2 cDNA synthesis

It is processed for the synthesis of single-stranded DNA (complementary DNA or cDNA) from RNA template by reverse transcription. After measuring RNA concentration, a volume equivalent to 1 µg of RNA was added to DNase free water to make a total of 15µL volume. A master mix of 5µL was prepared from High-Capacity cDNA Reverse Transcription Kits (Applied Biosystems) as follows:

Table 12: cDNA synthesis reaction mix

Reagents	Volume taken
10x PCR Buffer II	2µL
25x dNTPs	0.8µL
10X RT Random Primers	2µL
MultiScribe™ Reverse Transcriptase	1µL
RNase Inhibitor	1µL
ddH2O	3.2µL
Total	10 µL

The 10x PCR Buffer II need for the maintaining optimal pH and ionic strength for PCR amplification. The dNTPs include of dATP, dCTP, dGTP, and dTTP. Random Hexamer primers used as short oligodeoxyribonucleotides of random sequence, which annealed to random complementary sites on a target RNA to help for cDNA synthesis by reverse transcriptase. RNase Inhibitor (ribonuclease inhibitor) was used to prevent the degradation of RNA template by inhibiting the RNase activity. MultiScribe™ Reverse Transcriptase in the master mix was a recombinant RNA-dependent DNA polymerase for synthesizes a complementary

DNA (cDNA) strand. The reaction was carried out PCR cyclers (Bio-Rad) by following the steps in the program:

Table 13: PCR program for cDNA synthesis

Conditions	Step-1	Step-2	Step-3	Step-4
Temperature (°C)	25	37	85	4
Time (min)	10	120	5	∞

The cDNA was cooled down to 4 °C, and stored at -80°C.

2.2.2.3 Amplification of cDNA

Quantitative real-time PCR was performed using SYBR Green qPCR master mix (Applied Biosystems, Darmstadt, Germany) on a StepOnePlus™ 96 well Real-Time PCR System (Applied Biosystems, Carlsbad, CA). Generated cDNA was used as a template for amplification in q-PCR. β -actin was used as a reference housekeeping gene in all q-PCR reactions. Real-time PCR data were analyzed using the comparative cycle threshold (Cq: amplification cycle number) method. The amount of target gene was normalized to the housekeeping gene β actin (Δ Cq). Relative differences were determined using the equation 2 ($-\Delta\Delta$ Cq). Primers were generated using Primer 3 software. For PCR master mix, the following reagents were added to cDNA-Template 2 μ L to a total volume of 25 μ L:

Table 14: qPCR reaction mix for mRNA expression

Reagents	Volume taken (μ L)
SYBR Green Buffer	12
Primer forward	1
Primer reversed	1
dH ₂ O	4
cDNA template	2

Total	20
-------	----

SYBR Green buffer mix consists of pre-mixed SYBR green I fluorescent dye, magnesium ion, uracil-DNA glycosylase (UDG), proprietary stabilizers, and deoxyribonucleotide triphosphates (dNTPs) and Taq DNA polymerase. SYBR green I was a fluorescent dye that binds directly to double-stranded DNA (dsDNA). Primers were designed which were 20-22 base pairs long with 40-60% GC content and with 57 to 60°C melting temperature. A negative control was containing water instead of the template DNA. The PCR was performed in Step One plus PCR system using the following program:

Table 15: *qPCR program for mRNA expression analysis*

Cycle step	Temperature (°C)	Time	Cycles
Initial Denaturation	94	10 m	1
Denaturation	95	15 s	40
Annealing	60	1 m	
Extension	72	30 s	
Final extension	72	4 m	1

2.2.2.4 cDNA synthesis for miRNA expression

For miRNA expression analysis, RNA samples were diluted to the 2ng and the following PCR master mix was prepared to transcribe RNA into cDNA (Applied Biosystems® TaqMan® MicroRNA reverse transcription kit and TaqMan® MicroRNA assays)

Table 16: *miRNA RT- PCR master mix recipe for cDNA*

Component	Volume/reaction
100 mM dNTPs	0.15 µL
MultiScribe™ reverse transcriptase, 50 U/µL	1.00 µL
10x reverse transcription buffer	1.50 µL
RNase inhibitor, 20 U/µL	0.19 µL
Nuclease-free water	4.16 µL
Total volume	7.00 µL

In above master mix, 3 µL of 5x RT primer provided in the TaqMan® MicroRNA assay and 5 µL of 2ng RNA were added. All the components were mixed gently and centrifuged. The reaction was carried out PCR cycler (Bio-Rad) by following the steps in the program:

Table 17: *PCR program for cDNA for miRNA*

Conditions	Step-1	Step-2	Step-3	Step-4
Temperature (°C)	25	37	85	4
Time (min)	10	120	5	∞

2.2.2.5 Quantitative Real-Time PCR analyzes for miRNA profiling:

qRT PCR was performed on an Applied Biosystems® ViiA™ 7 System, a 7th generation real-time PCR system in a 96-well format. The qRT PCR was carried out by using the TaqMan® Fast Advanced Master Mix from Applied Biosystems® and the TaqMan® MicroRNA assay. RNU-48 was used as an endogenous control in both cDNA synthesis and qPCR for normalization

Next, the PCR master mix to conduct q-PCR was prepared as follows:

Table 18: *qPCR reaction mix for miRNA expression analyses*

Component	Volume
TaqMan® Fast Advanced Master Mix	10.00 µL
Nuclease-free water	7.50 µL
TaqMan® MicroRNA assay	1.00 µL
cDNA template	1.50 µL
Total volume	20.00 µL

All the samples were loaded in triplicates in the 96-well plate including the endogenous controls. No-template controls were also pipetted for verifying the contaminations and accuracy of the PCR. The plate was then briefly centrifuged, sealed with an adhesive film and loaded into the instrument. The experiment was set up in the ViiA™ 7 with setting up the specific parameter.

2.2.3 Protein expression analysis

2.2.3.1 Protein isolation from CFBE41o- and 16HBE14o-

Protein isolation from cells was carried out using lysis buffer (50 mM Tris, 100 mM NaCl, 5 mM EDTA, 1% Triton X-100, 0.5% Na-deoxycholate) containing proteases inhibitor (1 mM PMSF). The culture media was removed from the plate and further cells were washed 2 times with PBS. Immediately, 250µL of cell lysis buffer was directly added to Petri plate and each well of 6 well plates. After, cells were incubated at 4°C for 5-10 minute and scratched with cell scrapers and supernatants were collected in 2 mL Eppendorf tubes. Cell supernatant was sonicated for 30 seconds by sonicator to release of membrane-bound proteins. Further, supernatant used for protein quantification or stored at -80°C.

2.2.3.2 Protein quantification

Protein concentrations were determined with a bicinchoninic acid assay kit (Thermo Scientific, Dreieich, Germany). It is a biochemical assay for measuring the total concentration of protein in a solution which involving the reaction of protein with an alkaline copper in the solution. Further, BCA chelate with each Cu^+ ion and give rise to a purple-colored product, which absorbs light at a wavelength of 562 nm. Bovine serum albumin (BSA) with a different concentration in the range of 0.003-2000mg/mL was used as a standard. Protein lysates were pre-diluted in 1-10 dilution. 25 μL of protein sample and standards were pipetted in duplicated into 96 wells plate. Next 200 μL of BCA kit reagent solution A and B (50:1) was pipetted into each well of 96 wells plate. The reaction was incubated at 37°C for 30 min and the absorbance was measured at 562nm using a microplate reader (Tecan). Exact concentrations were measured by the standard curve in accordance with the standards. Then the volume of protein samples was calculated to reach 15 μg of total protein.

2.2.3.3 Sodium dodecyl sulfate-polyacrylamide gel electrophoresis (SDS-PAGE) and immunoblotting

SDS-PAGE is used to separate proteins in the samples as per their molecular weights by electrophoresis. Protein samples prepared for the gel electrophoresis by mixing 4X loading buffer at the ratio 3:1 and followed by denaturation at 95°C for 10 min. Gels were prepared depending upon the molecular weight of proteins.

Gel preparation

Gel Electrophoresis apparatus (Bio-Rad) used for the preparation of gels. The gel casting apparatus was assembled with the glass plates and spacers.

Resolving gel Component for 2 gels:

Table 19: Resolving gel preparation composition

Reagents	8%	12%
Rotiphorese Gel 30	2.655mL	4mL
Buffer B	3.33mL	3.33mL
10% SDS	100µL	100µL
Water	3.84mL	2.53mL
10 % APS	50µL	50µL
TEMED	10µL	10µL
Total	10 mL	10mL

All reagent mixed together with continuous stirring except the TEMED and 10 % APS. Prior to pouring the gel, 10% APS and TEMED were added and immediately poured in glass wells about 1.5 cm below the wells of the comb. Isopropanol was added on the top of gel solution to seal the gels to avoid oxygen getting in which inhibit polymerization. Further resolving gels were incubated for 45 min for solidification. After solidification isopropanol was removed. Then the stacking gel solution was poured on the top of resolving gel and comb were inserted immediately. Again, the gel was incubated for 35-40 min for polymerization.

Stacking gel Component for 2 gels:

Table 20: Stacking gel preparation composition

Reagent	Quantity taken
Rotiphorese Gel 30	655µL
Buffer C	1mL
10%SDS	50µL
Water	3.285mL
10 % APS	50µL
TEMED	5µL

Total	5mL
-------	-----

Further gels were set into the electrophoresis chamber filled with 1X running buffer. Proteins samples (15 μ g) were loaded carefully into each well of the gels and then 7 μ L of Protein ladder was loaded to compare the molecular weight of the proteins. Initially, gels were run at 100V until proteins reached to resolving gel and increased the volts up to 140V during migration through resolving gel for 1-2 hours. After separation of proteins on the gels, separated proteins were transferred to a PVDF-membrane by the wet transfer method. PVDF membrane was activated by methanol for 1 min followed by washing with water and then soak in transfer buffer. Cassette was prepared by loading up the sponge, Whatman filter, gels and membrane (presoaked in transfer buffer) in the following order:



Figure 7: Wet transfer

The transfer was carried out for 90 min at 100V in transfer buffer. The cooling pack was used to cool down the transfer buffer during transfer. After the transfer, membranes were removed and blocked in blocking buffer (5% non-fat milk in 1X TBST solution) for 2 hours at RT on the shaker. Further, the membrane was incubated with primary antibodies diluted in blocking buffer for overnight at 4°C.

Following day, membranes were washed 4 times with 1xTBST buffer for 15 min and subsequently incubated with secondary HRP-conjugated antibodies diluted in blocking buffer for 1hr at RT. After incubation, membranes were washed 4 times with 1x TBST for 15 min. HRP signal was detected by developing the membrane using ECL kit (Bio-Rad) detection reagents. 2 detection reagent mixed in 1:1 proportion which acts as a substrate for horseradish peroxidase (HRP) associated with the secondary antibody. Densitometric analysis of the immunoblots was calculated by image J software and value was normalized with β -actin.

2.2.3.4 Enzyme-linked immunosorbent assay (ELISA)

TGF- β is a multifunctional cytokine. It is known that most of the cytokine expressed in the supernatant of cells. In order to analyze the levels of TGF- β 1 and TGF- β 2, supernatants were collected from 5 different passages of CFBE41o- and 16HBE14o- cells. The TGF- β 1 and TGF- β 2 levels in the supernatants were measured by use of the TGF- β 1 and TGF- β 2 DuoSet Development Kits (R&D Systems, USA). Initially, TGF- β 1 and TGF- β 2 DuoSet Development Kit containing reagents were diluted as follows:

Table 21: Reagent preparation for ELISA

Reagents	TGF- β 1	TGF- β 2
Capture Antibody	360 μ g/mL of mouse anti-TGF- β 1 when reconstituted with 1 mL PBS	360 μ g/mL of mouse anti-TGF- β 2 after reconstitution with 1 mL PBS
Detection Antibody	54 μ g/mL of biotinylated chicken anti-human TGF- β 1 when reconstituted	27 μ g/mL of biotinylated goat anti-human TGF- β 2 when reconstituted with

MATERIALS AND METHODS

	with 1mL Reagent Diluent	1mL PBS
Standard	140 ng/mL of recombinant human TGF- β 1 when reconstituted with 0.5mL Reagent Diluent	70 ng/mL of recombinant human TGF- β 2 when reconstituted with 0.5 mL Reagent Diluent
Streptavidin-HRP	1.0 mL of streptavidin conjugated to horseradish-peroxidase	1 mL streptavidin conjugated to horseradish-peroxidase

Latent TGF- β 1 and TGF- β 2 activation were carried out by the addition of 3.5 μ L HCL on 100 μ L supernatant samples into each microcentrifuge tube. The samples were vortexed and incubated for 1 hour at 4°C or on the ice. Further, the samples were neutralized by addition of 7 μ L NaOH and 9 μ L HEPES.

Next, 100 μ L diluted Capture Antibody was pipetted in each well of the 96 wells plates and incubated overnight at 4°C. Following next day, each well was emptied and washed 3 times with 400 μ L wash buffer. 300 μ L block buffer was added to each well of the plate and incubated for 1hr at RT. Each well was emptied and washed 3 times with 400 μ L wash buffer. 100 μ L of Standard or sample or controls was added to respective wells of the plate and incubated for 2hrs at RT. Each well was emptied and washed 3 times with 400 μ L wash buffer. Further, 100 μ L diluted Detection Antibody was added to each well of the plate and incubated for 2 hours at RT. Each well was emptied and washed 3 times with 400 μ L wash buffer. After incubation, 100 μ L diluted Streptavidin-HRP was added into each well of the plate and incubated for 20 minutes at RT in the dark. Each well was emptied and washed 3 times with 400 μ L wash buffer 100 μ L TMB substrate was added to each well of the plate and incubated for 20 minutes at RT in the dark. The reaction was stopped by addition of 100 μ L Stop Solution into

each well of the plate. Optimal density was measured immediately at 570nm on a micro-plate reader.

2.2.3.5 Immunofluorescence:

It is cell imaging techniques, in which antibodies are used to label a specific target antigen with a fluorescent dye (also called as fluorophores). A chemically conjugated antibody with fluorophores allows visualization of the target distribution proteins on or in the cells.

Cells were grown and treated in BD falcon culture chamber slides. Cells were grown to 80–90% confluence, and further treated with TGF β (2ng/mL) for 9hr or EIPA (0.1, 1.0 and 10 μ M) for 4hrs. After treatment, media was removed and cells were washed twice with PBS (Gibco). Further cells were fixed by adding 4% paraformaldehyde (Sigma-Aldrich) on the cells for 15 min at room temperature. Cells were washed 3 times with PBS for 5 min each. Cells were incubated with 0.1% saponin (Sigma-Aldrich) for 10–15 min at room temperature for permeabilization. After, cells were again washed 3 times with PBS for 5 min. Cells were kept for blocking in 1% BSA for 30 min at room temperature, flowed by overnight incubation primary antibodies diluted in 1% BSA (1:200) at 4°C. The next day, cells were washed twice with PBS and incubated with secondary antibodies conjugated with appropriate fluorophores 488 or 555 (Alexa Fluor) diluted in 1% BSA (1:400) for 1hr at room temperature in dark. Followed by again PBS wash, chamber slides were detached from the glass slide, and nuclei were counterstained with mounting medium containing 4,6-diamidino-2-phenylindole (DAPI) before the mounting of the coverslip (VECTASHIELD Mounting Medium with DAPI). Slides were examined under Zeiss immunofluorescence microscope at 63X magnification.

2.2.4 Transfections

2.2.4.1 Transfection of miRNA mimics and inhibitor:

miRNA mimics and inhibitors were reverse transfected using the siPORT™ NeoFX™ transfection agent from Invitrogen™. Further cells were trypsinized and plated along with the transfection complex in 6-well culture plates. Negative controls each different for mimics and inhibitors were also transfected in another well. All the miRNA mimics, inhibitors, and negative controls were dissolved in the diluents provided by the manufacturer and further diluted to 10 μM working concentration. For negative control, a mock test was also performed in which the cells were treated with only the transfection reagent. Opti-MEM® I was used for the complex formation instead of serum-free medium. Then, in 2 Eppendorf cups each for miRNA inhibitor, miRNA mimic, miRNA inhibitor negative control, miRNA mimic negative control, and mock the components were mixed as follows:

Table 22: Reagent composition for miRNA transfection

	Components	Control	Mock	miRNA mimic/inhibitor
Tube A	Opti-MEM® I	-	47 μL	47 μL
	siPORT™ NeoFX™	-	3 μL	3 μL
Tube B	Construct	-	-	3 μL
	Opti-MEM® I	-	50 μL	47 μL
A + B mix		-	100 μL	100 μL
	Complete Medium	1,000μL	900 μL	900 μL
Total Medium		1,000μL	1,000μL	1,000μL

After mixing the described components, both tubes were incubated at room temperature for 15 min and mixed together. The further mixture was incubated at room temperature for 15 min. The cells were trypsinized prior to the start of complex formations and were dissolved in about 1mL MEM medium. After the complex formation, 80,000 cells/well along with the complete medium (900 μ L) and the complex (100 μ L) were plated to respective wells. The miRNA mimic or inhibitor effects were measured after 72 hours by western blotting to analyze specific protein regulation.

2.2.4.2 Transfection of TLR-4-yfp plasmid:

Transfection is the process of introducing foreign DNA or RNA into the eukaryotic cells. There are two important ways for transfection, which is Cationic lipid-mediated transfection and electroporation. In our experiments, lipofection was used as the method of transfection. It has positively charged surface, which interacts with negatively charged DNA and form lipid-DNA complex. Positive charged on liposome also allowing fusion of the liposome/nucleic acid transfection complex with the negatively charged cell membrane. Further, this transfection complex uptake is carried out by endocytosis.

CFBE41o- and 16HBE14o- cells were cultured until 60–70% confluence in BD falcon culture chamber slides and treated with EIPA (10 μ M) for 4 hrs. Further cells were transfected using transfection reagent lipofectamine with 1 μ g of reporter plasmids of TLR-4-YFP. 2 μ g of TLR-4-YFP plasmid and Lipofectamine 2000 transfection reagent (Invitrogen Carlsbad CA) were incubated separately in Opti-MEM (Gibco, Life Technologies) for 5 min and mixed together. The mixture was incubated for 20 min at room temperature. The further pre-incubated mixture was diluted with serum and antibiotic-free DMEM medium at the ratio of 1:1 and added dropwise to the cells. After 4hrs of transfection, cells medium was replaced with DMEM supplemented with antibiotics and incubated for 24hrs. Next

day, cells were fixed in 4% paraformaldehyde (Sigma-Aldrich) for 15 min at room temperature and washed twice with PBS. Mounting medium containing 4,6-diamidino-2-phenylindole (DAPI) used for counterstained the nuclei and mounting the coverslip. TLR-4-yfp signals were captured in Zeiss immunofluorescence microscope at 63X magnification.

2.2.5 Statistical analysis

Data are presented as means \pm SEMs and was given unless stated otherwise. Statistical analysis was performed using student's unpaired t-test for comparison of two groups and one-way ANOVA following Bonferroni post-test was used for multiple comparison studies with more than two groups. Prism 5 and Image-J was used to analyze the statistical data.

3 Results

3.1 TGF- β expression in CFBE41o- and 16HBE14o- cells

The transforming growth factor beta (TGF- β) not only controls proliferation and cellular differentiation also acts as a multifunctional cytokine, which exhibits immunosuppressive capacity.

TGF- β is elevated in bronchoalveolar lavage fluid from children with CF and in lung tissue sections from the CF patients [119]. Despite previously reported the elevated level of TGF- β in CF [69-71], expression of TGF- β was not studied in delta F508 mutation in CFTR gene (CFBE41o-) and normal human bronchial epithelial cells (16HBE14o-). So, we were interested in analyzing TGF- β expression in bronchial epithelial cells with a defective deltaF508 mutation in CFTR gene (CFBE41o-) and normal human bronchial epithelial cells (16HBE14o-) cells.

3.1.1 mRNA expression of TGF- β by q-PCR

To test the TGF- β levels, we analyzed mRNA expression of TGF- β in CF and normal epithelial cells by q-PCR. RNA extracted from CFBE41o- and 16HBE14o- cells, reverse-transcribed complementary DNA (cDNA) amplified by quantitative real-time PCR (q-PCR). We noticed a significant downregulation of TGF- β at mRNA level in CFBE41o- cells (* $p < 0.05$ and ** $p < 0.01$) compared to that of 16HBE14o- cells (Fig. 8).

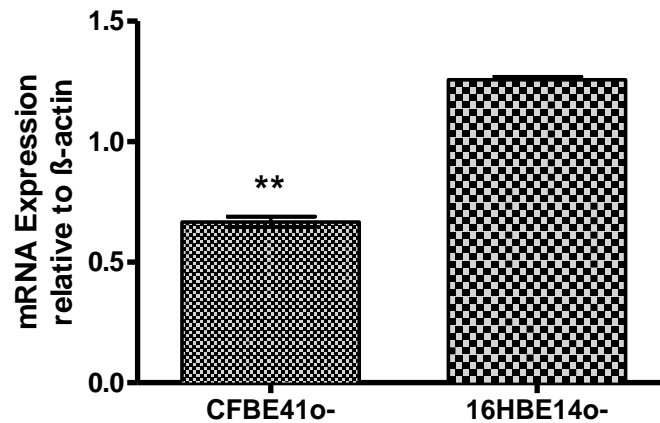


Figure 8: Relative mRNA expression of TGF- β in CFBE41o- vs. 16HBE14o- cells. Data presented are mean \pm SEM and asterisks indicate statistical significance determined by student's t-test (* p <0.05 and ** p <0.01). The experiments were repeated three times ($n=3$).

3.1.2 Protein expression of TGF- β by immunoblotting

Further, we analyzed protein expression of TGF- β in cell lysate of CF and normal epithelial cells by immunoblotting. At the protein level, we also noticed a significant downregulation of TGF- β in CFBE41o- cells (* p <0.05) compared to 16HBE14o- cells (Fig. 9A and 9B). β actin was used as loading control and served as the standard for densitometry analysis.

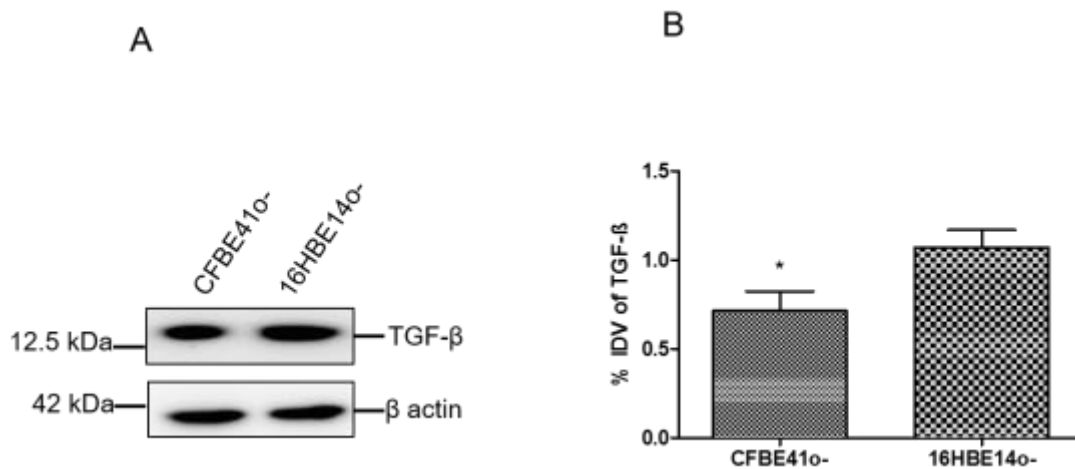


Figure 9: A) Representative immunoblotting for levels of TGF- β in cell lysate of CFBE410⁻ and 16HBE140⁻ cells. The molecular size of each protein is indicated on the right. (B) Densitometry analysis of immunoblotting for TGF- β . TGF- β -to- β -actin ratio was calculated and is represented as bar graphs. Data represent means \pm SEM and asterisks indicate statistical significance determined by Student's *t*-test ($*p < 0.05$, 16HBE140⁻ vs. CFBE410⁻ cells). IDV, intensity density values ($n=5$).

3.1.3 Level of TGF- β by ELISA

TGF- β is multifunction cytokine and plays an important role in regulating the immune system [120]. Cytokines often circulate as proteins bound to soluble receptors, carrier proteins, or inhibitors, which can be easy to detect by enzyme-linked immunosorbent assay (ELISA) [121]. To analyze the level of TGF- β in cells media supernatant, ELISA was performed in cell culture supernatant of CFBE410⁻ and 16HBE140⁻ cells. Relative to mRNA expression the protein levels of TGF- β 1 and TGF- β 2 were found less expressed in the medium supernatant of CFBE410⁻ compared to 16HBE140⁻ cells, but the differences were not significant (Fig. 10).

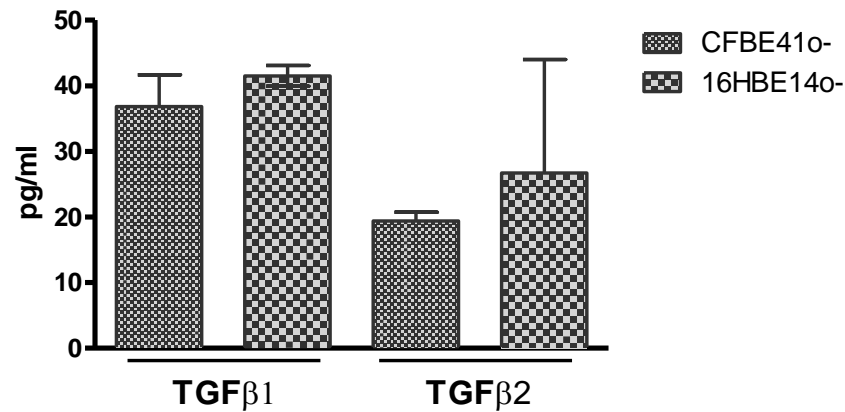
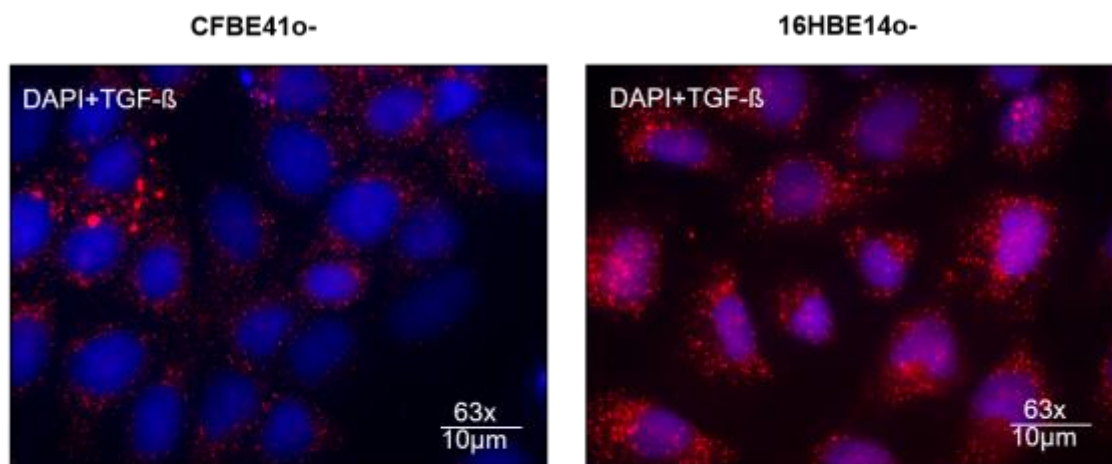


Figure 10: ELISA in CFBE41o- and 16HBE14o- assessed secretion of TGF-β1 and TGF-β2 cells supernatant (n=5).

3.1.4 Expression of TGF-β by immunofluorescence

To confirm the expression of TGF-β *in vitro*, immunofluorescence experiments were performed in CFBE41o- and 16HBE14o- cells. TGF-β signals were less in CFBE41o- cells whereas intense signals were observed in 16HBE14o- cells (Fig.11). The results obtained indicate the decrease in TGF-β expression in CFBE41o- compared to that of 16HBE14o- cells. This further supports our previous results and confirmed decreased TGF-β expression in CFBE41o- cells.



Dapi-Blue, TGF-β- Red

Figure 11: Immunofluorescence analysis of TGF- β expression in CFBE41o- and 16HBE14o- cells. Representative images from immunofluorescence were using an antibody against TGF- β (Dilution1: 400). Red: TGF- β positive stain, Nuclei is stained with DAPI (blue) ($n=3$), Scale bar: 10 μ m.

3.1.5 TGF- β expression in corrCFBE41o- cells

CF is caused by defective CFTR, which might be responsible for alteration of many genes. So, it was crucial to investigate whether defective CFTR might involve in downregulation of TGF- β . To confirm CFTR involvement in TGF- β expression immunoblotting was performed in the cell lysate of corrected (corr) CFBE41o- cell and compared with CFBE41o- and 16HBE14o- cells. (corrCFBE41o- cell line is CFBE41o-isogenic wild-type CFTR-complemented counterpart).

As shown before TGF- β expression is reduced in CFBE41o- cells as compare to the normal 16HBE14o- cells. When compared TGF- β expression in CFBE41o- cells and corrCFBE41o- cells, it was observed that TGF- β expression was slightly increased in corrCFBE41o- cell as compared to CFBE41o- cells but differences were not significant (Fig. 12A and 12B). Corrected CFTR increased the expression of TGF- β protein expression, suggesting that, defective CFTR might be associated with downregulation of TGF- β in cystic fibrosis. Taken together, these results confirmed that TGF- β expression is downregulated in CFBE41o- as compare to 16HBE14o- cells.

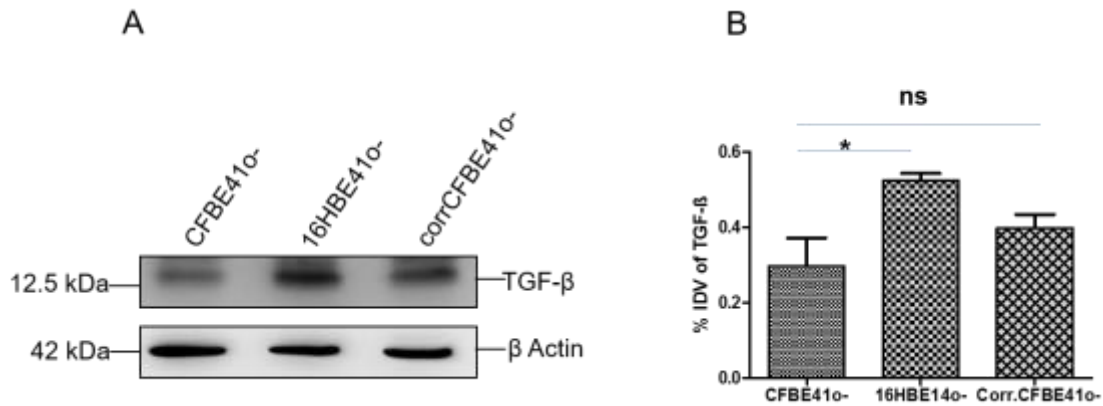


Figure 12: A) Representative immunoblotting for levels of TGF- β in cell lysate of CFBE41o⁻ and 16HBE14o⁻ cells and corrCFBE41o⁻ cells. β -actin was used as loading control. The molecular size of each protein is indicated on the right. B) Densitometry analysis of immunoblotting for TGF- β , relative to β -actin. CFBE41o⁻ versus corrCFBE41o⁻ cells. Data presented are mean \pm SEM (* p <0.05, student's t -test, ns-non-significance). The experiments were repeated thrice ($n=3$).

3.2 miRNA-16 dependent TGF- β expression

Various studies have been shown that the expression of ENaC is elevated in the respiratory epithelial cells in cystic fibrosis [122]. One such miRNA regulating the ENaC expression by down-regulating TGF- β is miR-16. A Recent study reported that miR-16 modulates the ENaC channel through downregulation of TGF- β in ALI [55]. We were interested in miR-16 regulation and its effect on TGF- β expression in CF cells.

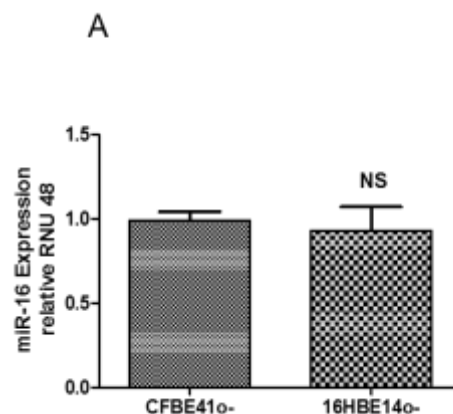
3.2.1 miR-16 expression

To determine whether the expression of miR-16 was altered in CF, quantitative real-time PCR (qPCR) on RNA lysates from CFBE41o⁻ and 16HBE14o⁻ cells

was performed. Results obtained showed that miR-16 was expressed similarly CFBE41o- and 16HBE14o- cell lines (Fig.13A).

3.2.2 TGF- β expression upon miR-16 mimic and anti-miR-16 transfection in 16HBE14o- cells and CFBE41o- cells

Although there was no elevated level of miR-16, TGF- β expression regulated by miR-16 was examined in CF cell lines. Therefore, to find the association between miR-16 and TGF- β , 16HBE14o- cells were transfected with miR-16 mimics to increase miR-16 expression and anti-miR-16 were transfected in CFBE41o- cells to block miR-16 expression. After transfection, immunoblotting was performed on cell lysate to analyze the TGF- β expression. β actin used as loading control and served as the standard for densitometry analysis. Over-expression of *miR-16* led to a reduction of TGF- β expression 16HBE14o- cells (Fig. 13B and 13C). Blocking of *miR-16* led to increasing of TGF- β expression in CFBE41o- cells (Fig. 13D and 13E). Collectively, these data suggested that miR-16 play role in TGF- β regulation, which might contribute to developing a new therapeutic approach in CF.



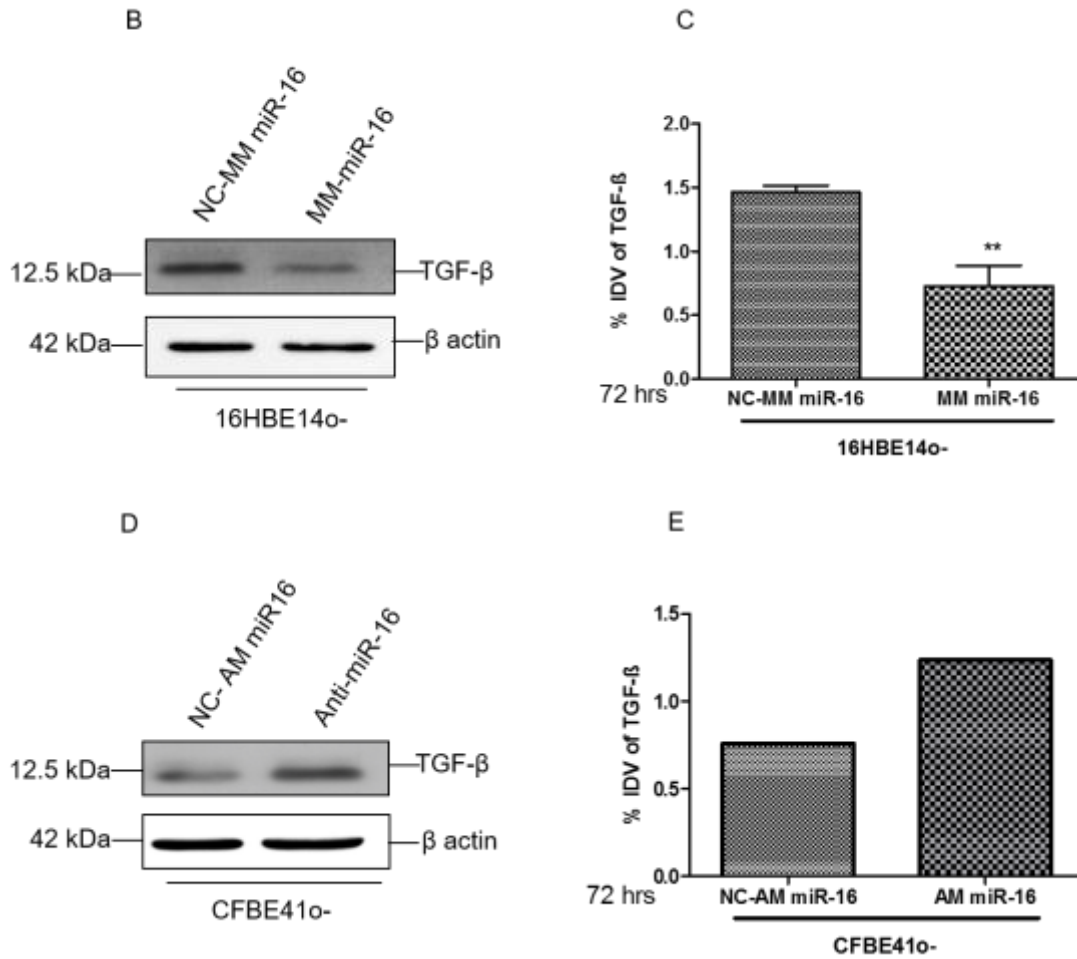


Figure 13: A) Relative miR-16 expression in CFBE41o- compared 16HBE14o- cells. RNU-48 was used for normalization. Cells were transfected with miR-16 mimic and anti-miR-16 for 72 hours and harvested for protein analysis. Untreated cells were taken as negative control. B) Representative immunoblot of TGF-β at protein levels in cell lysate of 16HBE14o- cells after transfection of mimic miR-16. β-actin was used as loading control. The size of each band is indicated on the right. C) Densitometry analysis of immunoblot for TGF-β, * $p < 0.05$, student's *t*-test, Transfected 16HBE14o- vs. non-transfected 16HBE14o- cells. Data are presented as mean \pm SEM ($n=5$). D) Representative immunoblot of TGF-β at protein levels in cell lysate of CFBE41o- cells after transfection of anti-miR-16. β-actin was used as loading control. The molecular size of each protein is indicated on the right. E) Densitometry analysis of immunoblot for TGF-β, Transfected CFBE41o- vs. non-transfected CFBE41o- cells ($n=1$).

3.3 Hypoxia stabilization associated TGF- β expression

We have previously demonstrated that altered iron homeostasis leads to hypoxia in cystic fibrosis [107]. This leads to HIF-1 α destabilization in cystic fibrosis. Previous studies reported by other groups suggest that the hypoxia increases the expression of TGF- β , which is regulated by its transcription factor, hypoxia response element (HRE) [123]. To confirm, impaired HIF-1 α in CF might be responsible for TGF- β downregulation, the expression of TGF- β under hypoxic condition (0.1% O₂) to stabilize the HIF-1 α in CFBE41o- and 16HBE14o- cells was analyzed. The immunoblotting analysis revealed a two-fold increase of TGF- β in 16HBE14o- cells. On the contrary, TGF- β expression was reduced in CFBE41o- under hypoxia (Fig. 14A and 14B). This might be due to HIF-1 α destabilization in CF cells since oxygen deprivation might also increase free radicals, damage DNA, and causes cell death [124].

Since hypoxic condition seems to fail in the stabilization of HIF-1 α and showed reduced TGF- β expression in CFBE41o- cells. To analyze this hypothesis a known hypoxia mimic agent Deferoxamine (DFO) was used. Deferoxamine is a hypoxia-mimetic agent which artificially induces hypoxia by blocking the degradation of HIF-1 α [125]. CFBE41o- and 16HBE14o- cells were treated with 100 μ M/mL of deferoxamine (DFO) for 30 minutes, 1, 2 and 4 hours).

Results obtained from immunoblotting revealed a time-dependent increase in TGF- β expression upon DFO in CFBE41o- and 16HBE14o- lines (Fig. 14C). Densitometry analysis of 3 biological repeats also showed slight increased TGF- β expression in CFBE41o- and no significant difference in 16HBE14o- cells (Fig. 14D). Hence, hypoxia in CFBE41o- cells might be responsible for downregulation of TGF- β .

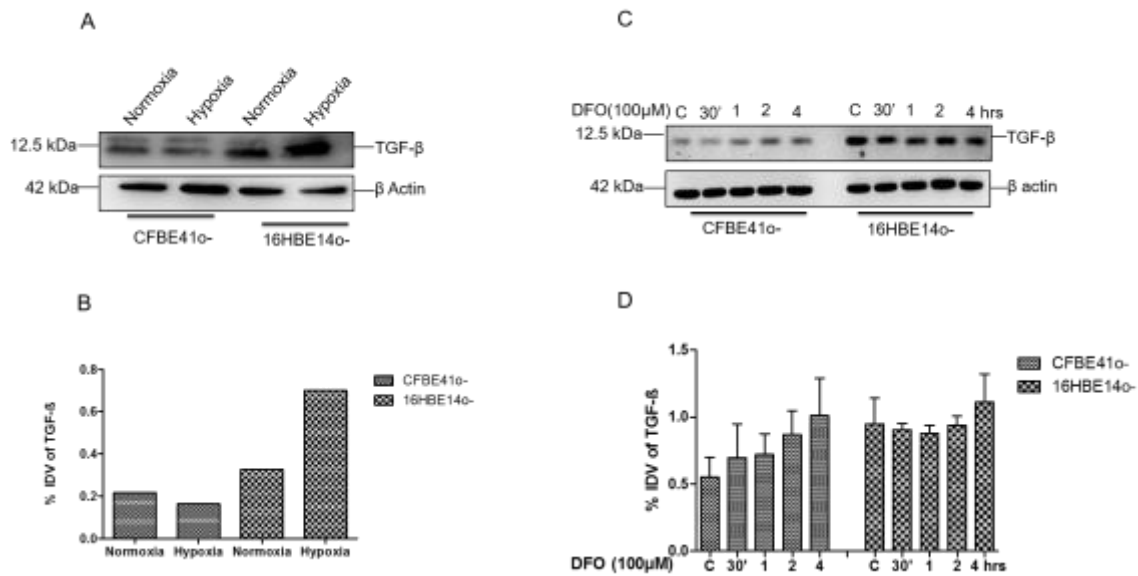


Figure 14: A) Representative immunoblot for levels of TGF-β in cell lysate of hypoxic condition (0.1% O₂) for 24 hours in CFBE41o- and 16HBE14o- cells. β-actin was used as loading control. The molecular size of each protein is indicated on the right. B) Densitometry analysis of immunoblotting for TGF-β, Normoxic condition served as a control of each cell line. Normoxic conditions were compared with the hypoxic condition in both 16HBE14o- and CFBE41o- cells. C) Representative immunoblotting for levels of TGF-β in cell lysate of DFO (100μM) at 30 minutes, 1, 2 and 4 hours. in CFBE41o- and 16HBE14o- cells. β-actin was used as loading control. The molecular size of each protein is indicated on the right. D) Densitometry analysis of immunoblotting for TGF-β, non-treated cells served as a control of each cell line. 16HBE14o- vs. CFBE41o- cells. Data are presented as mean ± SEM. The experiments were repeated 3 times (n=3).

3.4 Decreased expression of ferroportin in CF

Turi et al. 2008 showed that overexpression of ENaC leads to the higher import of Na⁺ ions and subsequent iron bypass into the cells thereby increasing the iron concentration [105]. This supports the published studies in Chillappagari et al. regarding the increased iron concentration and hypoxia in Cystic fibrosis [107]. It is known that ferroportin is an iron exporter, which up-regulate in the presence of

excess intracellular iron levels and involved in iron detoxification in the lung. To confirm the Ferroportin regulation in CF, Expression of ferroportin was analyzed in CFBE41o- and 16HBE14o- cells.

3.4.1 mRNA expression of ferroportin by q-PCR

Ferroportin levels were studied by analyzing mRNA expression of ferroportin in CFBE41o- and 16HBE14o- cells by using q-PCR. cDNA was synthesized from RNA extracted from CFBE41o- and 16HBE14o- cells and amplified by q-PCR. q-PCR results showed a significant downregulation of TGF- β at mRNA level in CFBE41o- cells (* $p < 0.05$ and ** $p < 0.01$) compared to that of 16HBE14o- cells (Fig. 15)

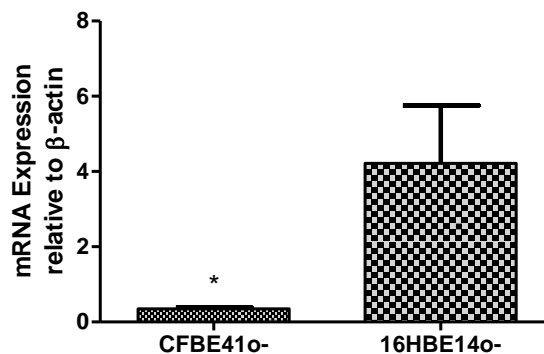


Figure 15: Relative mRNA expression of Ferroportin in CFBE41o- compared 16HBE14o- cells. Data presented are mean \pm SEM and asterisks indicate statistical significance determined by student's t-test (* $p < 0.05$ and ** $p < 0.01$). The experiments were repeated 3 times ($n=3$).

3.4.2 Protein expression of ferroportin by western blot

Further, protein expression of ferroportin was analyzed in cell lysate of CFBE41o- and 16HBE14o- by using immunoblotting. At the protein level, a significant downregulation of ferroportin was observed in CFBE41o- cells

(* $p < 0.05$) compared to 16HBE14o- cells (Fig. 16A and 16B), β actin used as loading control and served as the standard for densitometry analysis.

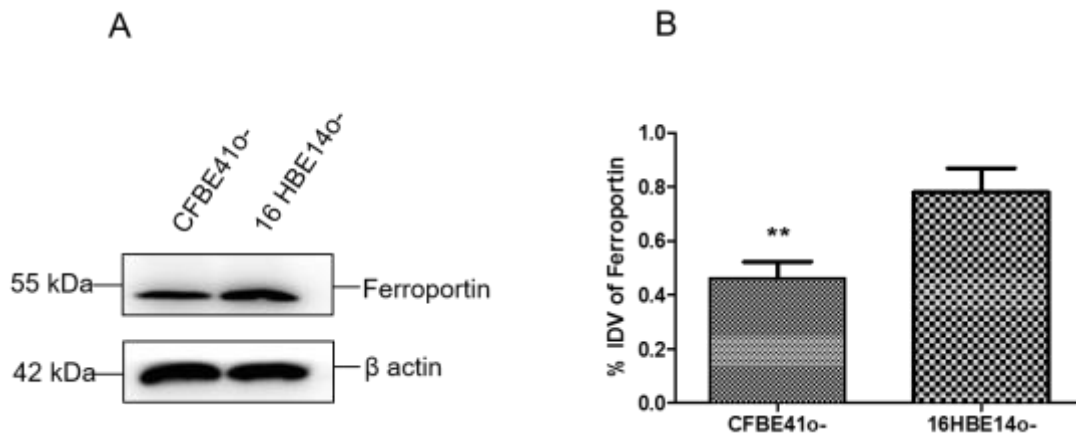


Figure 16: A) Representative immunoblot for expression of ferroportin in cell lysate of CFBE41o- and 16HBE14o- cells. The size of each band is indicated on the right. B) Densitometry analysis of immunoblotting for ferroportin. Data represent means \pm SEM and asterisks indicate statistical significance determined by Student's t-test (* $p < 0.05$, 16HBE14o- vs. CFBE41o- cells). The experiments were repeated 5 times ($n=5$).

3.4.3 Expression of ferroportin by immunofluorescence

To confirm the expression of ferroportin *in vitro*, immunofluorescence experiments were performed in CFBE41o- and 16HBE14o- cells. Ferroportin signals were reduced in CFBE41o- cells whereas intense signals were detected in 16HBE14o- cells (Fig.17). The results obtained indicate the decrease of ferroportin expression in CFBE41o- as compared to that of 16HBE14o- cells. This further confirmed the decreased ferroportin expression in CFBE41o- cells.

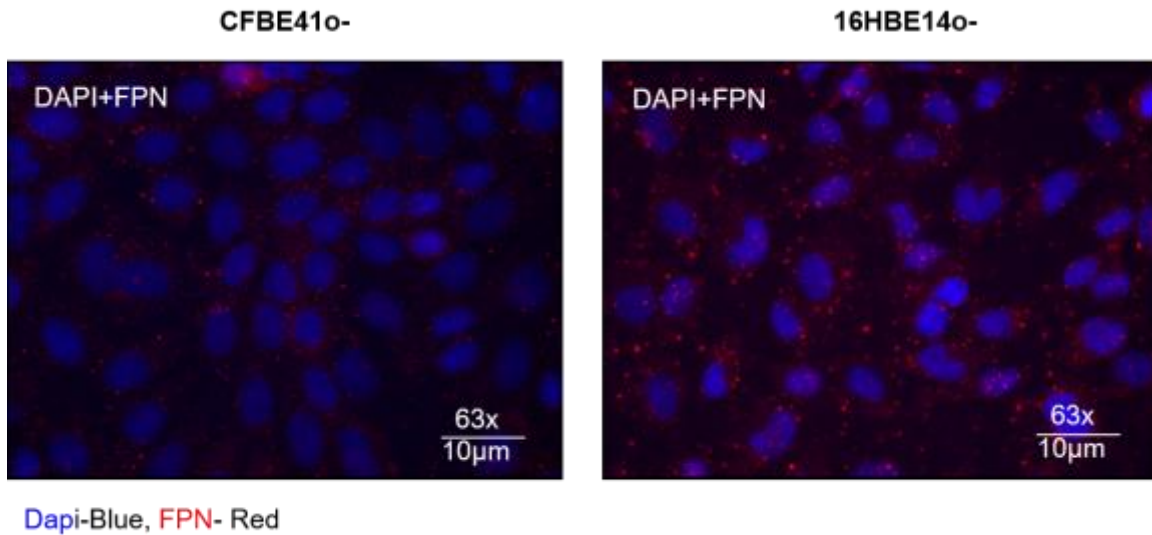


Figure 17: Immunofluorescence analysis of ferroportin expression in CFBE41o- and 16HBE14o- cells. Representative images from immunofluorescence were using an antibody against ferroportin (Dilution 1:400). Red: TGF- β positive stain, nuclei are stained with DAPI (blue). The experiments were repeated 3 times ($n=3$), Scale bar: 10 μ m.

3.4.4 Ferroportin expression in corrCFBE41o- cells

To verify the decrease of ferroportin in CFBE41o- cells, we analyzed the ferroportin expression in corrCFBE41o- cell line and compared with CFBE41o- and 16HBE14o- cells. Previous results showed that ferroportin expression is reduced in CFBE41o- cells as compared to that of normal 16HBE14o- cells. Further, comparative study of ferroportin expression in CFBE41o- cells and corrCFBE41o- cells revealed that ferroportin expression was significantly increased in corrCFBE41o- cell than CFBE41o- cells (Fig. 18A and 18B). Therefore, defective CFTR might also be associated with downregulation of ferroportin in CF.

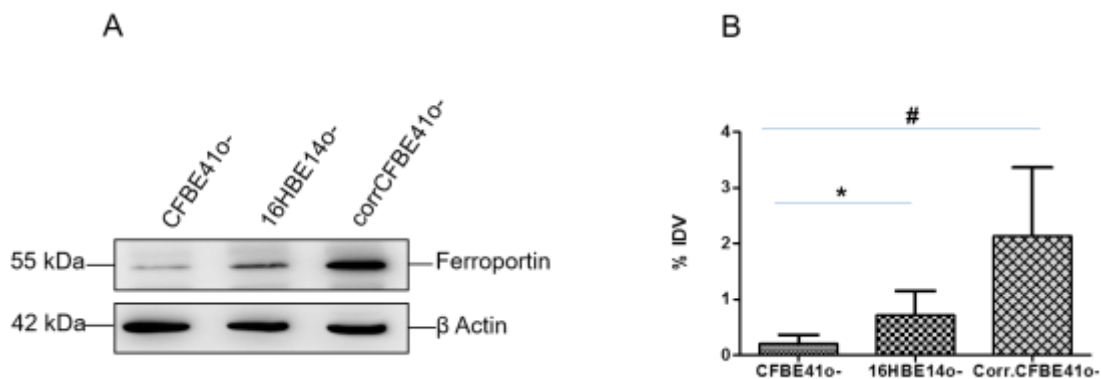


Figure 18: A) Representative immunoblot for expression of ferroportin in cell lysate of CFBE41o- and 16HBE14o- cells and corrCFBE41o- cells. The molecular size of each protein is indicated on the right. B) Densitometry analysis of immunoblot for ferroportin, relative to β -actin. CFBE41o- vs. corrCFBE41o-cells. Data presented are mean \pm SEM (* p <0.05, student's t -test, ns-non-significance). The experiments were repeated 3 times ($n=3$).

3.5 Hypoxia stabilization associated ferroportin expression

Since the ferroportin promoter contains HIF-Responsive Elements (HRE) in the promoter. Additionally, hypoxia in CF might be involved in regulation of ferroportin expression in CF cells[116]. Therefore, ferroportin expression was analyzed under the hypoxic condition and hypoxia mimetic agent by immunoblotting in CFBE41o- and 16HBE14o- cells. To create a hypoxic condition, both cell lines were incubated at 0.1% O₂ for 24hrs and cell lysates were collected immediately after the incubation. Further, protein expression of ferroportin by immunoblotting revealed, an up-regulation of ferroportin under hypoxic condition compared to that of the normoxic condition in both CFBE41o- and 16HBE14o- cells (Fig. 19A and 19C). To confirm these finding, the cells were treated with known hypoxia mimic agent deferoxamine (DFO). Cells were treated with 100mM of DFO for 30 minutes, 1, 2 and 4 hours. Immunoblotting was performed on cell lysate of treated cells to analyze the ferroportin expression.

RESULTS

Results showed that significant time-dependent increase of ferroportin expression ($*p<0.05$) in CFBE41o- whereas ferroportin expression remains unchanged in 16HBE14o- cells (Fig. 19B and 19D). These results conclude that stabilization of HIF-1 α led to increased ferroportin expression in CF epithelial cells.

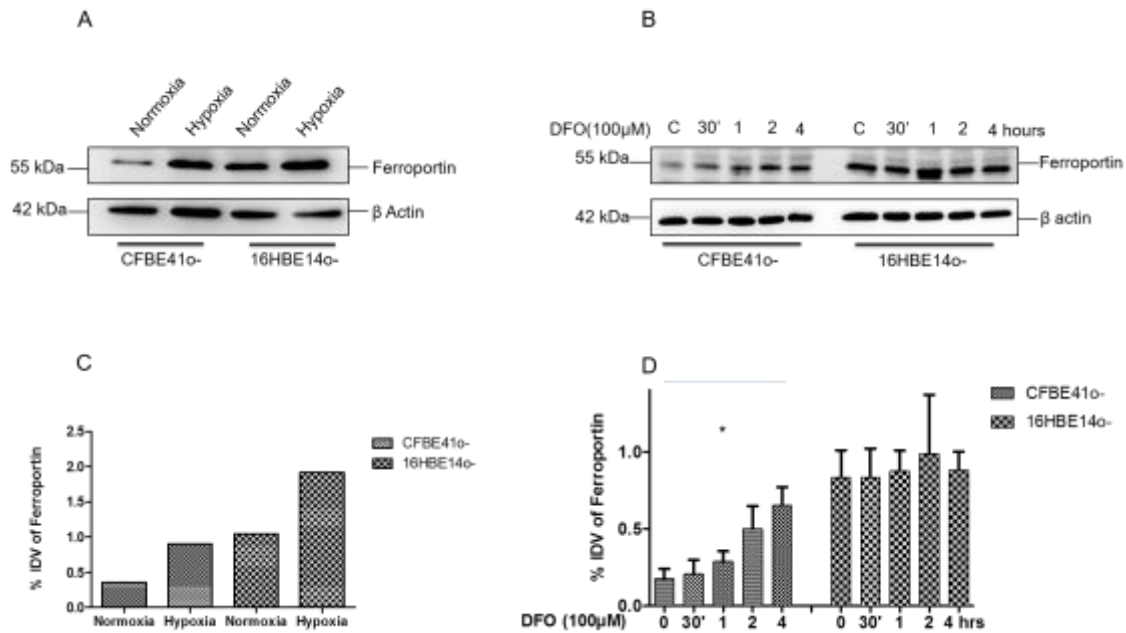


Figure 19: A) Representative immunoblot for levels of ferroportin in cell lysate of hypoxic condition (0.1% O₂) for 24 hours in CFBE41o- and 16HBE14o- cells. β -actin was used as loading control. The molecular size of each protein is indicated on the right. B) Representative immunoblotting for levels of ferroportin in cell lysate of DFO (100 μ M) for increased time (30', 1, 2 and 4 hours) in CFBE41o- and 16HBE14o- cells. β -actin was used as loading control. C) Densitometry analysis of immunoblot for TGF- β , Normoxic condition of cells served as a control of each cell line. Normoxic conditions were compared with hypoxia condition in both 16HBE14o- and CFBE41o- cells. D) Densitometry analysis of immunoblot for ferroportin, non-treated cells served as a control of each cell line. 16HBE14o- vs. CFBE41o- cells. Data are presented mean \pm SEM, $*p<0.05$, student's *t*-test. The experiments were repeated 3 times ($n=3$).

3.6 Effect of TGF- β treatment on expression of ferroportin expression

The previous result on TGF- β expression in CF cell lines led to a hypothesis that reduced TGF- β might be associated with ferroportin expression.

To verify the effect of TGF- β in ferroportin expression, we analyzed ferroportin protein expression by immunoblotting and immunofluorescence in both CFBE41o- and 16HBE14o- cells under TGF- β treatment.

Cells were stimulated with increasing concentration of TGF- β (0,2,5,10 20ng/mL) for 9 hours and 2ng/mL TGF- β was treated for different time points (0, 3, 6, 9 hours). Studies with increasing concentration of TGF- β showed an up-regulation of ferroportin expression until 10ng in both CFBE41o- and 16HBE14o- cells (Fig. 20A and 20C) and time-dependent studies also revealed, an up-regulation of ferroportin expression in CFBE41o- but no effect on 16HBE14o- cells (Fig. 20B and 20D).

Immunofluorescence was performed *in vitro* to confirm the ferroportin surface expression. Cells were treated with TGF- β (2ng) for 9hrs and further stained with ferroportin antibody. Obtained results also confirmed prominent staining of ferroportin in stimulated compared to that of none- stimulated CFBE41o- cells. No much difference was observed in 16HBE14o- cells (Fig. 20E).

Exogenous stimulation with TGF- β on CFBE41o- cells resulted in enhanced expression of ferroportin, which might be associated with maintaining iron homeostasis in CF.

RESULTS

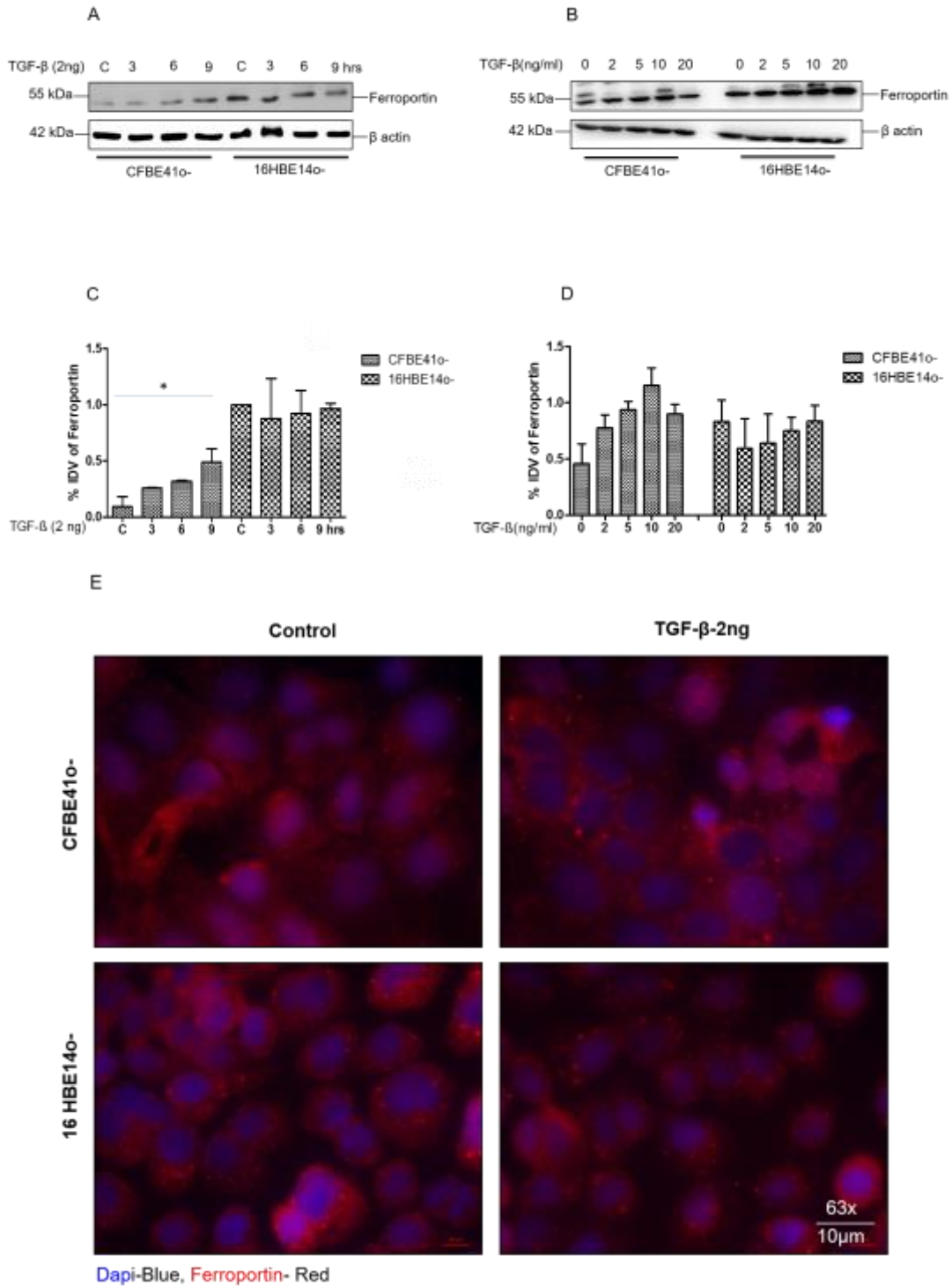


Figure 20: A) Representative immunoblot for detection of ferroportin in cell lysate of CFBE41o- and 16HBE14o- cells upon TGF-β treatment for indicated time interval (A) and concentration (B). β-actin was used as loading control. The molecular size of each

protein is indicated on the right. C) Densitometry analysis of ferroportin immunoblotting upon time and concentration (D) dependent treatment of TGF- β . TLR-4-to- β -actin ratio was calculated and represented as bar graphs. Data represent means \pm SEM, and asterisks indicate statistical significance determined by Student's *t*-test (* P <0.05). Significance was calculated and is relative to respective time points for each cell line. IDV, intensity density values. The experiments were repeated 3 times. E) Ferroportin staining (red) using immunofluorescence in CFBE41o- and 16HBE14o- cell lines upon TGF- β (2ng/mL) stimulation for 9 hours. The experiments were repeated 3 times (n =3). Non-treated cells served as control. Nuclei stained with DAPI (blue).

3.7 Effect of TGF- β treatment on expression of TLR-4 expression

TGF- β is known to act as ENaC channel inhibitor. Therefore, it might reduce ENaC mediated iron concentration in the cells. Further, this can stabilize the HIF-1 α and subsequently can enhance *TLR4* expression [114]. Therefore, TLR-4 expression was investigated upon external application of TGF- β on CFBE41o- and 16HBE14o- cells. Immunoblot and immunofluorescence were performed to analyze TLR-4 expression upon TGF- β treatment. Cells were stimulated with TGF- β in dose-dependent manner (0, 2, 5, 10, 20 ng/mL) for 9 hours and time-dependent manner (0, 3, 6, 9 hours) of 2 ng/mL TGF- β .

Immunoblot analysis in both time (Fig. 21A and 21C) and dose dependent (Fig. 21C and 21D) manner showed a slight increase in TLR-4 expression upon TGF- β treatment in both CFBE41o- and 16HBE14o- cells. β -actin used as loading control and served as the standard for densitometry analysis.

In vitro immunofluorescence was performed to confirm the TLR-4 surface expression. Cells were treated with TGF- β (2 ng) for 9 hrs and further stained with TLR-4 antibody. Obtained results also confirmed prominent staining of TLR-4 in stimulated compared to that of non-stimulated CFBE41o- and 16HBE14o- cells (Fig. 21E).

RESULTS

These results concluded that exogenous treatment with TGF- β on CFBE41o-cells result in enhanced expression TLR-4 surface expression in CF epithelial cells.

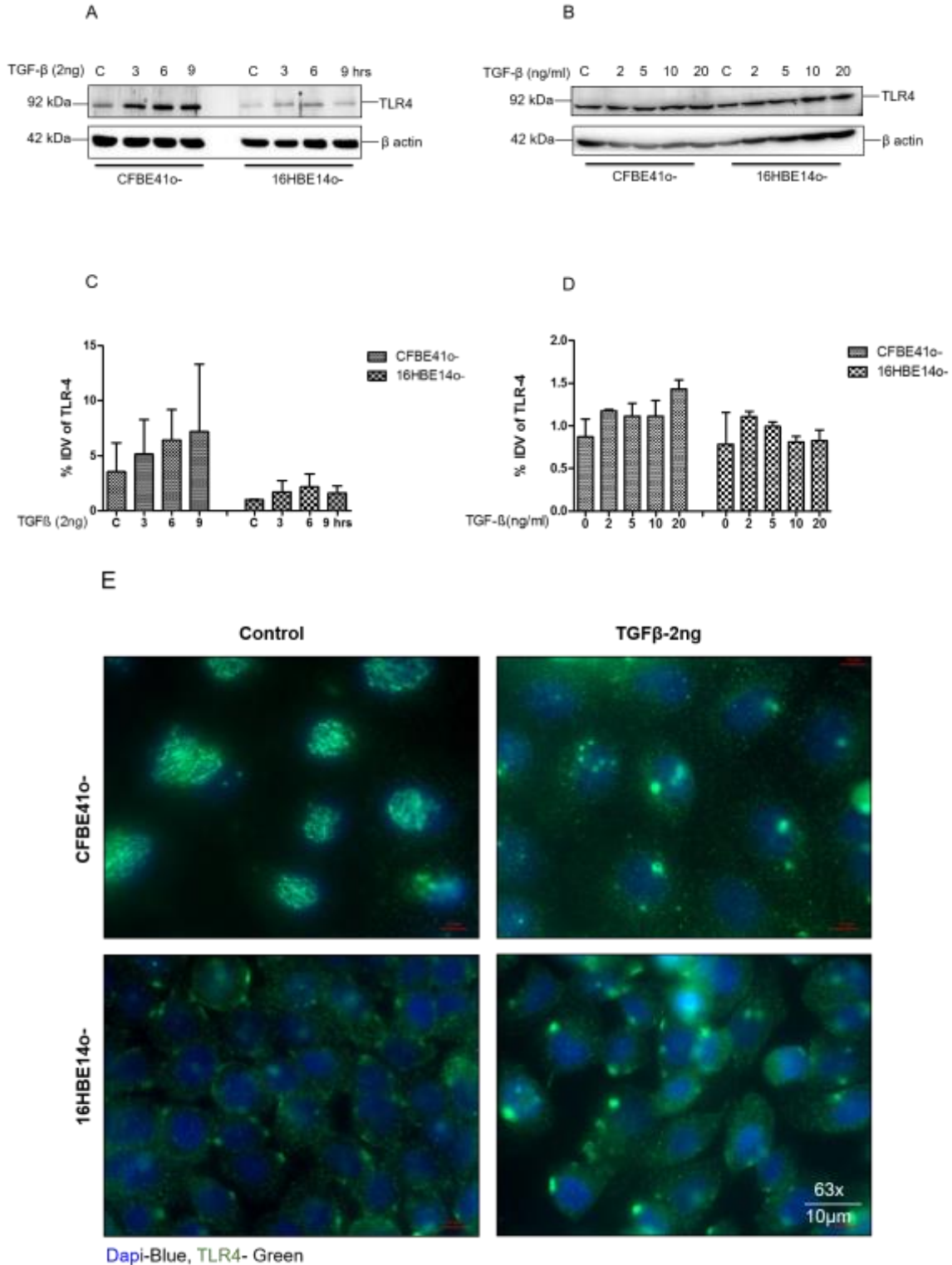


Figure 21: A) Representative immunoblot for detection of TLR-4 in cell lysate of CFBE41o- and 16HBE14o- cells upon TGF- β treatment for indicated time interval (A) and concentration (B). β -actin was used as loading control. The molecular size of each protein is indicated on the right. C) and D) Densitometry analysis of TLR-4 immunoblotting upon time and concentration dependent treatment of TGF- β . TLR-4 to β -actin ratio was calculated and represented as bar graphs. Data represent means \pm SEM, and asterisks indicate statistical significance determined by Student's t-test (* P <0.05). Significance was calculated and is relative to respective time points for each cell line. IDV, intensity density values. The experiments were repeated 3 times ($n=3$). E) TLR-4 staining (green) using immunofluorescence in CFBE41o- and 16HBE14o- cell lines upon TGF- β (2ng/mL) stimulation for 9 hours. The experiments were repeated 3 times ($n=3$). Non-treated cells served as control. Nuclei are stained with DAPI (blue).

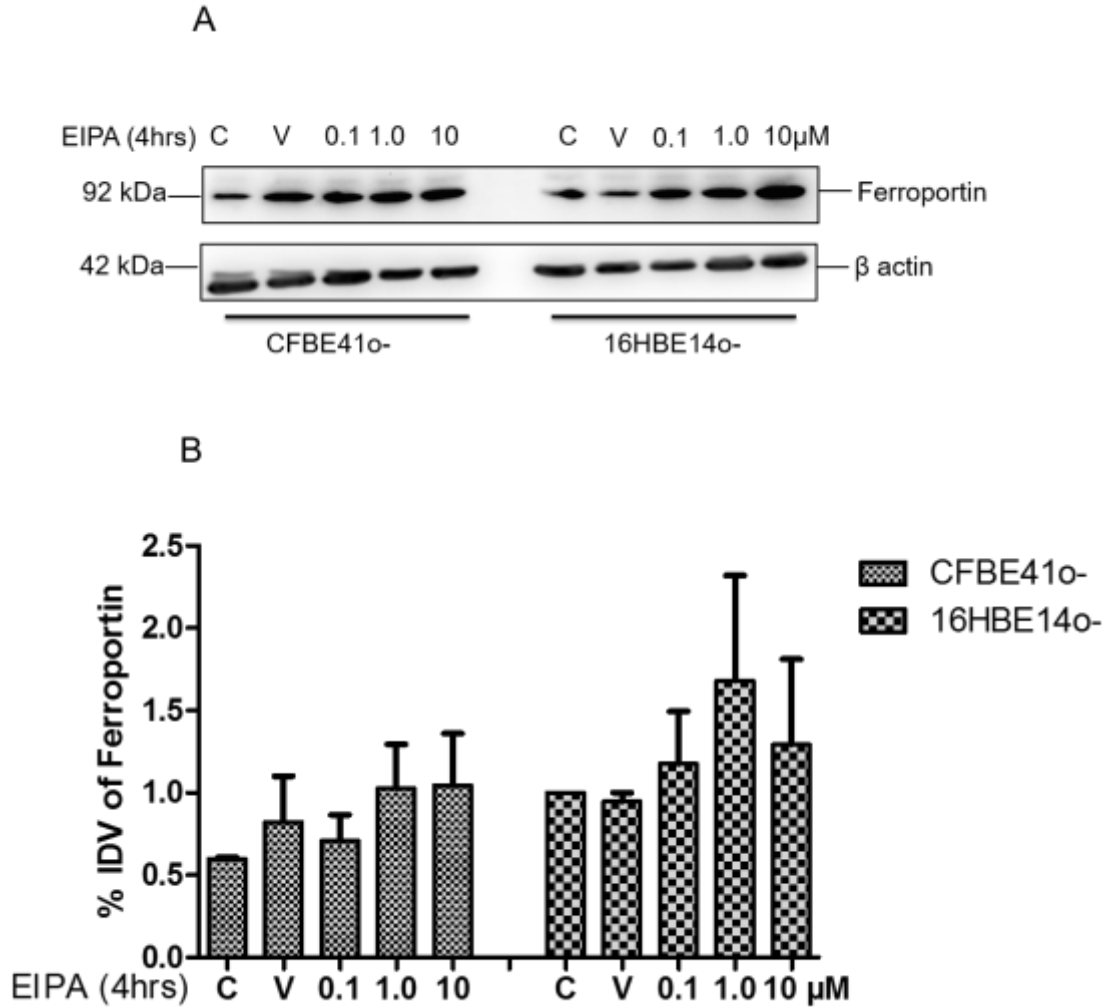
3.8 ENaC- channel inhibition by amiloride upregulates the expression of Ferroportin.

Previous literature showed that overexpression of ENaC associated with high intracellular Na⁺, subsequently leading to increased iron concentration.

The effect of ENaC channel inhibitor, EIPA [5-(N-Ethyl-N-isopropyl) amiloride] on ferroportin expression was investigated on CFBE41o- and 16HBE14o- cells. Therefore, CFBE41o- and 16HBE14o- cells were treated with increasing concentration of EIPA (0, 0.1, 1.0, 10 mM) for 4hrs. Ferroportin expression was investigated by immunoblot and immunofluorescence. Immunoblot analysis revealed, a concentration-dependent increase of ferroportin expression upon EIPA treatment in both CFBE41o- and 16HBE14o- cells with no significant differences (Fig. 22A and 22B). Immunofluorescence results also confirmed the increase of ferroportin staining upon increasing concentration of EIPA in both CFBE41o- and 16HBE14o- cells (Fig. 22C).

RESULTS

Collectively, these findings demonstrate that ENaC channel inhibition up-regulates ferroportin expression which might further assist to reduced iron overload in CF.



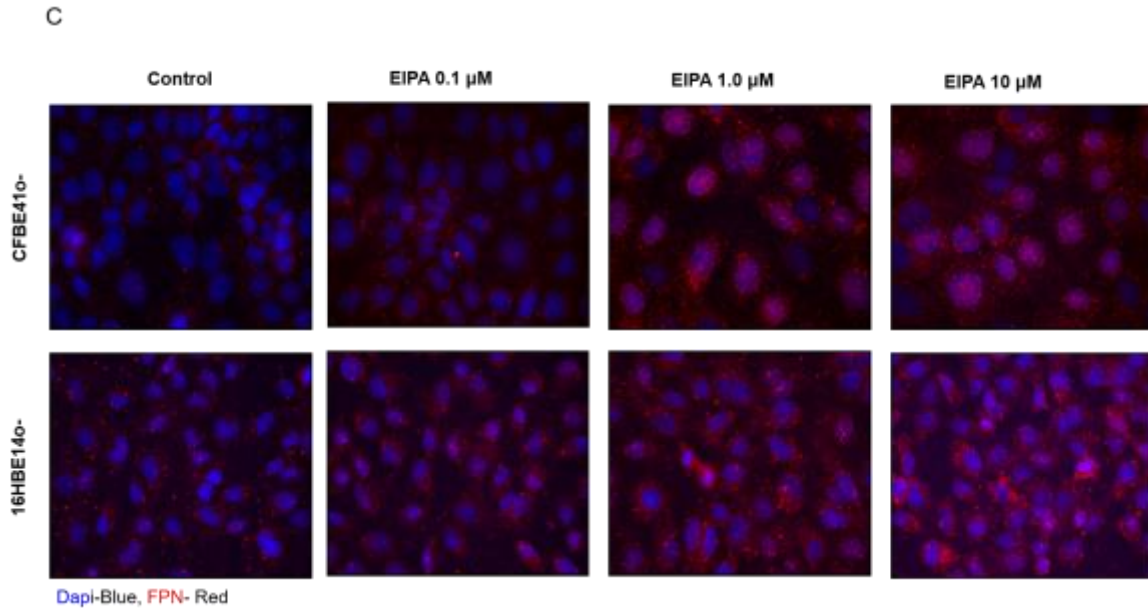


Figure 22: A) Representative immunoblotting for detection of ferroportin in cell lysate of CFBE41o- and 16HBE14o- cells upon EIPA treatment for concentration. β -actin was used as loading control. The molecular size of each protein is indicated on the right B) Densitometry analysis of ferroportin immunoblotting upon increasing concentration of EIPA. Ferroportin-to- β -actin ratio was calculated and is represented as bar graphs. Data represent means \pm SEM. IDV, intensity density values. C) Ferroportin staining (red) using immunofluorescence in CFBE41o- and 16HBE14o- cell lines upon EIPA stimulation for 4 hours. The experiments were repeated 2 times ($n=2$). Untreated cells served as control. Nuclei stained with DAPI (blue).

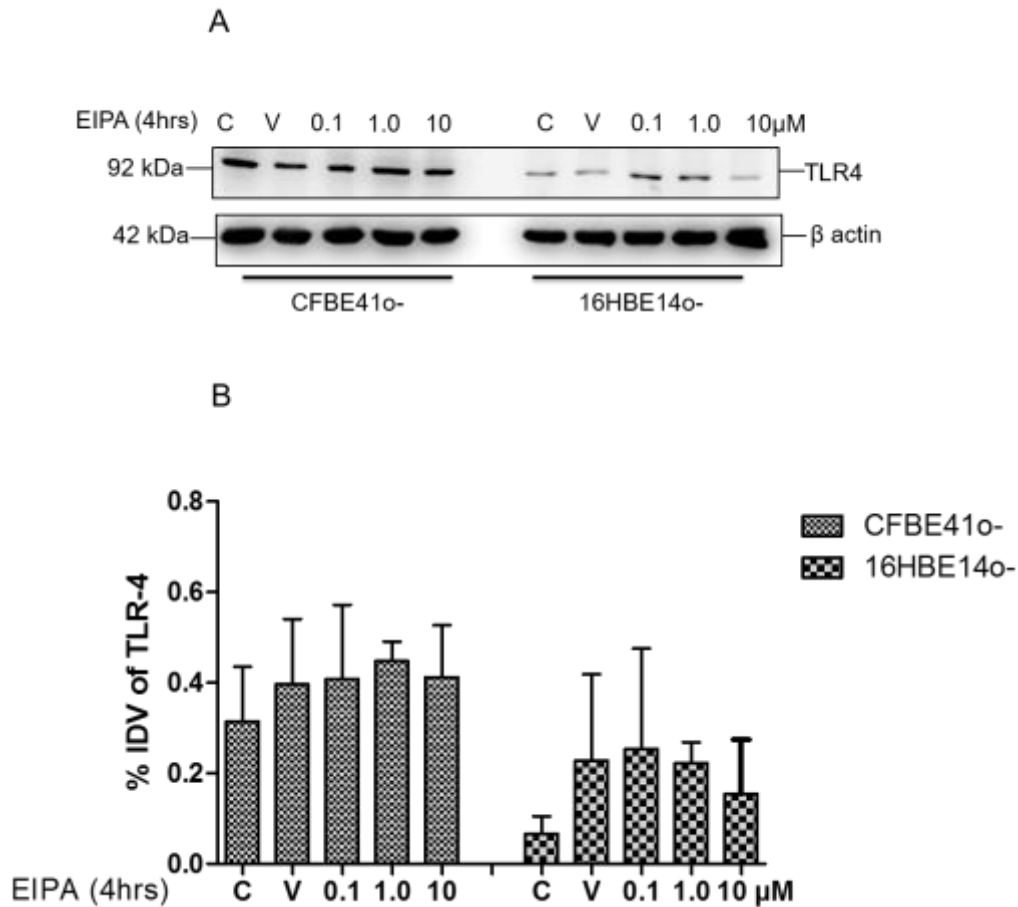
3.9 ENaC channel inhibition by amiloride restores TLR-4 expression in CFBE cell lines

ENaC channel inhibition associated ferroportin upregulation and reduced iron intake in the epithelial cells might lead to decrease intracellular iron concentration. Further, can cause HIF-1 α stabilization and might influence on TLR-4 expression in CF epithelial cells. Previously Kim et al. showed that HIF-1 α augments the TLR-4 expression. So TLR-4 expression upon ENaC inhibition was inspected.

RESULTS

Cells were treated with increasing concentration of EIPA (0, 0.1, 1.0, 10 mM) for 4 hours. Immunoblot and immunofluorescence studies were performed to analyze the TLR-4 expression. Results obtained from immunoblot analysis did not show much difference in TLR-4 protein expression upon EIPA treatment in both CFBE41o- and 16HBE14o- cells (Fig. 23A and 23B). Interestingly, immunofluorescence staining showed intact and punctate staining of TLR-4 on the surface in increasing concentration of EIPA in CFBE41o- and 16HBE14o- cells (Fig. 23C).

Therefore, these results provide evidence that ENaC inhibition improved the TLR-4 surface expression in Cystic fibrosis epithelial cells.



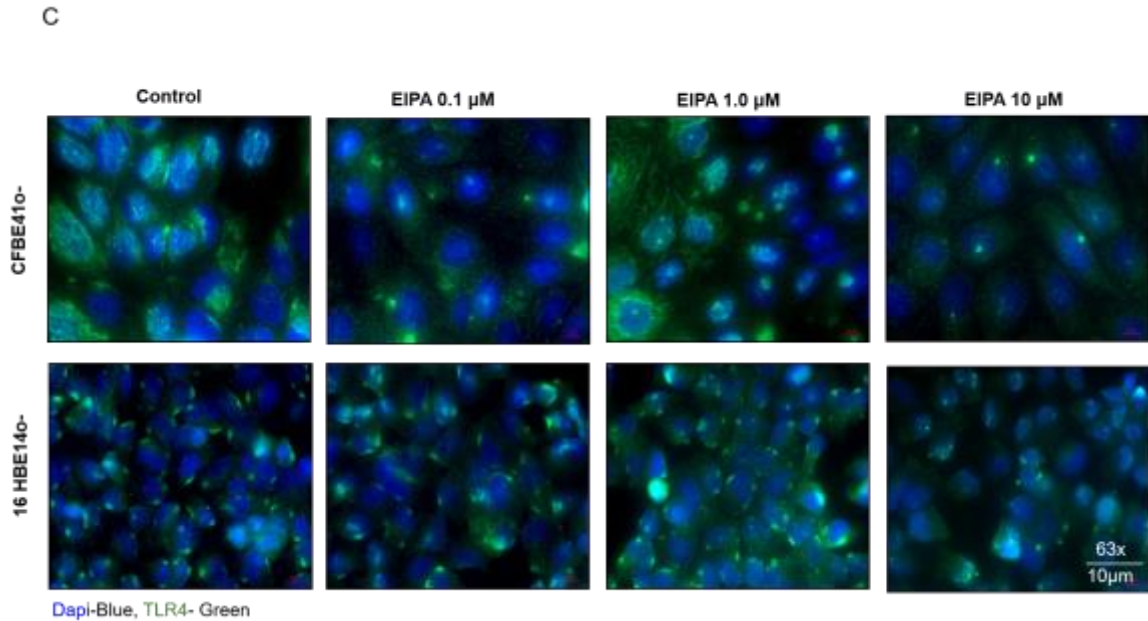
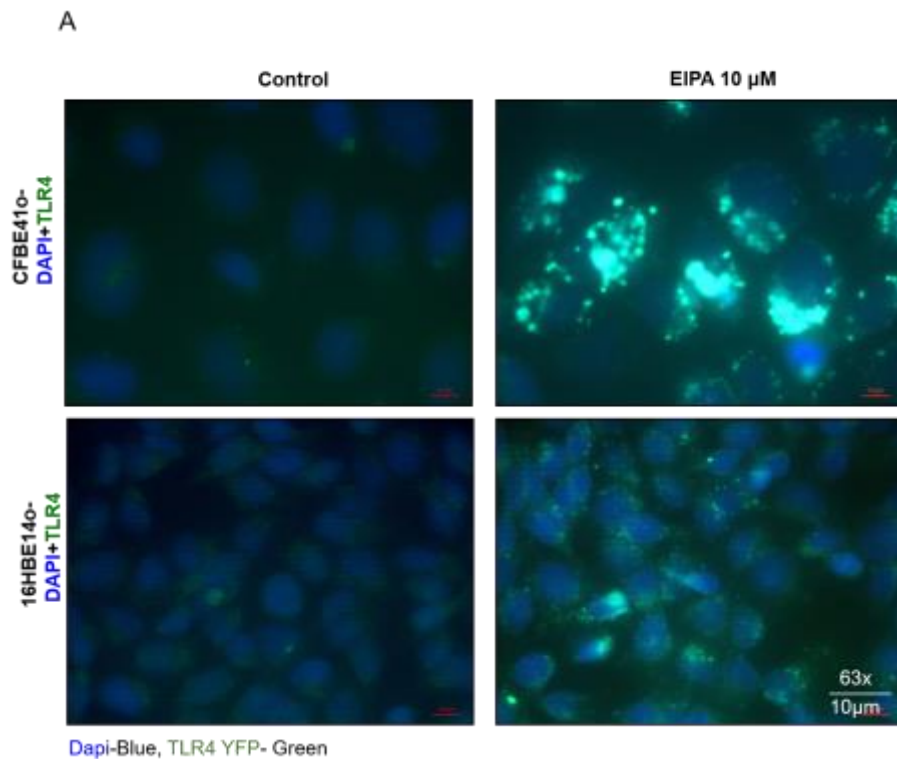


Figure 23: A) Representative immunoblot for detection of TLR-4 in cell lysate of CFBE410- and 16HBE140- cells upon treatment with increasing concentration of EIPA. β -actin was used as loading control. B) Densitometry analysis of TLR-4 immunoblotting upon increasing concentration of EIPA. TLR-4 to β -actin ratio was calculated and is represented as bar graphs. Data are representing means \pm SEM and asterisks indicate statistical significance determined by Student's *t*-test ($*P < 0.05$). Significance was calculated and is relative to respective time points for each cell line. IDV-intensity density values. C) TLR-4 staining (green) using immunofluorescence in CFBE410- and 16HBE140- cell lines upon EIPA stimulation for 4 hours. The experiments were repeated 2 times ($n=2$). Untreated cells served as control. Nuclei stained with DAPI (blue).

3.9.1 Transfection of TLR-4-yfp to CFBE410- and 16HBE140- cells

To support the previous finding, the impact of ENaC inhibition on TLR-4 surface expression, cells were transfected with TLR-4-yfp plasmid by lipofectamine to overexpress the TLR-4 in the cells. After transfection, cells were treated with EIPA (10 μ M/mL) for 4 hours. Nuclei were stained with DAPI and TLR-4-yfp signals were captured.

Observed results clearly indicated, restored TLR-4 expression upon EIPA treatment when compared with untreated CFBE410- and 16HBE140- cells (Fig. 24A). These further confirmed ENaC inhibition result in improve TLR-4 surface expression in CFBE410- cells. Collectively, these findings demonstrate that ENaC channel inhibition up-regulated ferroportin and improved TLR-4 surface expression in CF epithelial cells.



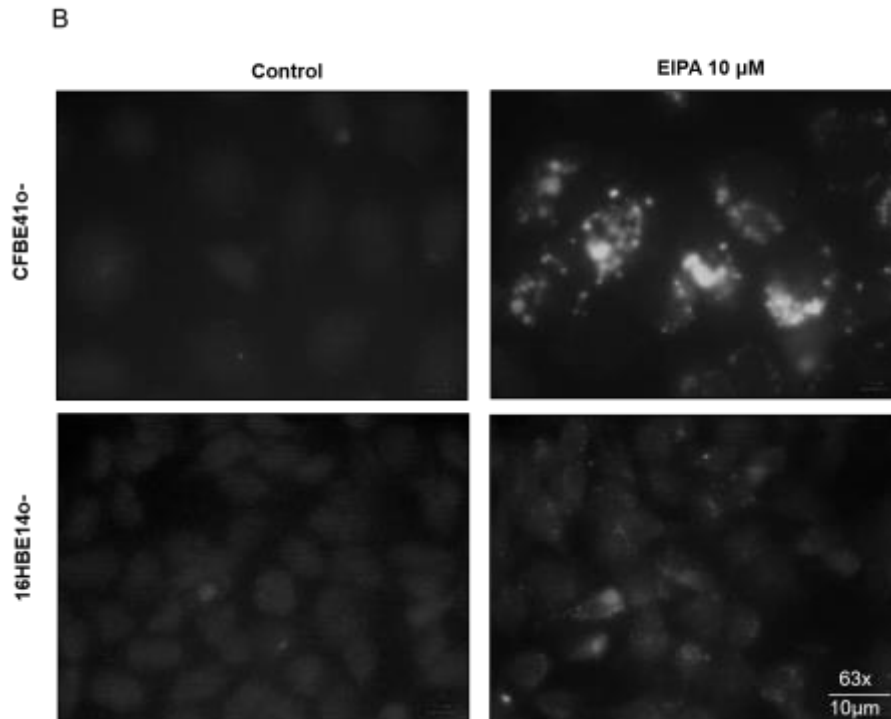


Figure 24: A) TLR-4 staining (green) using fluorescence microscope in CFBE41o- and 16HBE14o- cell lines upon TLR-4-yfp transfection (24 hours) followed by EIPA treatment for 4 hours. Non-treated cells served as control. Nuclei stained with DAPI (blue). B) Same images captured in white light to focus on the TLR-4 signals.

3.10 TLR-4 expression upon DFO, TGF- β and EIPA treatments

Finally, to prove the hypothesis, CFBE41o- and 16HBE14o- cells were treated with DFO, TGF- β and EIPA treatment for 5 hours and TLR-4 protein expression was analyzed by immunoblotting. This study confirmed the increase of TLR-4 expression in both cells lines (Fig. 25A and 25B). Therefore, DFO, TGF- β and EIPA increased TLR-4 expression through HIF-1 α stabilization, which might be due to reduced iron concentration in the cell.

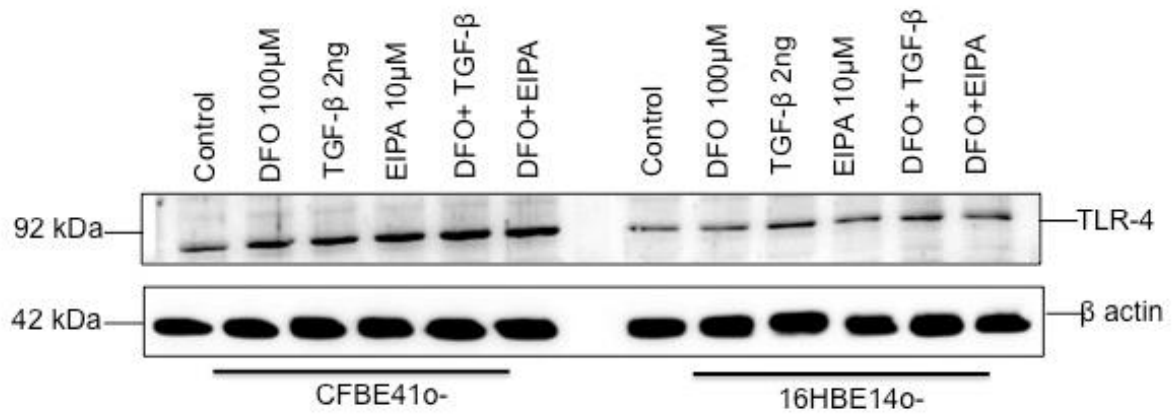


Figure 25: A) Representative immunoblot for detection of TLR-4 in cell lysate of CFBE41o- and 16HBE14o- cells upon DFO, TGF- β and EIPA. β-actin was used as loading control. B) Densitometry analysis of TLR-4 immunoblotting upon increasing concentration of EIPA. TLR-4-to- β-actin ratio was calculated and is represented as a bar graph. IDV, intensity density values.

4 Discussion

In CF, the $\Delta F508$ -CFTR mutation causes defective CFTR channels, which leads to defective chloride ion export from the airway epithelial cells. CFTR not only functions as chloride channel but also regulates the epithelial sodium channel (ENaC) [6]. Mutation of CFTR leads to imbalances in CFTR-mediated anion secretion and ENaC-mediated Na^+ absorption in airways epithelium and leads to dehydration of airway surface liquid level causing thickening of mucus secretion. This leads to reduced mucociliary clearance [126]. Further, it contributes to the bacterial infection of CF airways. Since CF airways fail to eradicate bacterial infection, it results in altered immune responses that lead to chronic colonization of CF airways by pathogens such as *P. aeruginosa* [32]. Along with defective TLR-4 surface expression, altered iron homeostasis and destabilization of hypoxia-inducible factor (HIF) was reported in CF airways [107]. ENaC channel is regulated via extrinsic and intrinsic factors including miR-16 and TGF- β and associated with iron uptake in airway epithelial cells [45, 54, 55].

In the current study, we have shown *in vitro* a reduced TGF- β expression in CF airway epithelial cells (CFBE41o-) compared to normal human bronchial epithelial cells (16HBE14o-). We have also demonstrated that hypoxia, defective CFTR, and miR-16 in CF might lead to decrease TGF- β expression. We also found decreased expression of iron exporter ferroportin in CF, which seem to be dependent on the stability of HIF-1 α . We further demonstrated that external application of TGF- β in CFBE41o-cells leads to increase levels of Ferroportin and rescue the TLR-4 surface expression in CF cells. Direct blocking of ENaC channel by ENaC inhibitor leads to increase the iron exporter ferroportin and further improve the TLR-4 surface expression in CF cells.

Previous studies have shown that TLR-4 surface expression is reduced in CF airway epithelial cells (CFBE41o- and IB-3), leading to a reduced MyD88-related

and Toll/IL-1 receptor domain-containing adaptor inducing IFN (TRIF)-related activation of IL-6/IL-8 and type I interferon's /interferon -inducible protein-10 [30, 37]. However, the principal mechanisms behind reduced TLR-4 surface expression are still unknown. We showed that reduced TLR-4 surface expression leads to altered iron homeostasis, which further affects the stability of the HIF-1 α through downregulation of hemeoxygenase-1 [107]. This might be the reason for an ineffective anti-inflammatory and antioxidant responses in CF, which might be associated with exaggerated airway inflammation in CF.

Therefore, we aimed to determine the influence of ENaC mediated regulation of TLR-4 surface expression and factors associated with ENaC channel regulation including TGF- β , miR-16 and iron-related protein (FPN).

To confirm our hypothesis, we used an immortalized CFBE41o-cell line, homozygous for the deltaF508 CFTR mutation and its corrected corrCFBE41o-cell line with a stable expression of the wild-type CFTR protein and normal human bronchial epithelial cells 16HBE14o-cells. Firstly, we analyzed the Expression of TGF- β , which is a potent inhibitor of ENaC channels and its regulating factors such as miR-16 and hypoxia.

4.1 TGF- β expression is reduced in CF

TGF- β is expressed in lungs respiratory epithelial cells and play a crucial role in cellular differentiation, lung development and homeostasis [127]. It is involved in chronic pulmonary diseases including pulmonary fibrosis and CF [71]. Previous data suggested that TGF- β plays role in downregulation of CFTR channels in CF [72]. However, most of the studies demonstrate up-regulation of TGF- β levels in CF. TGF- β levels in plasma from CF patients were found to be elevated compared to controls [69]. TGF- β levels were increased in bronchoalveolar lavage fluid (BAL) from children with CF and it was shown to be associated with

neutrophilic inflammation with reduced lung function [70]. Further, TGF- β signaling was increased in lung tissue sections from CF patients [71]. While some studies show high TGF- β levels in CF patients there is no evidence emphasizing on the adverse effects of high TGF- β 1 levels in CF so far [128]. In *in vitro* studies, Kelly et al. have postulated that SMAD3 levels are decreased in CF epithelial cells. As SMAD3 is a critical player in the TGF- β signaling pathway, they suggest decreased TGF- β levels in the CF cells [129]. This might be a reason for the controversial finding of *in vivo* versus *in vitro* studies since the expression of TGF- β has not been studied in delta F508 mutation in CFTR gene (CFBE41o-) and normal human bronchial epithelial (16HBE14o-) cells.

Our results show reduced TGF- β expression in CFBE41o- cells as compared to 16HBE14o- cells. Many studies show up-regulation of ENaC channels in CF. This might be the reason for TGF- β downregulation. TGF- β is also known as crucial ENaC channel blocker and has been shown to inhibit the epithelial sodium channels (ENaC) channel in acute lung injury [54, 55, 73]. It is also shown that TGF- β 1 might impede sodium reabsorption by a downregulation of prostasin expression and subsequent inhibition of ENaC activity in renal epithelial cells [130]. Our result indicates that reduced expression of TGF- β might be associated with ENaC regulation in CF, which might be interesting for further studies. Normal expression of TGF- β in CF airways might lead to a decrease of Na⁺ reabsorption by inhibiting the ENaC activity, which further reduces the iron bypass through ENaC channels. Altered TGF activity could be related to transcription, secretion, or processing in CF, which needs to be further investigated for the exact mechanism for TGF- β regulation. This might help in understanding the pathophysiology of CF and possibility of new therapeutic options for CF treatment.

4.2 miR-16 downregulate TGF- β expression in CF cells

MicroRNAs (miRNAs) are small nucleotide sequences for negative regulation of various genes and numerous biological processes.

In CF, mutation of CFTR leads to imbalances in CFTR-mediated anion secretion and ENaC-mediated Na⁺ absorption in airways epithelium and leads to dehydration of airway surface causing thickening of mucus secretion, which is associated with chronic bacterial infection. Previous studies have shown that miR-16 lead to increased ENaC expression and associated with a significant decrease in TGF- β levels. Therefore, miR-16 related dysregulation of ENaC expression is mediated through downregulation of TGF- β in acute lung injury (ALI) [55]. To determine whether miR-16 affects the TGF- β , we analyzed TGF- β expression in miR-16 overexpressed normal human bronchial cells and blocked miR-16 in CF bronchial epithelial cells.

Our study shows decreased TGF- β expression upon miR-16 overexpression and increased TGF- β upon blockage of miR-16 expression. Results indicate the role of miR-16 in downregulation of TGF- β in CF, which might further be associated with ENaC overexpression in CF. However, the level of miR-16 was not changed in CF airways cells as compare to normal bronchial airways cells (Fig. 3A).

In future, inhibition of miR-16 by anti-miR might provide a therapeutic strategy to reduce ENaC overexpression though TGF- β up-regulation and might serve as a therapeutic agent to treat CF.

4.3 Hypoxia regulates the TGF- β expression

Chronic bacterial infections and altered immune responses result in reduced ASL which leads to thickened mucus secretion on airways lining. Furthermore, this causes difficulty in gas exchange in the CF lungs. Due to chronic infection, iron-mediated reactive oxygen species are increased which alters the

microenvironment of the airway epithelial cells. It gives rise to low partial pressure of oxygen inside the lungs and subsequently induces hypoxia [108, 109]. It was shown that defective TLR-4 and altered iron homeostasis leads to hypoxic response (low HIF-1 α) in CF [107]. We hypothesized that hypoxia might be associated with reduced TGF- β expression in CF cells. So, we incubated the cells at hypoxia conditions to elicit a stronger hypoxic response in CF. Previous studies also reported that hypoxia increases the expression of TGF- β , which contains hypoxia response element (HRE) in promoter [123].

Under hypoxia, TGF- β expression was increased in 16HBE14o- cells. Contrast to this TGF- β expression was decreased in CFBE41o- cells. This might be the effect of HIF-1 α destabilization in CF cells. Oxygen deprivation might also increase free radicals, damage DNA, and cause cell death [124]. The hypoxic condition seems to fail in the stabilization of HIF-1 α and showed reduced TGF- β expression in CFBE41o- cells.

HIF activity is dependent on HIF-1 α stabilization and negatively regulated by prolyl hydroxylase domain (PHD) enzymes. PHD residues of HIF-1 α in the presence of O₂, Fe²⁺, and 2-oxoglutarate further lead to polyubiquitination and proteasomal degradation of HIF. Fe²⁺ is known to play important role in regulating the activity of PHD. Iron chelation (or substituting Fe²⁺ with other metal ions such as CO₂, Ni, and Mn) leads to diminishing the activity of PHDs [131]. Thus, we hypothesized that excess intracellular iron and HIF-1 destabilization in CF might be linked with TGF- β expression. We tested our hypothesis by a known hypoxia mimic agent deferoxamine (DFO). As DFO act as the hypoxia-mimicking agent through iron chelation, we believe that DFO chelate the excess iron and stabilize the HIF-1 α and increases the TGF- β expression.

4.4 Ferroportin expression is reduced in CF and regulated by hypoxia

It has been speculated that increased intracellular iron concentration could be the effect of ENaC overexpression and reduced hemoxygenase-1 (HO-1) leading to altered iron homeostasis in CF [105, 107].

Therefore, we were interested in iron regulatory proteins such as ferroportin. It is a single known iron exporter in the cells and is regulated by iron regulatory hormone hepcidin [132]. Ferroportin is essential for regulation of iron homeostasis and involved in iron detoxification by up-regulating in the presence of excessive intracellular iron levels. Ferroportin is shown to be up-regulated in lung tissue from CF patients [118]. Expression of ferroportin has not been studied in CF airway epithelial cells.

Despite increased intracellular iron in CF, we observed the downregulation of mRNA and proteins levels of ferroportin in the CFBE cells, which might be responsible for the increased iron concentration in CF epithelial cells. It is already known that ferroportin-deficient animals show accumulation of iron in enterocytes, macrophages, and hepatocytes [133].

A possible explanation for the observed reduced expression of ferroportin in CF airway epithelial cells might be a chronic bacterial infection and associated inflammation in CF. Previous studies have suggested that inflammation might play a role in the transcription of ferroportin [116]. Lipopolysaccharide (LPS) is inflammatory signals which are known to downregulate ferroportin mRNA and upregulate hepcidin mRNA in macrophages, leading to the cooperative suppression of ferroportin protein. Bacterial-produced LPS injected into mice or rats are associated with decreased ferroportin expression in spleen and intestine [134].

Ferroportin contains HIF-responsive elements (HRE) in promoter [116]. So, increased intracellular iron associated hypoxia in CF [107] could be another reason for reduced ferroportin expression in CF airways cells.

Deletion of HIF-2 α in *Hamp*^{-/-} mice causes decreased mRNA levels of DMT1 and ferroportin in the intestine, which demonstrates the significance of HIF in the regulation of ferroportin [135]. Several studies have suggested that increased HIF-1 α activity causes increased ferroportin levels, suppression of hepcidin, and increased serum iron availability [136]. Our immunoblotting results also show increased ferroportin expression under hypoxic conditions (1% O₂). A similar strategy employed by using iron chelators (desferroxamine, DFO) to inhibit Fe²⁺-dependent PHD activation and HIF-1 α stabilization. In our investigation, after DFO treatment, we found an increased ferroportin expression in CF compared to normal condition.

Thus, we speculate that destabilization of HIF-1 α in CF is not only related to reduced TGF- β expression but also involved in downregulation of ferroportin.

4.5 Exogenous TGF- β upregulates the ferroportin and TLR-4 expression

Previous results on TGF- β expression in CF cell lines led us to speculate that reduced TGF- β might be associated with ferroportin expression since TGF- β and Ferroportin both contain hypoxia response element in the promoter. It was also shown in astrocytes that TGF- β 1 promoted iron efflux and increased the expression of ferroportin [137]. We analyzed whether exogenous treatment with TGF- β affects ferroportin in CFBE41o- and 16HBE14o- cells. Our research showed that ferroportin expression was increased upon TGF- β treatment. TGF- β mediated HIF-1 α stabilization could be responsible for increased ferroportin in CF cells.

Recently, transforming growth factor- β 1 (TGF- β 1) has emerged as an agonist, which induces HIF-1 α accumulation in various cell lines including human HT1080 fibrosarcomas and vascular smooth muscle cells under normoxic conditions [138, 139]. However, the mechanism underlying how TGF- β 1 stabilizes HIF-1 α remains unclear.

McMahon et al. showed that TGF- β decreased the transcription of PHD2 gene by the activation of SMAD proteins. It was also shown that SMAD signaling pathway plays an important role to the TGF- β since inhibition of SMAD led to the restoration of PHD2 mRNA and protein levels and impaired HIF-1 α protein accumulation in response to the growth factor in HepG2 and HT1080 cells [140].

Based on earlier evidence and our *in vitro* results of HIF-1 α stabilization by hypoxia (1% O₂) and DFO leading to increased ferroportin expression, it can be speculated that exogenous application of TGF- β might increase the ferroportin expression. This might lead to maintain the iron homeostasis by reducing the intracellular iron in CF cells.

In the present study, TGF- β was applied to CFBE410- and 16HBE14o- cells. According to previously reported data, we suppose that sodium transport machinery was most likely targeted by TGF- β . External treatments of TGF- β (10 ng/mL) can down-regulate the gene encoding α ENaC (SCNN1A) in alveolar epithelial cells [73]. TGF- β is known to inhibit the ENaC channel in acute lung injury [54, 55, 73]. Inhibition of ENaC might lead to a reduction of sodium intake in the epithelial cells. Turi et al. demonstrated that intracellular iron accumulation is increased in the presence of augmented extracellular Na⁺. Furthermore, it was shown that inhibition of Na⁺ channels leads to lack of iron accumulation in the cells [105].

In CF cells, exogenous application of TGF- β can also act as ENaC inhibitor and might lead to reducing ENaC mediated iron bypass to maintain the iron

homeostasis. Due to reduced iron intake in the cells, the intracellular concentration of iron might be reduced. Further, reduced iron intake might stabilize the HIF-1 α , by degradation of prolyl hydroxylase (PHD). This might be responsible for increased ferroportin expression in CF cells.

Recent data from our lab demonstrated that defective TLR-4 in CF might contribute to decreased HIF-1 α under normoxia and vice versa under hypoxia [107]. So we were interested to find out the effect of exogenous treatment of TGF- β on TLR-4 expression. In our investigation, we observed increment of TLR-4 protein expression upon both times as well as concentration-dependent treatment of TGF- β . These results suggest that HIF-1 α stabilization by TGF- β treatment enhances the TLR-4 expression. Our immunofluorescence results also confirmed the improvement of TLR-4 surface expression in both cell lines (CFBE41o- and 16HBE14o-) (Fig. 8E).

As we discussed earlier, TGF- β is responsible for the HIF-1 α stabilization, this may explain our finding of increased TLR-4 protein and surface expression in the CF cells. Previous research was done by Kim et al. in macrophages showed that TLR-4 expression was up-regulated in hypoxia stress via hypoxia-inducible factor. In this study, they found small interfering RNA-mediated knockdown of HIF-1 α expression repressed TLR-4 expression in macrophages, whereas over-expression of HIF-1 α lead to increase TLR-4 expression. Additionally, their chromatin immunoprecipitation assays revealed that under hypoxic conditions, HIF-1 α binds to the TLR-4 promoter region [114].

Therefore, it can be speculated that exogenous TGF- β treatment enhances TLR-4 expression via HIF-1 α stabilization in CF cells.

4.6 Direct inhibition of ENaC up-regulate the ferroportin and TLR-4 expression

Recently, CF mice model with defective Cl^- secretion resulted in an increase of Na^+ and water absorption in lung epithelium, which is the consequence of overexpression of ENaC channel [141]. Deregulation of ENaC channels leads to depletion of airway surface liquid causing the thickening the mucus secretion, which reduce the mucociliary clearance of bacterial infections.

ENaC channel play role in transportation of iron into the epithelial cells. Epithelial transport of iron into the cell seems to be associated with transcellular movement of sodium ions [105]. Overexpression of ENaC leads to not only increase Na^+ intake in the cells but also increases the iron bypass in the cells [105]. In CF, an excess of Fe^{2+} suggests the interference with stability and activity of HIF-1 α expression under hypoxia [107]. We hypothesize that blocking of ENaC might reduce the iron intake in the cells which reduce the increased iron concentration in the epithelial cells. Further, this might lead to HIF-1 α stabilization due to reduced iron in the CF cells.

In this study, we used EIPA (5-(N-Ethyl-N-isopropyl) amiloride) to inhibit ENaC channels. We observed the increase of ferroportin in CFBE41o- cells, which also might be the result of HIF-1 α stabilization in cells. TLR-4 surface expression was found reduced in CF airways, which might compromise the innate immune responses. Less responsive CF airways during at the time of early bacterial infection might cause due to reduced TLR-4 surface expression. Consequently, this will delay neutrophil chemotaxis and migration across the epithelium and favor bacterial growth and biofilm formation [37]. So we examined the TLR-4 expression upon ENaC channel inhibitor (EIPA) in CFBE41o- and 16HBE14o- cell lines. Although protein expression of TLR-4 did not show many differences upon increasing concentration of EIPA when compared to untreated cells. But

immunofluorescence experiments suggested an induction of TLR-4 surface expression upon EIPA treatments (Fig-10C). Further experiments of TLR-4-YFP plasmid transfection also confirmed that ENaC inhibition was linked with increased TLR-4 surface expression (Fig.10 1A).

A possible explanation for the observed increased surface expression of TLR-4 could be HIF-1 α stabilization. As discussed earlier, blocking of ENaC might reduce the iron uptake in the epithelial cells [105], which can stabilize the HIF-1 α in CF cells and associate with the TLR-4 up-regulation in CF cells.

Not much study has been carried out in context with the ENaC and TLR-4 regulation. Elucidating molecular pathways regarding direct inhibition of ENaC associated with improved TLR surface expression needs further investigation.

Previously, it has been shown that epithelial sodium channel silencing facilitates restoration of the airway surface liquid level to allow usual mucociliary clearance [52]. Silencing ENaC using specific siRNAs can recover the surface hydration of CF and non-CF primary human bronchial epithelia (HBE) and can be one of the strategies to correct the airway surface fluid deficit in CF [142].

5 Conclusion

Based on the current study, the pathways by which TGF- β , ferroportin, and TLR-4 linked to CF, are presented in the schematic diagram in Figure- 26.

Reduced TGF- β and ferroportin expression might be a consequence of impaired HIF1 α and could be restored by hypoxia/DFO mediated HIF1 α stabilization. In addition, antagomirs miR-16 can be used to up-regulate the TGF- β .

Thus, the current *in vitro* data gives us an idea that treatments such as exogenous TGF- β , EIPA (5-(N-Ethyl-N-isopropyl) amiloride) could be potentially successful in increasing ferroportin expression which might be an approach to overcoming the increasing iron load and improving the TLR-4 surface expression in CF.

Further studies are necessary to elucidate downstream mechanism to reveal the increment of ferroportin and TLR-4 expressions in CF. Further confirmation in the primary airway epithelial cells from CFTR knockout mice or nasal epithelial cells obtained from patients with CF will support our findings and revealed the factors that play a role in the pathophysiology of CF.

The potential clinical implications of the findings are profound because increased ferroportin expression will reduce iron concentration and maintain the iron homeostasis in CF airways. Further restoring the TLR-4 surface expression can prevent the chronic colonization of gram-negative bacteria such as *Pseudomonas aeruginosa*.

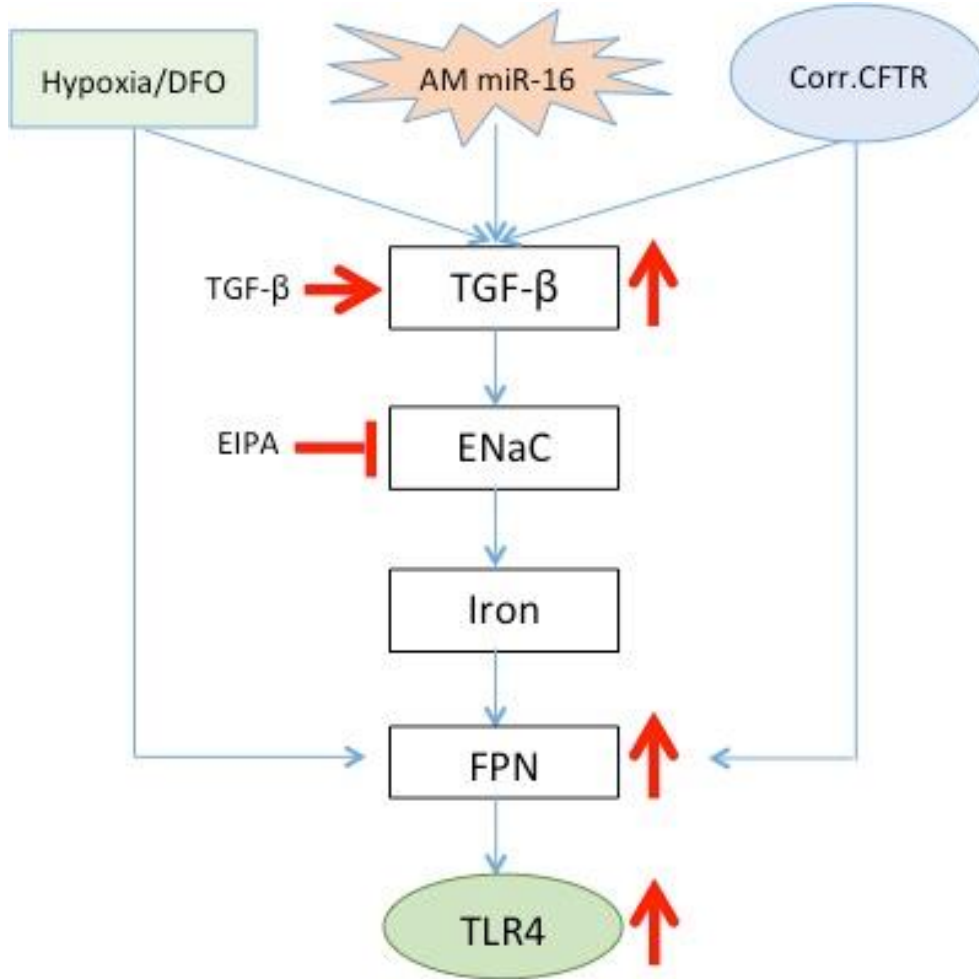


Figure 26: Schematic representation of pathways involved in TLR-4 and ferroportin expression in CF. Upregulation or downregulation of the respective targets is indicated with block arrows.

6 References

1. Riordan, J.R., et al., *Identification of the cystic fibrosis gene: cloning and characterization of complementary DNA*. Science, 1989. **245**(4922): p. 1066-73.
2. Rommens, J.M., et al., *Identification of the cystic fibrosis gene: chromosome walking and jumping*. Science, 1989. **245**(4922): p. 1059-65.
3. Rowntree, R.K. and A. Harris, *The phenotypic consequences of CFTR mutations*. Ann Hum Genet, 2003. **67**(Pt 5): p. 471-85.
4. Cutting, G.R., *Cystic fibrosis genetics: from molecular understanding to clinical application*. Nat Rev Genet, 2015. **16**(1): p. 45-56.
5. Kern, S.E., et al., *Clinical and pathological associations with allelic loss in colorectal carcinoma, corrected*. JAMA, 1989. **261**(21): p. 3099-103.
6. Reddy, M.M., M.J. Light, and P.M. Quinton, *Activation of the epithelial Na⁺ channel (ENaC) requires CFTR Cl⁻ channel function*. Nature, 1999. **402**(6759): p. 301-304.
7. Lubamba, B., et al., *Cystic fibrosis: insight into CFTR pathophysiology and pharmacotherapy*. Clin Biochem, 2012. **45**(15): p. 1132-44.
8. Frezal, J., C. Baumann, and J. Kaplan, *Cystic fibrosis: a gene at the end of the road*. Rev Prat, 1990. **40**(17): p. 1543-7.
9. Kreindler, J.L., *Cystic fibrosis: exploiting its genetic basis in the hunt for new therapies*. Pharmacol Ther, 2010. **125**(2): p. 219-29.
10. Anderson, M.P., et al., *Demonstration that CFTR is a chloride channel by alteration of its anion selectivity*. Science, 1991. **253**(5016): p. 202-5.
11. Xue, R., et al., *Expression of Cystic Fibrosis Transmembrane Conductance Regulator in Ganglia of Human Gastrointestinal Tract*. Scientific Reports, 2016. **6**: p. 30926.
12. O'Sullivan, B.P. and S.D. Freedman, *Cystic fibrosis*. Lancet, 2009. **373**(9678): p. 1891-904.
13. McKiernan, P.J. and C.M. Greene, *MicroRNA Dysregulation in Cystic Fibrosis*. Mediators Inflamm, 2015. **2015**: p. 529642.
14. Lyczak, J.B., C.L. Cannon, and G.B. Pier, *Lung infections associated with cystic fibrosis*. Clin Microbiol Rev, 2002. **15**(2): p. 194-222.

REFERENCES

15. Rajan, S. and L. Saiman, *Pulmonary infections in patients with cystic fibrosis*. *Semin Respir Infect*, 2002. **17**(1): p. 47-56.
16. Kopp, B.T., et al., *Exaggerated inflammatory responses mediated by Burkholderia cenocepacia in human macrophages derived from Cystic fibrosis patients*. *Biochem Biophys Res Commun*, 2012. **424**(2): p. 221-7.
17. Watt, A.P., et al., *Neutrophil cell death, activation and bacterial infection in cystic fibrosis*. *Thorax*, 2005. **60**(8): p. 659-64.
18. Bals, R., D.J. Weiner, and J.M. Wilson, *The innate immune system in cystic fibrosis lung disease*. *J Clin Invest*, 1999. **103**(3): p. 303-7.
19. Fearon, D.T. and R.M. Locksley, *The instructive role of innate immunity in the acquired immune response*. *Science*, 1996. **272**(5258): p. 50-3.
20. Doring, G. and E. Gulbins, *Cystic fibrosis and innate immunity: how chloride channel mutations provoke lung disease*. *Cell Microbiol*, 2009. **11**(2): p. 208-16.
21. Akira, S., S. Uematsu, and O. Takeuchi, *Pathogen recognition and innate immunity*. *Cell*, 2006. **124**(4): p. 783-801.
22. Akira, S. and K. Takeda, *Toll-like receptor signalling*. *Nat Rev Immunol*, 2004. **4**(7): p. 499-511.
23. Hartl, D., et al., *Innate immunity in cystic fibrosis lung disease*. *J Cyst Fibros*, 2012. **11**(5): p. 363-82.
24. Li, J., et al., *Toll-like receptors as therapeutic targets for autoimmune connective tissue diseases*. *Pharmacol Ther*, 2013. **138**(3): p. 441-51.
25. Martin, T.R. and C.W. Frevert, *Innate Immunity in the Lungs*. *Proceedings of the American Thoracic Society*, 2005. **2**(5): p. 403-411.
26. Iwasaki, A. and R. Medzhitov, *Toll-like receptor control of the adaptive immune responses*. *Nat Immunol*, 2004. **5**(10): p. 987-95.
27. Medzhitov, R., et al., *MyD88 is an adaptor protein in the hToll/IL-1 receptor family signaling pathways*. *Mol Cell*, 1998. **2**(2): p. 253-8.
28. Adachi, O., et al., *Targeted disruption of the MyD88 gene results in loss of IL-1- and IL-18-mediated function*. *Immunity*, 1998. **9**(1): p. 143-50.
29. Mukaida, N., Y. Mahe, and K. Matsushima, *Cooperative interaction of nuclear factor-kappa B- and cis-regulatory enhancer binding protein-like factor binding elements in activating the interleukin-8 gene by pro-inflammatory cytokines*. *J Biol Chem*, 1990. **265**(34): p. 21128-33.

REFERENCES

30. Parker, D. and A. Prince, *Innate immunity in the respiratory epithelium*. Am J Respir Cell Mol Biol, 2011. **45**(2): p. 189-201.
31. Ueno, K., et al., *MUC1 mucin is a negative regulator of toll-like receptor signaling*. Am J Respir Cell Mol Biol, 2008. **38**(3): p. 263-8.
32. Cohen, T.S. and A. Prince, *Cystic fibrosis: a mucosal immunodeficiency syndrome*. Nat Med, 2012. **18**(4): p. 509-19.
33. Brubaker, S.W., et al., *Innate immune pattern recognition: a cell biological perspective*. Annu Rev Immunol, 2015. **33**: p. 257-90.
34. Schletter, J., et al., *Molecular mechanisms of endotoxin activity*. Arch Microbiol, 1995. **164**(6): p. 383-9.
35. Poltorak, A., et al., *Defective LPS signaling in C3H/HeJ and C57BL/10ScCr mice: mutations in Tlr4 gene*. Science, 1998. **282**(5396): p. 2085-8.
36. John, G., et al., *TLR-4-mediated innate immunity is reduced in cystic fibrosis airway cells*. Am J Respir Cell Mol Biol, 2010. **42**(4): p. 424-31.
37. John, G., et al., *Reduced surface toll-like receptor-4 expression and absent interferon-gamma-inducible protein-10 induction in cystic fibrosis airway cells*. Exp Lung Res, 2011. **37**(6): p. 319-26.
38. Henke, M.O., et al., *MUC5AC and MUC5B Mucins Are Decreased in Cystic Fibrosis Airway Secretions*. Am J Respir Cell Mol Biol, 2004. **31**(1): p. 86-91.
39. Picot, R., I. Das, and L. Reid, *Pus, deoxyribonucleic acid, and sputum viscosity*. Thorax, 1978. **33**(2): p. 235-42.
40. Lethem, M.I., et al., *The origin of DNA associated with mucus glycoproteins in cystic fibrosis sputum*. Eur Respir J, 1990. **3**(1): p. 19-23.
41. Garty, H. and L.G. Palmer, *Epithelial sodium channels: function, structure, and regulation*. Physiol Rev, 1997. **77**(2): p. 359-96.
42. Ben-Shahar, Y., *Sensory functions for degenerin/epithelial sodium channels (DEG/ENaC)*. Adv Genet, 2011. **76**: p. 1-26.
43. Borgnia, M., et al., *Cellular and molecular biology of the aquaporin water channels*. Annu Rev Biochem, 1999. **68**: p. 425-58.
44. Schild, L., *The epithelial sodium channel: from molecule to disease*. Rev Physiol Biochem Pharmacol, 2004. **151**: p. 93-107.

REFERENCES

45. Bhalla, V. and K.R. Hallows, *Mechanisms of ENaC regulation and clinical implications*. J Am Soc Nephrol, 2008. **19**(10): p. 1845-54.
46. Eaton, D.C., et al., *Regulation of Na⁺ channels in lung alveolar type II epithelial cells*. Proc Am Thorac Soc, 2004. **1**(1): p. 10-6.
47. Hummler, E., et al., *Early death due to defective neonatal lung liquid clearance in alpha-ENaC-deficient mice*. Nat Genet, 1996. **12**(3): p. 325-8.
48. Mall, M., et al., *Wild type but not deltaF508 CFTR inhibits Na⁺ conductance when coexpressed in Xenopus oocytes*. FEBS Lett, 1996. **381**(1-2): p. 47-52.
49. Lazrak, A., et al., *Enhancement of alveolar epithelial sodium channel activity with decreased cystic fibrosis transmembrane conductance regulator expression in mouse lung*. Am J Physiol Lung Cell Mol Physiol, 2011. **301**(4): p. L557-67.
50. Mutesa, L., et al., *Genetic analysis of Rwandan patients with cystic fibrosis-like symptoms: identification of novel cystic fibrosis transmembrane conductance regulator and epithelial sodium channel gene variants*. Chest, 2009. **135**(5): p. 1233-42.
51. Matalon, S., R. Bartoszewski, and J.F. Collawn, *Role of epithelial sodium channels in the regulation of lung fluid homeostasis*. Am J Physiol Lung Cell Mol Physiol, 2015. **309**(11): p. L1229-38.
52. Butler, R., T. Hunt, and N.J. Smith, *ENaC inhibitors for the treatment of cystic fibrosis*. Pharm Pat Anal, 2015. **4**(1): p. 17-27.
53. Frizzell, R.A. and J.M. Pilewski, *Finally, mice with CF lung disease*. Nat Med, 2004. **10**(5): p. 452-4.
54. Peters, D.M., et al., *TGF-beta directs trafficking of the epithelial sodium channel ENaC which has implications for ion and fluid transport in acute lung injury*. Proc Natl Acad Sci U S A, 2014. **111**(3): p. E374-83.
55. Tamarapu Parthasarathy, P., et al., *MicroRNA 16 modulates epithelial sodium channel in human alveolar epithelial cells*. Biochem Biophys Res Commun, 2012. **426**(2): p. 203-8.
56. Assoian, R.K., et al., *Transforming growth factor-beta in human platelets. Identification of a major storage site, purification, and characterization*. J Biol Chem, 1983. **258**(11): p. 7155-60.
57. Feng, X.H. and R. Derynck, *Specificity and versatility in tgf-beta signaling through Smads*. Annu Rev Cell Dev Biol, 2005. **21**: p. 659-93.

REFERENCES

58. Zhu, H.J. and A.W. Burgess, *Regulation of transforming growth factor-beta signaling*. Mol Cell Biol Res Commun, 2001. **4**(6): p. 321-30.
59. Roberts, A.B., *Molecular and cell biology of TGF-beta*. Miner Electrolyte Metab, 1998. **24**(2-3): p. 111-9.
60. Shi, Y. and J. Massague, *Mechanisms of TGF-beta signaling from cell membrane to the nucleus*. Cell, 2003. **113**(6): p. 685-700.
61. Eickelberg, O., *Endless healing: TGF-beta, SMADs, and fibrosis*. FEBS Lett, 2001. **506**(1): p. 11-4.
62. Aubert, J.D., et al., *Transforming growth factor beta 1 gene expression in human airways*. Thorax, 1994. **49**(3): p. 225-32.
63. Coker, R.K., et al., *Diverse cellular TGF-beta 1 and TGF-beta 3 gene expression in normal human and murine lung*. Eur Respir J, 1996. **9**(12): p. 2501-7.
64. Wu, J.W., et al., *Crystal structure of a phosphorylated Smad2. Recognition of phosphoserine by the MH2 domain and insights on Smad function in TGF-beta signaling*. Mol Cell, 2001. **8**(6): p. 1277-89.
65. Shi, Y., et al., *A structural basis for mutational inactivation of the tumour suppressor Smad4*. Nature, 1997. **388**(6637): p. 87-93.
66. Itoh, F., et al., *Promoting bone morphogenetic protein signaling through negative regulation of inhibitory Smads*. EMBO J, 2001. **20**(15): p. 4132-42.
67. Huang, F. and Y.-G. Chen, *Regulation of TGF-beta receptor activity*. Cell & Bioscience, 2012. **2**(1): p. 1-10.
68. Hui, A.Y. and S.L. Friedman, *Molecular basis of hepatic fibrosis*. Expert Rev Mol Med, 2003. **5**(5): p. 1-23.
69. Peterson-Carmichael, S.L., et al., *Association of lower airway inflammation with physiologic findings in young children with cystic fibrosis*. Pediatr Pulmonol, 2009. **44**(5): p. 503-11.
70. Harris, W.T., et al., *Plasma TGF-beta(1) in pediatric cystic fibrosis: potential biomarker of lung disease and response to therapy*. Pediatr Pulmonol, 2011. **46**(7): p. 688-95.
71. Harris, W.T., et al., *Myofibroblast differentiation and enhanced TGF-B signaling in cystic fibrosis lung disease*. PLoS One, 2013. **8**(8): p. e70196.

72. Sun, H., et al., *Tgf-beta downregulation of distinct chloride channels in cystic fibrosis-affected epithelia*. PLoS One, 2014. **9**(9): p. e106842.
73. Frank, J., et al., *Transforming growth factor-beta1 decreases expression of the epithelial sodium channel alphaENaC and alveolar epithelial vectorial sodium and fluid transport via an ERK1/2-dependent mechanism*. J Biol Chem, 2003. **278**(45): p. 43939-50.
74. Davis, M. and S. Clarke, *Influence of microRNA on the maintenance of human iron metabolism*. Nutrients, 2013. **5**(7): p. 2611-28.
75. Kozomara, A. and S. Griffiths-Jones, *miRBase: integrating microRNA annotation and deep-sequencing data*. Nucleic Acids Res, 2011. **39**(Database issue): p. D152-7.
76. Georgantas, R.W., 3rd, et al., *CD34+ hematopoietic stem-progenitor cell microRNA expression and function: a circuit diagram of differentiation control*. Proc Natl Acad Sci U S A, 2007. **104**(8): p. 2750-5.
77. Poy, M.N., et al., *A pancreatic islet-specific microRNA regulates insulin secretion*. Nature, 2004. **432**(7014): p. 226-30.
78. Gauthier, B.R. and C.B. Wollheim, *MicroRNAs: 'ribo-regulators' of glucose homeostasis*. Nat Med, 2006. **12**(1): p. 36-8.
79. Kozakowska, M., et al., *Role of heme oxygenase-1 in postnatal differentiation of stem cells: a possible cross-talk with microRNAs*. Antioxid Redox Signal, 2013.
80. Zhao, Y. and D. Srivastava, *A developmental view of microRNA function*. Trends Biochem Sci, 2007. **32**(4): p. 189-97.
81. Booton, R. and M.A. Lindsay, *Emerging role of MicroRNAs and long noncoding RNAs in respiratory disease*. Chest, 2014. **146**(1): p. 193-204.
82. Gillen, A.E., et al., *MicroRNA regulation of expression of the cystic fibrosis transmembrane conductance regulator gene*. Biochem J, 2011. **438**(1): p. 25-32.
83. Oglesby, I.K., et al., *Regulation of cystic fibrosis transmembrane conductance regulator by microRNA-145, -223, and -494 is altered in DeltaF508 cystic fibrosis airway epithelium*. J Immunol, 2013. **190**(7): p. 3354-62.
84. Hassan, F., et al., *MiR-101 and miR-144 regulate the expression of the CFTR chloride channel in the lung*. PLoS One, 2012. **7**(11): p. e50837.

REFERENCES

85. Oglesby, I.K., et al., *miR-126 is downregulated in cystic fibrosis airway epithelial cells and regulates TOM1 expression*. J Immunol, 2010. **184**(4): p. 1702-9.
86. Bhattacharyya, S., et al., *Elevated miR-155 promotes inflammation in cystic fibrosis by driving hyperexpression of interleukin-8*. J Biol Chem, 2011. **286**(13): p. 11604-15.
87. Kumar, P., et al., *miR-16 rescues F508del-CFTR function in native cystic fibrosis epithelial cells*. Gene Ther, 2015. **22**(11): p. 908-16.
88. Greene, C.M., *MicroRNA Expression in Cystic Fibrosis Airway Epithelium*. Biomolecules, 2013. **3**(1): p. 157-67.
89. Reid, D.W., G.J. Anderson, and I.L. Lamont, *Role of lung iron in determining the bacterial and host struggle in cystic fibrosis*. Am J Physiol Lung Cell Mol Physiol, 2009. **297**(5): p. L795-802.
90. MacKenzie, E.L., K. Iwasaki, and Y. Tsuji, *Intracellular iron transport and storage: from molecular mechanisms to health implications*. Antioxid Redox Signal, 2008. **10**(6): p. 997-1030.
91. Goralska, M., et al., *Iron metabolism in the eye: a review*. Exp Eye Res, 2009. **88**(2): p. 204-15.
92. Ghio, A.J., *Disruption of iron homeostasis and lung disease*. Biochim Biophys Acta, 2009. **1790**(7): p. 731-9.
93. Frazer, D.M. and G.J. Anderson, *The orchestration of body iron intake: how and where do enterocytes receive their cues?* Blood Cells Mol Dis, 2003. **30**(3): p. 288-97.
94. Steele, T.M., D.M. Frazer, and G.J. Anderson, *Systemic regulation of intestinal iron absorption*. IUBMB Life, 2005. **57**(7): p. 499-503.
95. Britigan, B.E., et al., *Transferrin and lactoferrin undergo proteolytic cleavage in the Pseudomonas aeruginosa-infected lungs of patients with cystic fibrosis*. Infect Immun, 1993. **61**(12): p. 5049-55.
96. Kang, G.S., et al., *Effect of metal ions on HIF-1alpha and Fe homeostasis in human A549 cells*. Mutat Res, 2006. **610**(1-2): p. 48-55.
97. Yang, F., et al., *Iron increases expression of iron-export protein MTP1 in lung cells*. Am J Physiol Lung Cell Mol Physiol, 2002. **283**(5): p. L932-9.
98. Chua, A.C., et al., *The regulation of cellular iron metabolism*. Crit Rev Clin Lab Sci, 2007. **44**(5-6): p. 413-59.

REFERENCES

99. Ghio, A.J., et al., *Divalent metal transporter-1 decreases metal-related injury in the lung*. Am J Physiol Lung Cell Mol Physiol, 2005. **289**(3): p. L460-7.
100. Yang, F., et al., *Haptoglobin reduces lung injury associated with exposure to blood*. Am J Physiol Lung Cell Mol Physiol, 2003. **284**(2): p. L402-9.
101. Turi, J.L., et al., *The iron cycle and oxidative stress in the lung*. Free Radic Biol Med, 2004. **36**(7): p. 850-7.
102. Yang, F., et al., *Apical location of ferroportin 1 in airway epithelia and its role in iron detoxification in the lung*. Am J Physiol Lung Cell Mol Physiol, 2005. **289**(1): p. L14-23.
103. Reid, D.W., et al., *Airway iron and iron-regulatory cytokines in cystic fibrosis*. Eur Respir J, 2004. **24**(2): p. 286-91.
104. Moreau-Marquis, S., et al., *The DeltaF508-CFTR mutation results in increased biofilm formation by Pseudomonas aeruginosa by increasing iron availability*. Am J Physiol Lung Cell Mol Physiol, 2008. **295**(1): p. L25-37.
105. Turi, J.L., et al., *Iron accumulation in bronchial epithelial cells is dependent on concurrent sodium transport*. Biometals, 2008. **21**(5): p. 571-80.
106. Rafii, B., et al., *Oxygen induction of epithelial Na(+) transport requires heme proteins*. Am J Physiol Lung Cell Mol Physiol, 2000. **278**(2): p. L399-406.
107. Chillappagari, S., et al., *Impaired TLR4 and HIF expression in cystic fibrosis bronchial epithelial cells downregulates hemeoxygenase-1 and alters iron homeostasis in vitro*. Am J Physiol Lung Cell Mol Physiol, 2014. **307**(10): p. L791-9.
108. Davis, P.B., M. Drumm, and M.W. Konstan, *Cystic fibrosis*. Am J Respir Crit Care Med, 1996. **154**(5): p. 1229-56.
109. Wang, J., et al., *Iron-mediated degradation of IRP2, an unexpected pathway involving a 2-oxoglutarate-dependent oxygenase activity*. Mol Cell Biol, 2004. **24**(3): p. 954-65.
110. Fandrey, J., T.A. Gorr, and M. Gassmann, *Regulating cellular oxygen sensing by hydroxylation*. Cardiovasc Res, 2006. **71**(4): p. 642-51.
111. Rius, J., et al., *NF-kappaB links innate immunity to the hypoxic response through transcriptional regulation of HIF-1alpha*. Nature, 2008. **453**(7196): p. 807-11.

REFERENCES

112. van Uden, P., N.S. Kenneth, and S. Rocha, *Regulation of hypoxia-inducible factor-1alpha by NF-kappaB*. *Biochem J*, 2008. **412**(3): p. 477-84.
113. Spirig, R., et al., *Effects of TLR agonists on the hypoxia-regulated transcription factor HIF-1alpha and dendritic cell maturation under normoxic conditions*. *PLoS One*, 2010. **5**(6): p. e0010983.
114. Kim, S.Y., et al., *Hypoxic stress up-regulates the expression of Toll-like receptor 4 in macrophages via hypoxia-inducible factor*. *Immunology*, 2010. **129**(4): p. 516-24.
115. Johnson, E.E. and M. Wessling-Resnick, *Iron metabolism and the innate immune response to infection*. *Microbes Infect*, 2012. **14**(3): p. 207-16.
116. Ward, D.M. and J. Kaplan, *Ferroportin-mediated iron transport: expression and regulation*. *Biochim Biophys Acta*, 2012. **1823**(9): p. 1426-33.
117. Abboud, S. and D.J. Haile, *A novel mammalian iron-regulated protein involved in intracellular iron metabolism*. *J Biol Chem*, 2000. **275**(26): p. 19906-12.
118. Ghio, A.J., et al., *Iron accumulates in the lavage and explanted lungs of cystic fibrosis patients*. *J Cyst Fibros*, 2013. **12**(4): p. 390-8.
119. Harris, W.T., et al., *Transforming growth factor-beta(1) in bronchoalveolar lavage fluid from children with cystic fibrosis*. *Pediatr Pulmonol*, 2009. **44**(11): p. 1057-64.
120. Li, M.O., et al., *Transforming growth factor-beta regulation of immune responses*. *Annu Rev Immunol*, 2006. **24**: p. 99-146.
121. Sullivan, K.E., et al., *Measurement of cytokine secretion, intracellular protein expression, and mRNA in resting and stimulated peripheral blood mononuclear cells*. *Clin Diagn Lab Immunol*, 2000. **7**(6): p. 920-4.
122. Collawn, J.F., et al., *The CFTR and ENaC debate: how important is ENaC in CF lung disease?* *Am J Physiol Lung Cell Mol Physiol*, 2012. **302**(11): p. L1141-6.
123. Falanga, V., et al., *Hypoxia upregulates the synthesis of TGF-beta 1 by human dermal fibroblasts*. *J Invest Dermatol*, 1991. **97**(4): p. 634-7.
124. Alarifi, S., et al., *Oxidative stress contributes to cobalt oxide nanoparticles-induced cytotoxicity and DNA damage in human hepatocarcinoma cells*. *Int J Nanomedicine*, 2013. **8**: p. 189-199.

125. Zeng, H.L., et al., *Hypoxia-mimetic agents inhibit proliferation and alter the morphology of human umbilical cord-derived mesenchymal stem cells*. BMC Cell Biol, 2011. **12**: p. 32.
126. Hobbs, C.A., C. Da Tan, and R. Tarran, *Does epithelial sodium channel hyperactivity contribute to cystic fibrosis lung disease?* J Physiol, 2013. **591**(18): p. 4377-87.
127. Bartram, U. and C.P. Speer, *The role of transforming growth factor beta in lung development and disease*. Chest, 2004. **125**(2): p. 754-65.
128. Eickmeier, O., et al., *Transforming growth factor beta1 genotypes in relation to TGFbeta1, interleukin-8, and tumor necrosis factor alpha in induced sputum and blood in cystic fibrosis*. Mediators Inflamm, 2013. **2013**: p. 913135.
129. Kelley, T.J., H.L. Elmer, and D.A. Corey, *Reduced Smad3 protein expression and altered transforming growth factor-beta1-mediated signaling in cystic fibrosis epithelial cells*. Am J Respir Cell Mol Biol, 2001. **25**(6): p. 732-8.
130. Tuyen, D.G., et al., *Inhibition of prostatic expression by TGF-beta1 in renal epithelial cells*. Kidney Int, 2005. **67**(1): p. 193-200.
131. Ke, Q. and M. Costa, *Hypoxia-inducible factor-1 (HIF-1)*. Mol Pharmacol, 2006. **70**(5): p. 1469-80.
132. Ganz, T., *Cellular iron: ferroportin is the only way out*. Cell Metab, 2005. **1**(3): p. 155-7.
133. Donovan, A., et al., *The iron exporter ferroportin/Slc40a1 is essential for iron homeostasis*. Cell Metab, 2005. **1**(3): p. 191-200.
134. Viatte, L., et al., *Deregulation of proteins involved in iron metabolism in hepcidin-deficient mice*. Blood, 2005. **105**(12): p. 4861-4.
135. Mastrogiannaki, M., et al., *Deletion of HIF-2alpha in the enterocytes decreases the severity of tissue iron loading in hepcidin knockout mice*. Blood, 2012. **119**(2): p. 587-90.
136. Peyssonnaud, C., et al., *Regulation of iron homeostasis by the hypoxia-inducible transcription factors (HIFs)*. J Clin Invest, 2007. **117**(7): p. 1926-32.
137. Rathore, K.I., A. Redensek, and S. David, *Iron homeostasis in astrocytes and microglia is differentially regulated by TNF-alpha and TGF-beta1*. Glia, 2012. **60**(5): p. 738-50.

REFERENCES

138. Gorlach, A., et al., *Thrombin activates the hypoxia-inducible factor-1 signaling pathway in vascular smooth muscle cells: Role of the p22(phox)-containing NADPH oxidase*. *Circ Res*, 2001. **89**(1): p. 47-54.
139. Shih, S.C. and K.P. Claffey, *Role of AP-1 and HIF-1 transcription factors in TGF-beta activation of VEGF expression*. *Growth Factors*, 2001. **19**(1): p. 19-34.
140. McMahon, S., et al., *Transforming growth factor beta1 induces hypoxia-inducible factor-1 stabilization through selective inhibition of PHD2 expression*. *J Biol Chem*, 2006. **281**(34): p. 24171-81.
141. Donaldson, S.H. and R.C. Boucher, *Update on pathogenesis of cystic fibrosis lung disease*. *Curr Opin Pulm Med*, 2003. **9**(6): p. 486-91.
142. Gianotti, A., et al., *Epithelial sodium channel silencing as a strategy to correct the airway surface fluid deficit in cystic fibrosis*. *Am J Respir Cell Mol Biol*, 2013. **49**(3): p. 445-52.

7 Abbreviation

16 HBE14o-cells	Human bronchial epithelial cells
AEC	Alveolar epithelial cell
AM	Alveolar macrophages
AP	Alkaline phosphatase
APCs,	Antigen-presenting cells
APS	Ammonium persulfate
ASL	Airways surface liquid
ATP	Adenosine triphosphate
BAL	Bronchoalveolar lavage
BMP	Bone morphogenetic protein
BSA	Bovine serum albumin
cDNA	Complementary deoxyribonucleic acid
CF	Cystic fibrosis
CFBE41o-	Cystic fibrosis bronchial epithelial cells
CFTR	Cystic fibrosis transmembrane conductance regulator
COPD	Chronic obstructive pulmonary disease
Ct	Threshold cycle
Da	Dalton
DAMPs	Danger- associated molecular patterns
DAPI	4',6-diamidino-2-phenylindole
DCs	Dendritic cells

— ABBREVIATION —

DFO	Deferoxamine
DMT1	Divalent metal transporter 1
EDTA	Ethylenediaminetetraacetic acid
EIPA	(5-(N-Ethyl-N-isopropyl)amiloride)
ELISA	Enzyme-linked immunosorbent assay
EMT	Epithelial - mesenchymal transition
ENaC	Epithelial sodium channel
ER stress	Endoplasmic reticulum stress
FPN	Ferroportin
gms	Grams
HCP1	Heme carrier protein 1
HIF	Hypoxia-inducible factor
HIF1α	Hypoxia-inducible factor-1 α
HJV	Hemojuvelin
HO-1	Hemeoxygenase-1
HRP	Horseradish peroxidase
i-SMADs	Inhibitory SMADs
IFN-γ	Interferon- γ
IL	Interleukin
IP-10	Interferon- γ inducible protein – 10
IPF	Idiopathic pulmonary fibrosis
IRE	Iron-responsive element
Kb	Kilobase pairs

— ABBREVIATION —

KCl	Potassium chloride
kDa	Kilodalton
KH₂PO₄	Monopotassium phosphate
LPS	Lipopolysaccharide
LTGF-β	Latent precursor molecules of TGF- β
M	Molar (mole/litre)
MCC	Mucociliary clearance
mg	Milligram
min	Minute(s)
miRNA	MicroRNA
mL	Milliliter
mM	Millimolar
MMP	Matrix metalloproteinase
MUC5B	Mucin 5B
NaCl	sodium chloride
NADPH	nicotinamide adenine dinucleotide phosphate-oxidase
nm	Nanometer
nM	Nanomolar
NO	Nitric oxide
PAMPs	Pathogen-associated molecular patterns
PBS	Phosphate-buffered saline
PCR	Polymerase chain reaction
PFA	Paraformaldehyde

ABBREVIATION

PHDs	Prolyl hydroxylases
PPRs	Pattern recognition receptors
q-PCR	Quantitative real-time- polymerase chain reaction
RISC	RNA-induced silencing complex
ROS	Reactive oxygen species
RPM	Revolution per minute
RT	Room temperature
SDS-PAGE	SDS-polyacrylamide gel electrophoresis
TBST	Tris-buffered saline and Tween 20
TEMED	Tetramethylethylenediamine
Tf	Protein transferrin
TGF-β receptor	Transforming growth factor receptor
TLR	Toll-Like receptors
UPR	Unfolded protein response
V	Volt
α-SMA	Alpha smooth muscle actin
μg	Microgram
μL	Microliter
μm	Micrometer
μM	Micromolar

8 Curriculum vitae

Gaurav Sarode

Date of Birth 24th December 1987
Nationality Indian
Address Felsennelkenanger 17/300, 80937, München, Germany
Email gaurav.v.sarode@gmail.com

Education

July 2014-August 2017 **Ph.D. in Pulmonary Medicine, Ludwig-Maximilians-Universität, München, Germany**
Dissertation- Analysis of the altered intracellular pathways in reduced Toll-like receptor-4 (TLR-4) expression in cystic fibrosis

August 2014-Dec 2011 **Master of science (M.S.) in Biomedicine, University of Skövde, Skövde, Sweden**

August 2005–July 2009 **Bachelor of Pharmaceutical sciences, Pune University, Pune, India**

Work Experience

June 2014-August 2017 **Helmholtz Zentrum München, Germany Ludwig-Maximilians-Universität (LMU), Germany**
Ph.D. Student: Molecular Pulmonology, Pneumology
Guide: PD Dr. Markus Henke and Prof Dr. Jürgen Behr

January 2012-May 2014 **Justus-Liebig Universität, Germany**

- Research Associate- Molecular andrology
Guide - Prof. Dr. Klaus Steger
- June 2011–Dec 2011 **Philipps Universität, Marburg, Germany**
Universitäts Klinikum of Giessen and Marburg
(UKGM) Germany
- Internship in Pneumology
Guide: PD Dr. Markus Henke
- August 2009–July 2010 **Haffkine Ajantha Pharmaceuticals Ltd. India**
- Production/manufacturing chemists

Molecular and Cell Biology technical skills

- RNA/DNA methods PCRs, Cloning, RNA/DNA-gels, RNA/DNA-Isolation and purification, Purification and isolation of plasmid DNA, Combined Bisulphite Restriction Assay (COBRA), Bisulfite Sequencing (BS), Pyro-sequencing.
- Protein biochemistry SDS-PAGE, Western blot analysis, Chromatin Immunoprecipitation (ChIP), Co-Immuno-precipitation (co-IP), Luciferase reporter gene assay, Immunohistochemistry, Immunofluorescence.
- Cell culturing Bacterial cells (risk group 1/2), Human cells (risk group 1), Transformation, Transfection, and Establishment of the stable cell line, Iron assay.
- Computer skills Good skills in MS Office suite, ImageJ, Finch TV, Fluorescence LAS AF Microscope Software, MxPro QPCR, Prism GraphPad, SPSS Statistic

Achievements

Publications:

Sarode G, Garapati V, Mahavadi P, Guenther A, Behr J, Chillappagari S, Henke MO Role of epithelial sodium channel ENaC and its regulating factors associated increased ferroportin expression and improved TLR-4 surface expression in cystic fibrosis bronchial epithelial cells *in vitro* (Under Preparation).

Samans B, Yang Y, Krebs S, **Sarode GV**, Blum H, Reichenbach M, Wolf E, Steger K, Dansranjavin T, Schagdarsurengin U. Uniformity of nucleosome preservation pattern in Mammalian sperm and its connection to repetitive DNA elements. *Developmental cell*. 2014;30(1):23-35. Epub 2014/07/08. doi: 10.1016/j.devcel.2014.05.023. PubMed PMID: 24998597

Chillappagari S, Venkatesan S, Garapati V, Mahavadi P, Munder A, Seubert A, **Sarode G**, Guenther A, Schmeck BT, TummLer B, Henke MO. Impaired TLR-4 and HIF expression in cystic fibrosis bronchial epithelial cells downregulates hemeoxygenase-1 and alters iron homeostasis in vitro. *American journal of physiology Lung cellular and molecular physiology*. 2014;307(10): L791-9. Epub 2014/09/23. doi: 10.1152/ajplung.00167.2014. PubMed PMID: 25239913.

Chillappagari S, Preuss J, Licht S, Muller C, Mahavadi P, **Sarode G**, Vogelmeier C, Guenther A, Nahrlich L, Rubin BK, Henke MO. Altered protease and antiprotease balance during a COPD exacerbation contribute to mucus obstruction. *Respir Res*. 2015;16:85. doi: 10.1186/s12931-015-0247-x. PubMed PMID: 26169056; PMCID: PMC4501272.

Published abstracts (peer reviewed):

Velagala S.R., Seifer P., Dansranjavin T., **Sarode G.V.**, Weidner W., Wagenlehner F., Schagdarsurengin U Epigenetic analyses on inflammatory factors in patients with prostatitis, BPH and prostate cancer: Discovering the link between inflammation and carcinogenesis. *Eur Urol Suppl* 2014;13;e568

Yang Y., Samans B., Krebs S., **Sarode G.V.**, Wolf E., Blum H., Dansranjavin T., Weidner W., Schagdarsurengin U. Repetitive DNA elements act as a landmark in establishment and function of sperm chromatin. *Eur Urol Suppl* 2014;13;e152

S Chillappagari, **G Sarode**, H Shah, MO Henke. Cellular stress and homeostatic mechanisms involved in reduced innate immunity in cystic fibrosis cell lines. *Pneumologie* 2011; 65 - A12 DOI: 10.1055/s-0031-1296103.

9 Eidesstattliche Versicherung

Gaurav Sarode

Name, Vorname

Ich erkläre hiermit an Eides statt,

dass ich die vorliegende Dissertation mit dem Thema,

Analysis of altered intracellular pathways leading to a reduced TLR-4 expression
in cystic fibrosis

selbständig verfasst, mich außer der angegebenen keiner weiteren Hilfsmittel
bedient und alle Erkenntnisse, die aus dem Schrifttum ganz oder annähernd
übernommen sind, als solche kenntlich gemacht und nach ihrer Herkunft unter
Bezeichnung der Fundstelle einzeln nachgewiesen habe.

Ich erkläre des Weiteren, dass die hier vorgelegte Dissertation nicht in gleicher
oder in ähnlicher Form bei einer anderen Stelle zur Erlangung eines
akademischen Grades eingereicht wurde.

München (01.03.2017)

Gaurav Sarode

Ort, Datum

Unterschrift Doktorand

10 Acknowledgements

Firstly, my heartiest gratitude goes to my direct supervisor PD Dr. Markus Henke for his cordial help, relentless support and advice throughout my Ph.D. life. I have deep respect and admiration for his great support and believe that acted as a driving force for me to carry out my current thesis project. I would also like to sincerely thank my Doctor father Prof. Dr. med. Jürgen Behr for his invaluable support and encouragements.

I want to especially thank Dr. Shashi Chillappagari, Department of Internal Medicine II, Justus Liebig University Giessen, without him my masters and Ph.D. thesis would not have been finished. I deeply thank him for his valuable guidance, framing, and monitoring of the progress of my work.

I am humbly grateful to all of them, as they have been a strong support and positive influence on my project by acting as my thesis committee. I would like to thank Dr. Poornima Mahavadi and Prof. Dr. Andreas Günther for providing their support for facilitating few techniques at their labs. I also thank Ali Önder Yildirim for providing me initial support to start my lab work in his lab at Helmholtz Zentrum München.

I deeply acknowledge the help of my dear fellow lab mate Virajith Garapati during my project work. I also thank my friend Pradeep Kudipudi, Department of Obstetrics and Gynecology Giessen for performing ELISA experiments.

I would like to thank all my colleagues and friends: Gayathri Viswanathan, Vivek Patil, Balram Neupane, Zaneta Sibiska, Dharmesh Hirani and Moritz Schäfer offering experimental tips and help during my thesis with all those enjoyable moments outside the work.

Lastly, I am grateful to my family for all for their unconditional love, inspiration, and support through all my live.